VISUALIZATION OF INTERACTIONS BETWEEN FLUORESCENTLY TAGGED
G PROTEIN α_{11}, $\alpha_{12/13}$ SUBTYPES AND ADENOSINE 2A, DOPAMINE 2 OR
HOMODIMER ADENOSINE 2A/2A RECEPTORS

A THESIS SUBMITTED TO
THE GRADUATE SCHOOL OF NATURAL AND APPLIED SCIENCES
OF
MIDDLE EAST TECHNICAL UNIVERSITY

BY

IRMAK BEGÜM KOSTROMİN

IN PARTIAL FULFILLMENT OF THE REQUIREMENTS
FOR
THE DEGREE OF MASTER OF SCIENCE
IN
BIOLOGY

JANUARY 2018

.

Approval of the thesis

VISUALIZATION OF INTERACTIONS BETWEEN FLUORESCENTLY TAGGED G PROTEIN α_{11}, $\alpha_{12/13}$ SUBTYPES AND ADENOSINE 2A, DOPAMINE 2 OR HOMODIMER ADENOSINE 2A/2A RECEPTORS

submitted by **IRMAK BEGÜM KOSTROMİN** in partial fulfillment of the requirements for the degree of **Master of Science in Biology Department, Middle East Technical University** by,

Prof. Dr. Gülbin DURAL ÜNVER   _____
Dean, Graduate School of **Natural and Applied Sciences**

Prof. Dr. Orhan Adalı   _____
Head of Department, **Biology**

Assoc. Prof. Dr. Çağdaş Devrim Son   _____
Supervisor, **Biology Dept., METU**

Examining Committee Members:

Assoc.Prof.Dr. A.Elif Erson-BENSAN   _____
Biology Dept., METU

Assoc. Prof. Dr. Çağdaş Devrim SON   _____
Biology Dept., METU

Assoc. Prof. Dr. Can ÖZEN   _____
Biotechnology Dept., METU

Prof. Dr. Sreeparna BANERJEE   _____
Biology Dept., METU

Assoc.Prof.Dr. Banu PEYNİRCİOĞLU   _____
Medical Biology Dept., Hacettepe University

Date: 31/01/2018

I hereby declare that all information in this document has been obtained and presented in accordance with academic rules and ethical conduct. I also declare that, as required by these rules and conduct, I have fully cited and referenced all material and results that are not original to this work.

Name, Last name: IRMAK BEGÜM KOSTROMİN

Signature:

ABSTRACT

VISUALIZATION OF INTERACTIONS BETWEEN FLUORESCENTLY TAGGED G PROTEIN α_{11}, $\alpha_{12/13}$ SUBTYPES AND ADENOSINE 2A, DOPAMINE 2 OR HOMODIMER ADENOSINE 2A/2A RECEPTORS

Kostromin, Irmak Begüm

M.S., Department of Biology

Supervisor: Assoc. Prof. Dr. Çağdaş Devrim Son

January 2018, 130 pages

G-Protein-coupled receptors (GPCRs) belong to one of the largest family of cell surface receptors, which transmit extracellular signals to intracellular responses by interacting with G- proteins. The G proteins are known as molecular switches that regulates different pathways via control of secondary messengers and signaling proteins. Adenosine 2A (A_{2A}) and Dopamine 2 (D_2) receptors belong to G-Protein-coupled receptors (GPCRs) family and are located mostly in striatopallidal γ-aminobutyric acid (GABA) containing neurons. Therefore, problems related to these receptors are associated with physiological disorders such as schizophrenia, and Parkinson disease.

A_{2A} receptors regulate neurotransmission, cardiovascular system and immune response; On the other hand, D_2 receptors modulate the regulation of locomotion, food intake, learning, emotion and behavior. Studies showed that, A_{2A} and D_2 receptors change the cAMP level by stimulating or inhibiting adenylyl cyclase via interacting with $G\alpha_s$ and $G\alpha_i$ proteins. When D_1 and D_2 receptors heterodimerize, $G\alpha_{q11}$ signal pathway was preferred and activate PIP2 and DAG secondary messengers. However, interaction

between $G\alpha_{q11}$ protein and A_{2A}, D_{2R} or A_{2A}/A_{2A} homodimer is not reported. GPCRs could also signal through $G\alpha_{12/13}$ which regulates actin cytoskeleton and cell migration through activation of Rho kinases. It is established that, $G\alpha_{12/13}$ mutant cells show neuronal over migration and dysfunction at cerebral cortex. In addition, cell migration is effected positively by A_{2A} receptor activation while it could be negatively regulated by D_2R receptor activation. However, it is not clear if $G\alpha_{12/13}$ proteins are interacting with A_{2A} and D_2 receptors triggering related pathways.

The aim of this study is to analyze possible physical interaction between $G\alpha_{q11}$-A_{2A}, $G\alpha_{q11}$-D_2R, $G\alpha_{q11}$-A_{2A}/A_{2A}; $G\alpha_{12/13}$-A_{2A}, $G\alpha_{12/13}$ -D_2R and $G\alpha_{12/13}$ -A_{2A}/A_{2A} using Fluorescence Resonance Energy Transfer (FRET) method. For this purpose, G-protein α subunits ($G\alpha_{11}$, $G\alpha_{12}$ and $G\alpha_{13}$) were labeled with mCherry or EGFP fluorescent proteins from five different internal locations; receptors were labelled with split-EGFP fragments, and full length EGFP fluorophore, and then transfected to *Mus musculus* Neuroblastoma-2a (N2a) cells as various combinations. To analyze the possible interactions, images were taken *via* spinning disc confocal microscopy and FRET efficiency was calculated by using pixFRET Plugin for ImageJ software. Images obtained from $G\alpha_{11}$+mCherry and D_2R+EGFP transfected N2a cells; $G\alpha_{13}$+mCherry and A_{2A}+EGFP have high FRET signal mostly located on cell membrane. $G\alpha_{13}$-D_2R, $G\alpha_{11}$-A_{2A} and $G\alpha11$-A_{2A}/A_{2A} pairs had lower signal than $G\alpha11$-$D2R$ and $G\alpha13$-$A2A$ pairs. Further experiments are necessary to prove an interaction between these pairs if it ever exists. On the othe hand $G\alpha12$-$A2A$ and $G\alpha13$-$A2A/A2A$ pairs had very low signal that was impossible to difrentiate from background signal indicating a lack of interaction. Protein interaction studies like the ones detailed in this study could help us understand signal transduction pathways much better, thus will be useful to design new treatment models and discover drug candidates in future.

ÖZ

FLORESAN İŞARETLİ G PROTEİN α_{11}, $\alpha_{12/13}$ ALT GRUBUNUN ADENOZİN 2A, DOPAMİN 2 VEYA HOMODİMER ADENOZİN 2A/2A RESEPTÖRLERİYLE ETKİLEŞİMİNİN GÖRÜNTÜLENMESİ

Kostromin, Irmak Begüm

Yüksek Lisans, Biyoloji Bölümü

Tez Yöneticisi: Doç. Dr. Çağdaş Devrim Son

Aralık 2017, 130 sayfa

G-proteine kenetli reseptörler (GPKR), G proteinlerle etkileşime girerek hücre dışı sinyalleri, hücre içi cevaplara dönüştüren hücre zarı moleküllerine ait büyük bir reseptör ailesidir. G proteinleri, ikincil mesajcılar ve sinyal proteinleri ile farklı sinyal yolaklarını düzenleyen moleküler düzenleyicilerdir. Adenozin 2A (A_{2A}) ve Dopamin (D_2) reseptörleri de G-proteine kenetli reseptör (GPKR) ailesine aittir ve daha çok striatopallidal γ-aminobutyric acid (GABA) içeren nöronlarda bulunur. Bu nedenle bu reseptörlerle ilgili problemler şizofreni, Parkinson gibi pisikolojik hastalıklarla bağlantılıdır.

Adenozin A_{2A} reseptörü, nörotransmisyonu, kardiyovasküler sistemi ve immun sistemini düzenler. Diğer bir yandan, Dopamin reseptörü ise hareket, gıda alımı, öğrenme, duygu ve davranış durumlarını kontrol eder. Yapılan çalışmalara göre A_{2A} ve D_2 reseptörleri cAMP seviyesini $G\alpha_s$ ve $G\alpha_i$ ptoteinleri aracılığıyla adenylyl siklazı uyararak ya da

engelleyerek değiştirmektedir. Dopamin 1 (D_1) ve Dopamin 2 (D_2) reseptörleri heterodimer oluşturduklarında $G\alpha_{q11}$ sinyal yolu tercih edilerek PIP2 ve DAG ikincil mesajcıları active ederler; ancak $G\alpha_{q11}$ proteinin A_{2A}, D_2 ve A_{2A}/A_{2A} homodimeri reseptörleri ile etkileşimi rapor edilmemiştir. GPCR'lar aynı zamanda Rho kinazın aktive edilmesiyle aktin hücre iskeleti ve hücre göçünü düzenleyen $G\alpha_{12/13}$ sinyal yolunu kullanır. $G\alpha_{12/13}$ mutant hücrelerin aşırı nöral göçe ve serebral korteksin fonksiyon bozukluğuna neden olduğu tespit edilmiştir. Buna ek olarak, hücre göçü A_{2A} reseptörü ile pozitif, D_2 reseptörü ile negatif bir şekilde etkilenmektedir. Ancak, $G\alpha_{12/13}$ proteinlerinin A_{2A} ve D_2 reseptörleri ile farklı bir sinyal yolu olarak etkileşimi olup olmadığı bilinmemektedir.

Çalışmanın amacı; $G\alpha_{q11}$-A_{2A}, $G\alpha_{q11}$-D_2R, $G\alpha_{q11}$-A_{2A}/A_{2A}; $G\alpha_{12/13}$-A_{2A}, $G\alpha_{12/13}$ -D_2R ve $G\alpha_{12/13}$ -A_{2A}/A_{2A} arasında fiziksel etkileşimi Fluoresans Rezonans Enerji Transfer (FRET) metodu ile tespit etmektir. Bu amaçla G-proteinlerin α alt ünitesi ($G\alpha_{11}$, $G\alpha_{12}$ ve $G\alpha_{13}$) mCherry veya EGFP floresant proteinleri ile beş farklı konumdan işaretlenmiş; reseptörler ise bölünmüş EGFP fragmenti ve EGFP floroforları ile işaretlenerek farkı kombinasyonlarda *Mus musculus* Neuroblastoma-2a (N2a) hürelerine transfekte edilmiştir. Proteinler arası etkileşimin görülmesi için spinning disk konfokal mikroskobu ile görüntüler alınmış ve FRET verimi ImageJ programının pixFRET eklentisi ile hesaplanmıştır. $G\alpha_{11}$+mCherry ve D_2R+EGFP ile $G\alpha_{13}$+mCherry ve A_{2A}+EGFP transfeksyonu gerçekleşen N2A hücrelerinin hücre membranından gelen yüksek FRET sinyali tespit edilmiştir. $G\alpha_{13}$-D_2R, $G\alpha_{11}$-A_{2A} ve $G\alpha11$-A_{2A}/A_{2A} çiftleri, $G\alpha_{11}$-D_2R ve $G\alpha_{13}$-A_{2A} protein çiftlerine göre daha az sinyal vermiştir. Bu proteinlerin kesin olarak etkileşime girdiğini belirlemek için daha fazla deneyle desteklenmesi gerekmektedir. Diğer bir yandan, $G\alpha_{12}$-A_{2A} ve $G\alpha_{13}$-A_{2A}/A_{2A} çiftleri ise background sinyalden ayrılamayacak kadar düşük FRET sinyali vermiştir. Bu da etkileşimin olmadığının göstergesidir. Bu çalışmada olduğu gibi protein etkileşimlerinin çalışılması, sinyal

yolaklarının daha iyi anlaşılmasına ve ileride bunların yeni tedavi modelleri ile ilaç adaylarının keşfedilmesine yardımcı olabilir.

Anahtar kelimeler: Förster Resonans Enerji Transfer (FRET), Dopamin D_{2R}, Adenosine A_{2A}, G-Protein Coupled Receptors, G-Protein, $G\alpha_{11}$, $G\alpha_{12}$ and $G\alpha_{13}$

To my family,

ACKNOWLEDGEMENTS

TABLE OF CONTENTS

LIST OF TABLES

LIST OF FIGURES

FIGURES

LIST OF ABBREVIATIONS

A1R	Adenosine A1 Receptor
A2AR	Adenosine A2A Receptor
AC	Adenylyl Cyclase
ADHD	Attention Deficit Hyperactive Disorder
ADP	Adenosine Diphosphate
AGE	Agarose gel electrophoresis
AMP	Adenosine Monophosphate
ATP	Adenosine Triphosphate
bp	base pair
BiFC	Bimolecular Fluorescence Complementation
BRET	Bioluminescence Resonance Energy Transfer
BSA	Bovine Serum Albumin
cAMP	cyclic AMP
CaCl2	Calcium chloride
CFP	Cyan Fluorescent Protein
cDNA	Complementary Deoxyribonucleic Acid
CNS	Central Nervous System
DAG	Diacylglycerol
D2R	Dopamine D2 Receptor
D-MEM	Dulbecco's Modified Eagle Medium
DMSO	Dimethyl sulfoxide
DNA	Deoxyribonucleic Acid
EDTA	Ethylenediamine tetraacetic acid
EGFP	Enhanced Green Fluorescent Protein

CHAPTER 1

INTRODUCTION

1.1 G-Protein Coupled Receptors (GPCRs)

G-Protein-coupled receptors (GPCRs) also known as seven-transmembrane domain receptors (7TM receptors), heptahelical receptors, serpentine receptors, and G-protein-linked receptors (GPLR) (Wu J. *et al.*, 2012). GPCRs belong to a large family of cell surface receptors that transmit extracellular signals including light, hormones and neurotransmitters to intracellular responses. These responses play role in major biological processes such as secretion, neurotransmission, growth, cellular differentiation and the immune response (Siehler S. *et al.,* 2007; Latek D. *et al.,* 2012, Wu J. *et al.*, 2012). Receptors in this protein family consist of three intracellular loops and three extracellular loops. Intracellular loops interact with G proteins; on the other hand extracellular loops have a role in ligand binding (Latek D. *et al.,* 2012).
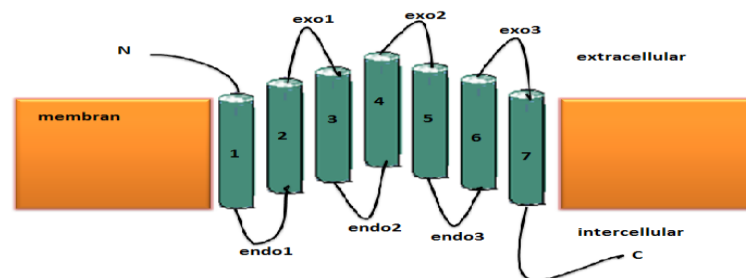
Figure.1.1 The image shows common structure of GPCRs. Transmembrane helices have been numbered 1-7. Intracellular loops have been called endo and extracellular loops called exo. (Taken from Flower D.R. 1999)

GPCRs contain three major receptor sub-families according to sequence similarities. These are class A including Rodopsin, adenosine, melanocortin, neuropeptide, olfactory, chemokine, and melatonin receptors; class B containing the gastrointestinal peptide hormone family (secretin, glucagon, vasoactive intestinal peptide); while class C covering metabotropic glutamate receptors (mGluR), the calcium-sensing receptor (CaSR), $GABA_B$ receptors, some potential taste receptors, and is characterized by a very long *N*-terminal domain (Schoneberg T. *et al.,* 2004)

In human genome over 1000 genes, encode G protein-coupled receptors (GPCRs) (Thomsen W. et al. 2005). This indicates that, GPCRs are one of the most diverse group of proteins in humans thus it is not surprising that nearly 30 % of the drugs in the market target these receptors (Oldham W. M. and Hamm E. H. 2008).

The intracellular region of GPCRs interact with heterotrimeric G proteins which are known as molecular switches that regulate secondary messengers and signaling proteins (Bhattacharyya R. and Wedegaertner B.P. 2000). When the agonist binds to GPCR at extracellular surface, structural changes in the receptor protein is believed to induce conformational changes in heterotrimeric G protein (αβγ) which would cause exchange of guanosine diphosphate (GDP), inactive form of G proteins, to guanosine triphosphate (GTP) bound active form. Activation of G proteins by catalyzing the exchange of GDP for GTP causes α subunit dissociation from βγ subunits and lead to effector protein modulation. This reaction cascade is very important for signal transduction inside the cell (Siehler S. *et al.,* 2007). Active G proteins mediate various cell signaling pathways by changing the function of downstream effectors including adenylyl cyclase, guanylyl cyclase, phospholipase C, and others (Purves D. *et al.,*1999) (See in Figure 1.2)
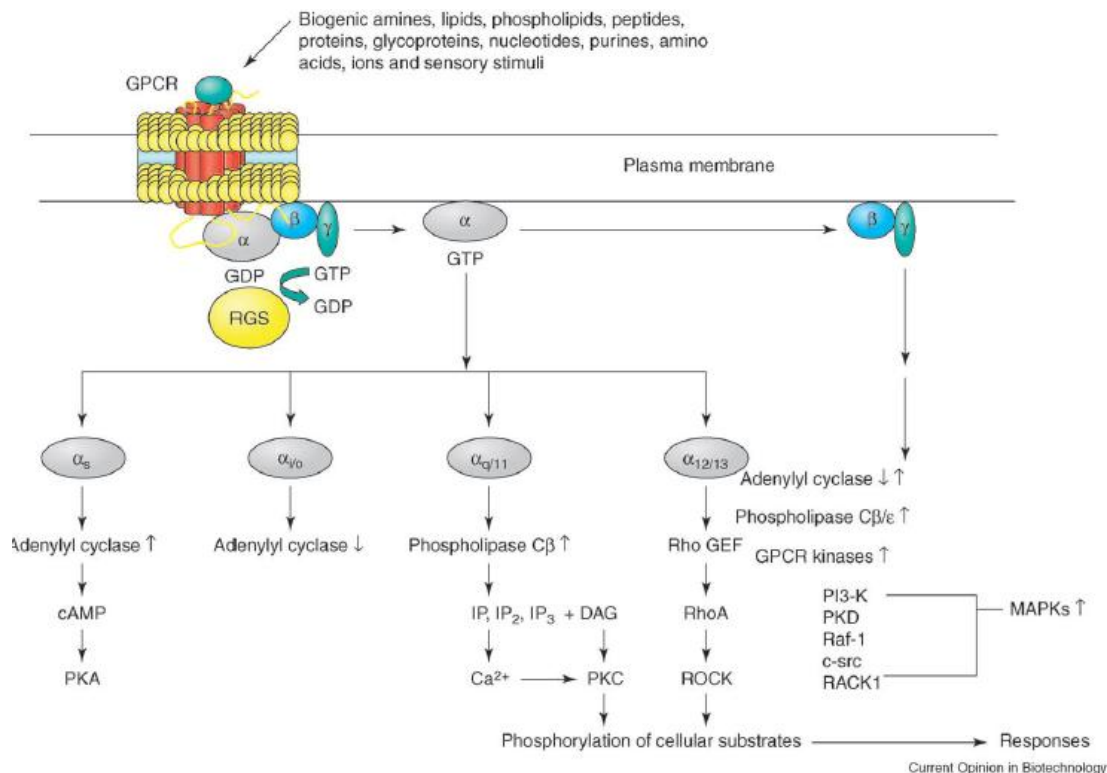
Figure 1.2 GPCR signaling pathways. Members of the $G\alpha_s$, $G\alpha_{i/o}$, $G\alpha_{q/11}$, $G\alpha_{12/13}$ subfamilies primarily act to stimulate different secondary messengers (Taken from Thomsen W. *et al.,* 2005)

1.1.1   Adenosine Receptors and Adenosine Signaling

Adenosine is an endogenic nucleoside generally created from degradation of adenosine triphosphate (ATP) and minor amount from S-adenosyl-L-homocysteine (SAH) metabolism (Ciruela F *et al.*, 2011). Adenosine is important for regulation of many physiologic actions such as platelet functions, coronary and systemic vascular tone, lipolysis in adipocytes. Also extracellular adenosine plays regulatory role in the brain including neuronal membrane potential, astrocytic function, neuronal viability,

propagation of action potentials and microglia reactivity. Since adenosine takes a part in

several functions, potential therapeutic use of adenosine has been increased over the last years (Sebastiao A.M. *et al*., 2000; Fredholm B.B.*et al*., 2005; Jacobson K.A. *et al*., 2006; Abbracchio M.P *et al*., 2009).

Adenosine acts via GPCRs called adenosine receptors which are grouped in to four subtypes; A_1, A_{2A}, A_{2B}, and A_3 (Ciruela F. *et al.* 2011). A_1 receptor is the most abundantly and homogeneously distributed adenosine receptor in the brain and mostly coupled with $G\alpha_{i/o}$ proteins which regulates adenylate cylase, Ca^{2+} and K^+ channels and phospholipase C (Palmer T.M., Stiles and G.L 1995; Dupre D.J *et al.,* 2006). On the other hand, A_{2A} receptor is highly expressed in some regions of the brain including, striatum, nucleus accumbens and olfactory tubercle (Fredholm B.B. 1995) and it generally interacts with $G\alpha_s$ in periphery and with $G\alpha_{olf}$ in the striatum to activate adenylyl cyclase (Marala R.B *et al.,* 1993). In human endothelial cells, it has been suggested that A_{2A} receptor signaling through $G\alpha_{12/13}$ proteins but it has not been shown experimentally (Feoktistov I. *et al.*, 2002). In addition, A_{2B} receptor mostly coupled to $G\alpha_s$ and $G\alpha_q$ proteins to activate adenylyl cyclase and PLC respectively (Ryzhov S. *et al.,* 2006) in human microvascular cells, A_{2B} receptor has a role in angiogenic factor expression via $G\alpha_q$, and possibly via $G\alpha_s$ (Feoktistov I. *et al.,* 2002). In contrast, it has been found that A_3 receptor inhibits adenylyl cyclase but promotes calcium mobilization via G protein $G\beta\gamma$ subunits' PLC activation (Jacobson K.A. *et al*., 2006).

Intracellular signal transduction occurs from receptors embedded in the cellular membrane to second messengers or protein kinases (Schulte G. 2002). Generally, Adenosine receptor signaling appear through adenylyl cyclase by inhibiting or stimulating the pathway, however it is also related with other pathways like phospholipase C (PLC), Ca^{2+} and mitogen-activated protein kinases (MAPKs) (Jacobson

A.K. and Gao Z.G 2006). Adenylyl cylase is a transmembrane protein with nine different isoforms that catalyzes the formation of cAMP from ATP. Gα, Gβγ and intracellular calcium influence these isoforms in different ways (Hanoune J. and Defer N. 2001). Thus, protein phosphorylation and calcium regulate cAMP by feedback loop. cAMP binds to regulatory domains of PKA, this release active subunits that phosphorylate cytoplasmic or nuclear targets like GPCRs, AC, ion channels, transcription factors (Schulte G. 2002).

Phospholipases have a role in phospholipid hydrolysis that activates secondary messengers. When PLCβ is activated by $Gα_{q/11}$ and Gβγ subunit; IP3 and DAG are released (Dickenson J.M. and Hill S.J., 1998). IP3 released to the cytoplasm and binds to its receptors on the endoplasmic reticulum which is an ion channel. This results in increased cytoplasm reticulum concentration which activates protein kinases, calmodulin or AC. When A_{1A} receptor is activated by pertussis toxin-sensitive G proteins, adenylyl cyclase activity is inhibited and as a result PLC activity is increased (Reid EA, *et al.*; 2005).

In the peripheral systems, $Gα_s$ is the major protein which is activated by A_{2A} receptor and increase adenylyl cyclase activity. However, in striatum where A_{2A} receptor concentration is higher, $Gα_{olf}$ is stimulated (Kull B. *et al.,* 2000). Moreover, via $Gα_{15}$ and $Gα_{16}$ proteins, A_{2A} receptors induce inositol phosphates formation that cause to increase intracellular calcium and activates protein kinase C. (Offermanns S. *et al.,* 1996). Similarly, A_{2B} receptors also activate adenylyl cyclase and PLC pathways via $Gα_q$ proteins. In mast cells, A_{2B} receptors are related to inositol phosphate formation and arachidonic acid pathways (Feoktistov I. *et al.,* 1995; Donoso M.V. *et al.*, 2005). On the other hand, A_{3A} receptors couple to secondary messengers that inhibit adenylyl cyclase but stimulate PLC and calcium mobilization. Also, A_{3A} receptors bind to MAPK that has

a role in cell growth, survival, death and differentiation (Jacobson A.K. and Gao Z.G 2006). Summary of adenosine receptor interaction according to subtypes is given in Table1.1.

Table 1.1 Summary of adenosine receptor subtypes, their interactions with G proteins and effects of signaling pathway.

Adenosine Receptor Subtypes	A_1	A_{2A}			A_{2B}		A_3	
G protein	$G\alpha_{i/o}$ $G\alpha_{12/13}$	$G\alpha_s$	$G\alpha_{olf}$	$G\alpha_{15/16}$	$G\alpha_s$	$G\alpha_{/11}$	$G\alpha_{i2,3}$	$G\alpha_q$
Effects of G protein coupling	↓cAMP ↑IP3/DAG (PLC) βy-mediated ↑Arachidonate (PLA2) {General, CHO cells} ↑choline, DAG (PLD) {DDT, MF-1} ↑K^+ channels {Atrial cells, neurons} ↓Q, P, N-type Ca^{2+} channels {Neurons}	↑cAMP {General}	↑cAMP {Striatum, CHO cells}	↑IP3 {COS-7 cells}	↑cAMP {General}	↑IP3/DAG (PLC) {Xenopus oocytes HMC-1, HEK-293}	↓cAMP {Neurons CHO cells} ↑IP_3/DAG (PLC) ßy-mediated {Neurons CHO cells} ↑choline, DAG (PLD) {Rat mast cells} ↑K^+-ATP channels {Cardiac cells} ↑Cl⁻ channels {Human cliary epithelial cells}	↑IP₃/DAG (PLC) {CHO cells}

1.1.1.1. Adenosine Receptor Oligomerization and A_1R/A_2R Heterodimerization

In recent studies, different biophysical techniques including resonance energy transfer (RET), like bioluminescence-RET (BRET) and Föster-RET (FRET) were used to detect receptor-receptor oligomerization (F. Ciruela *et al*., 2005).

A_1R and $A_{2A}R$ function via antagonistic signal transduction pathways. It has been suggested that dimerization of A_1R and $A_{2A}R$ shows molecular or functional cross-talk when they are part of the same molecular signaling complex. When $A_1R/A_{2A}R$ heterodimerize, A_1R affinity to its agonist and A_1R mediated calcium mobilization decline (Ciruela F. et al. 2011). Furthermore, A_1R and $A_{2A}R$ have distinct affinity for adenosine. When the adenosine concentration is low, the A_{1A} receptor stimulated primarily and glutamate release is inhibited. On the other hand, both $A_{2A}R$ and $A_{1A}R$ were activated primarily at high concentration of adenosine but $A_{2A}R$ stimulation abolishes the A_1R glutamate function (Fredholm B.B. *et al.,* 2001).

1.1.1.2. A_1 Receptor (A_1R) And Dopamine D_1 Receptor (D_1R) Oligomerization

It has been reported that adenosine dopamine interaction can inhibit effects of dopamine in cerebral cortex and basal ganglia. As it is seen in previous studies, after pretreatment with D_2R agonist, A_1R/D_1R heterodimerization disappears but when they are treated with D_1R and A_1R agonists, this result is not observed (Gines S. *et al.,* 2000). A_1R activation could adjust D_1R signaling such as activation of A_1R within heteromer that

effect dopamine binding characteristics to the D_1R. It has been suggested that A_1R/D_1R heteromer stimulation, may prevent receptor interaction that cause D_1R uncouple to $G\alpha_s$ protein (Ciruela F. *et al*. 2011).

Morphologically and functionally A_{2A} receptors are similar to D_1 receptors. Their third intracellular loop is short and they both have long acidic C-terminus. Thus in striatum, they both couple to G_{olf}. A_{2A} and D_1 receptors might be using the same epitope while interacting with D_2 receptor; which is sugested as a phosphorylated serine in the C-terminus (Surmeier D.J. 2007).

1.1.2. Dopamine Receptors and Dopamine Signaling

Dopamine is a major catecholamine plays an important role in Central nervous system functions such as attention and reward control, regulates locomotor activity, responsible from short-term memory and neuroendocrine secretion (Ciruela F. *et al.,* 2011; Jaber *et al.,* 1996). Dopaminergic neurotransmission dysfunction has been related with Central nervous system changes in stress condition and psychiatric, neurological disorders (Surmeier D.J. *et al.,* 1995). It also has an important role in hormone secretion, cardiovascular function and gastrointestinal modulation (Missale C. *et al*., 1998).

Dopamine receptors are divided into two classes according to their signaling pathway; D_1 like and D_2 like receptors. D_1 like receptors classified as D_1R and D_5R; D_2 like receptors including D_2R isoforms, D_3R and D_4R (Sedaghat K. *et al.,* 2006; Neve A.K. *et al.,* 2004). D_2R has short (D_2S) and long (D_2L) isoform. D_2S is differ from D_2L form with its 29 amino acid insertion in the third cytoplasmic loop (Sedaghat K. *et al.,* 2006). The detailed information about Dopamine receptor subtypes and location summarized in **Table1.2.**

Table 1.2 Summary of dopamine receptor subfamily and their location (adapted from Vallone 2000 and Ares-Santos S. 2013)

		Receptor subfamily	Location
D1like receptor	Adenylyl ↑ cyclase	D1R	CP, nucleus accumbens, OT, cerebral cortex and amygdala, subthalamic nucleus.
		D5R	Hippocampus, lateral mammillary nucleus and in the thalamus.
D2like receptor	Adenylyl ↓ cyclase	D2R	CP, OT, nucleus accumbens substantia nigra pars compacta. Also in Retina, kidney, vascular system and pituitary gland.
		D3R	Island of calleja, hypothalamus, thalamus and cerebellum.
		D4R	Frontal cortex, amygdala, olfactory bulb, hippocampus, hypothalamus and mesenchephalon.

D_1-like receptor subtypes regulate cyclic AMP (cAMP) level positively and stimulation of these receptors activates protein kinase A (PKA) that phosphorylates cytoplasmic and nuclear proteins (Vallone D. *et al.,* 2000). D_1 receptor affects intracellular Ca^{2+} stores by cAMP pathway without stimulating phosphoinositide (PI) hydrolysis. On the other hand, D_2R was first described as intracellular cAMP inhibitor in pituitary gland and striatal cells. D_3R and D_4R are also inhibitor of cAMP level in lots of cells but D_3R, inhibit AC less than D_2R (Missale C. *et al.,* 1998).
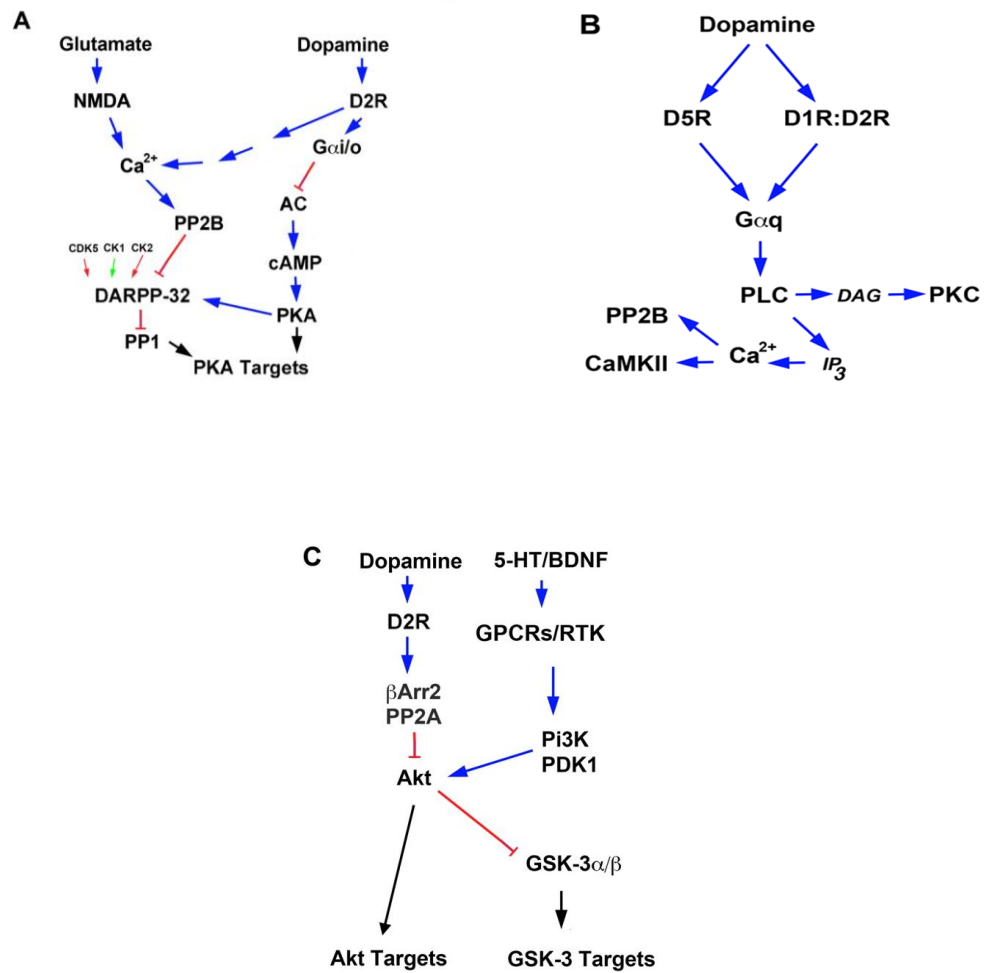
Figure 1.3 Signal pathway regulated by D_1 and D_2 like family (adapted from Beaulieu J.M. *et al.*, 2011).

It has been reported that D_1 like receptors are couple to $G\alpha_s$ that stimulate adenylate cyclase (Neve A.K *et al.*, 2004). D_2R reduces N-type Ca^{2+} in rat neostriatal cholinergic interneurons via coupling to $G\alpha_{i/o}$ protein. On the other hand, D_2R modulate intracellular

Ca^{2+} levels important for DA biosynthesis. Like D_2 receptors, D_4 activates G proteins such as $G\alpha_{i2}$, $G\alpha_{i3}$ and $G\alpha_o$ (Liu LX. *et al.*, 1999; Taraskevich PS. *et al.*, 1990).

Moreover, D_4 receptor couples to $G\alpha_z$ and $G\alpha_{t2}$ (Obadiah J. *et al*., 1999). D_3R, which is the member of D_2 like receptors signal via $G\alpha_o$, $G\alpha_z$ and $G\alpha_{q/11}$ with regard to different cell types (Neve A.K *et al.,* 2004). $G_{q/11}$ also interacts with D_1 like receptors and activates phospholipase C (PLC) and intracellular calcium release (Rashid A.J. *et al.,* 2007). Dopamine receptor interaction mediates different pathways. While D_2 receptors coupled to $G\alpha_{i/o}$ and inhibit adenylyl cyclase, D_1/D_2 heteromer formation interacts with $G_{q/11}$ and regulates PLC signaling (Ferré S. *et al*., 2008; Lee S.P. *et al*., 2004).

1.1.2.1 Adenosine 2 (A2AR) And Dopamine D2 Receptor (D2R) Oligomerization

The adenosine A_{2A} receptor ($A_{2A}R$) and dopamine D_2 receptor (D_2R) are coexpressed in the striatum of the basal ganglia especially localized in (GABA)-containing neurons. These neurons have an important role in the basal ganglia disorders, like Parkinson's disease (Canals M. *et. al.,* 2003).

It has been reported that, there is a relationship between $A_{2A}R$ and D_2R at biochemical, functional and behavioral levels. $A_{2A}R$ and D_2R have an antagonistic interaction modulating dopaminergic activity in the striatum or in cell lines (Kamiya T. *et. al.,* 2003). This interaction occurs between the third intracellular loop (3IL) of the D_2R and C terminal tail of $A_{2A}R$. Third intracellular loop (3IL) of the D_2R has a positively charged arginine rich motif interacting with negatively charged motif located at C-terminal tail of the $A_{2A}R$ (Woods A.S., *et al*. 2005). Stimulation of D_2R inhibits cAMP accumulation. However, cAMP is increased by the stimulation of $A_{2A}R$ through

$G\alpha_{s/olf}$ proteins. When D_2R interacts with $A_{2A}R$ (D_2R/A_2 Heterodimer); D_2R switches coupling to $G\alpha_{q/11}$ protein signaling (Ciruela F. *et al*. 2011).

1.2   GTP-Binding Proteins

The heterotrimeric guanine-binding proteins known as G proteins have roles as signal transducers. They take many signals from GPCRs triggered by different hormones, neurotransmitters chemokines, autocrine and paracrine factors and transfer signals to different intracellular pathways that regulate broad range of cellular metabolic effectors such as enzymes, ion channels, transporters, and activities like transcription, motility and secretion. These metabolic processes also affect systemic functions including embryonic development, gonadal development, learning and memory (Neves R.S.*et al*., 2002).

There are two general classes of GTP-binding proteins; heterotrimeric and monomeric G-proteins. Heterotrimeric G proteins are consisting of three different subunits (α, β and γ). α subunit binds to guanine nucleotides GTP or GDP. Similarly, monomeric G-proteins also called as small G-proteins transmit signals from activated cell surface to intracellular targets like the vesicle trafficking apparatus (Purves D. *et al.*, 2001).

1.2.1. Classification and Molecular Structure of Heterotrimeric G proteins

There are 16 different Gα subunit genes identified in mammalian cells (Cabrera-Vera *et al.,* 2003). They interact with different combinations of 5 Gβ and 12 Gγ subunits (Nina

Wettschureck and Stefan Offermanns 2005). Gα subunit of heterotrimeric G proteins is divided into four families based on the homology of their amino acid sequences: $G\alpha_s$, $G\alpha_i/G\alpha_o$, $G\alpha_q/G\alpha_{11}$, and $G\alpha_{12}/G\alpha_{13}$ (Siehler S. *et al*. 2007).

Gα subunits consist of two domains; that are Ras-like GTPase domain and α-helical domain. Ras-like GTPase domain has a role in binding and hydrolysis of GTP. All

members of G protein superfamily have Ras-like GTPase domain which has 6-stranded β sheet surrounded by 6α-helices. G-1 to G-5 regions are necessary for GDP/GTP Mg^{2+} binding and exchange. G-1/P loop is phosphate-binding loop that bind to guanine nucleotide phosphate groups. G-2 sequence has threonine residue containing Mg^{2+} cation. Also, G-3 has Mg^{2+}/β-phosphate-binding motif; G-4 and G-5 are guanine binding sites (Rens-Domiano and Hamm, 1995).

G protein's α-helical domain has an arginine residue that cause to increase intrinsic GTP hydrolysis. When there is a mutation of this residue, oncogenic symptoms occur, because GTP-bound structure remains and G protein stays in the active (Scheffzek *et al.*, 1997).

The 3D structure of Gα protein shows that guanine nucleotide is located between α-helical domain and the GTPase domain. Switch regions helps the molecule conformational change (figure 1.4 A) (Warner and Weinstein, 1999).

Gγ subunits are small polypeptides that are nearly 7-9 kD and contain two α-helices connected by a loop so it's hard to make long-range intramolecular connection. On the other hand it can interact strongly with Gβ subunit which is about 35-39kD weight, bind to N-termini as a parallel coiled-coil formed not by covalent manner (figure 1.4 B) (Garritsen *et al.*, 1993, Clapham and Neer, 1997).

A   **B**
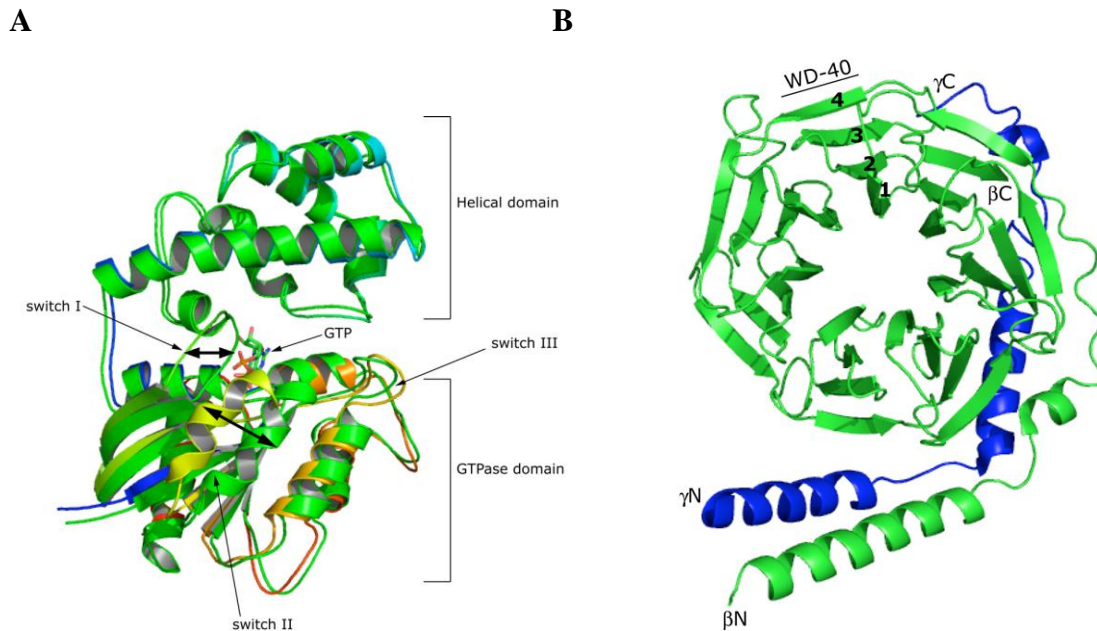
Figure 1.4 The crystal structure of Gα subunits. The arrows show switch regions of the protein (A). The crystal structure of Gβγ subunits. Gβ is colored green and Gγ is colored blue (B) (Hermans M.J.W 2008).

In our study, the information about molecular structure of Gα protein was used to decide tagging region. RCSB PDB (protein databank), Swiss-Model Expasy and NCBI computer programs helped us to see 3D structure of Gα protein.

1.2.2. Membrane Localization of G-Proteins

Gα proteins are subjected to co-translational or post-translational lipid modifications such as myristoylation and/or Palmitoylation at the N termini. These lipid modifications play an important role in acting as hydrophobic anchors for G proteins membrane localization (Marrari Y.*et al*. 2008). Myristoylation is a 14 carbon myristate attachment to glycine via amine bond which is a reversible co-translational attachment

(Bhattacharyya R. and Wedegaertner B.P. 2000; Suzuki N. *et al*. 2009). Gα subunits that have MGxxxS/T can be myristoylated by N-Myristoyl Transferase (NMT) like $Gα_t$. However, myristoyl group does not trigger high affinity for plasma membranes. That is why $Gα_t$ cannot bind tightly to the membrane. On the other hand Palmitoylation is a 16 carbon palmitate attachment to cysteine residues through thioester bond and it is a reversible post-translational modification. Palmitoylated Gα's contain cysteine residue is a substrate for palmitoyl transferase enzyme (Hallak *et al.*, 1994). $Gα_t$ is modified by only myristoylation; $Gα_i$, $Gα_o$ and $Gα_z$ are both myristoylated and palmitoylated; $Gα_s$ and $Gα_{12}$ are singly, $Gα_{13}$ and $Gα_q$ are dually palmitoylated (Yamazaki J. *et al*. 2005).

It has been reported that palmitoylation of $Gα_{13}$ is important for its association with the plasma membrane, interaction of Rho A and movement of effector protein p115RhoGEF; (Suzuki N. *et al.* 2009). It has been observed that mutations of palmitoylated cystein residues in $Gα_q$ $Gα_{11}$ and $Gα_{12}$ result in detection of Gα protein in soluble fractions and also partially or complete loss of signal (Wise A. *et al.,* 1997). The immunofluorescence microscopy experiment with palmitoylation deficient single cystein mutants (C14S, C18S); double cystein mutants (C14S and C18S) of $Gα_{13}$ showed no observable plasma membrane staining but displayed a spread out cytoplasmic staining (Bhattacharyya R *et al.*, 2000).

In addition studies, report mutations that prevent binding of Gα to Gβγ, disturb Gα subunits' membrane association. Though Gα subunits are modified by palmitoylation, this is not enough for a stable membrane association due to the Gα-Gβγ binding mutations. Therefore for successful Gα membrane localization both lipid modifications and Gβγ association are required (Michaelson D. *et al.* 2002).

1.2.3 G-protein Signal Pathways

Most of the G protein pathways' connections have been investigated via biochemical studies. Distinct extracellular signals through different types of receptors transmit to specific G proteins. For example: Epinephrine's signal is carried through the β-adrenergic receptor bind to $G\alpha_s$, while the α2- type of adrenergic receptor binds to $G\alpha_i$ and α1- type couples with $G\alpha_q$ or $G\alpha_{11}$ (see in Figure 1.5).
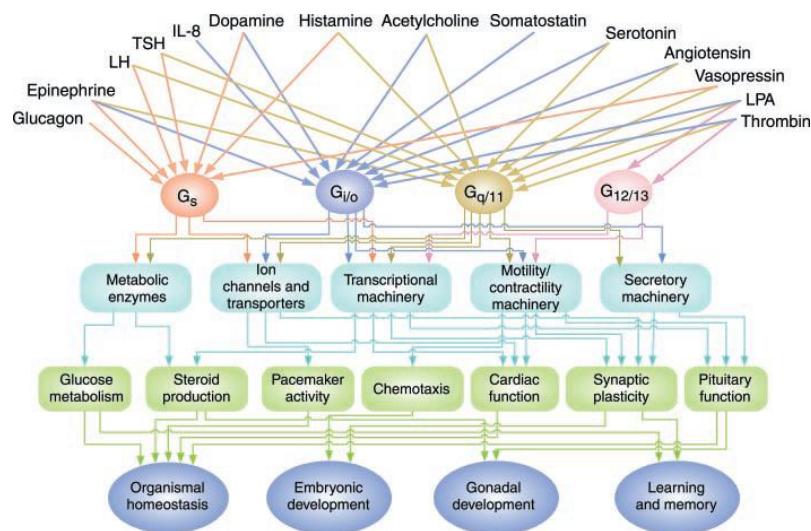
Figure 1.5 The cascade representing different types of signals transmit throug receptors interacted with distinct G proteins to produce many cellular responces (Taken from Nina Wettschureck and Stefan Offermanns 2005).

The broadly expressed G protein families $G\alpha_i/G\alpha_o$. $G\alpha_{i1}$, $G\alpha_{i2}$ and $G\alpha_{i3}$ are the members of this family has a role in inhibition of different kinds of adenylyl cyclases (Nina Wettschureck and Stefan Offermanns 2005). $G\alpha_i$ name was given due to the ability of inhibition of adenylyl cyclase. $G\alpha i/G\alpha o$ pathway is used by lots of hormones and

neurotransmitters such as epinephrine, serotonine, acetylcholine and dopamine. This pathway can be inhibited by pertussis toxin that catalyzes adenosine diphosphate ribosilation of G protein α subunits. Therefore it prevents the interaction of Gα subunits and the receptor (Neves R.S.*et al.*, 2002). In addition, in this pathway Gβγ can couple to different effector molecules and activate MAPKs. These effectors include PLC-β, K^+ channels, adenylyl cyclase and phosphatidylinositol 3 kinase (PI3K). M2 muscarinic receptor couples to $G\alpha_i$ and it release Gβγ subunit which activates K^+ channels. Also $G\alpha_i$ and $G\alpha_o$ can regulate signals from c-Src to STAT3 and rap pathways (Ram P.T. and Iyengar R. 2001).

On the contrary, $G\alpha_s$ protein activates adenylyl cyclases, thus intracellular cAMP levels and the activity of the cAMP-dependent protein kinase (PKA) increase. Also it signals to activation of mitogen activated protein kinase (MAPK) (Siehler S. *et al.* 2007, Neves R.S.*et al.*, 2002).

Studies showed that, when $G\alpha_q$ family protein is stimulated by calcium-mobilizing hormones, it activates PLC-β and produces inositol three phosphates (IP3) that help to release calcium from intracellular stores. Also $G\alpha_q$ activates transcription factor NF-kB through PYK2 C (Shi S. and Kehrl J. H., 2001).

$G\alpha_{12/13}$ family has two proteins $G\alpha_{12}$ and $G\alpha_{13}$ with high sequence similarity. $G\alpha_{12}$ interacts with GTPase-activating protein to stimulite Ras, RasGap and Bruton's tyrosine kinase (Btk) (Jiang Y. *et al.*, 1998). It is not well understood but suggested that $G\alpha_{12}$ can stimulate phospholipase C, c-Src and PKC. Extracellular signal-related kinase 5 (ERK5) and c-jun NH2-terminal kinase (JNK), which are MAPK family members are also activated by $G\alpha_{12}$ pathway and effect the regulation of gene expression (Neves R.S. *et al.*, 2002).

Gα$_{13}$ is coupled to lysophosphatidic acid (LPA) and thromboxane A2 receptors. Gα$_{13}$ activates Rho and it triggers regulation of the Na+-H+ exchanger. It has been suggested that Gα$_{13}$ may activate PI3K pathway which stimulates the activation of Akt and regulation of NF-kB (S. Shi and J. H. Kehrl, 2001). Also, Monomeric GTPase RhoA is activated by the Gα$_{12/13}$ family (Siehler S. *et al.* 2007).

Table 1.3 Classification of Gα-subtypes and their effectors (Adapted from Cabrera-Vera M.T. *et al*., 2003 and Milligan G. and Kostenis E. Heterotrimeric 2006)

Family	Subtype	Effector
G_s	$G\alpha_{s(S)}$	↑ AC
	$G\alpha_{s(L)}$	↑ GTPase of tubulin ↑ src
	$G\alpha_{s(olf)}$	↑ AC
G_i	$G\alpha_{i1}$	↓ AC
	$G\alpha_{i2}$	Rap 1 GAP
	$G\alpha_{i3}$	GRIN 1 and 2
	$G\alpha_{oA}$	↑ GTPase of tubulin
	$G\alpha_{oB}$	↑ src
	$G\alpha_z$	Ca^{2+} and K^+ channels
	$G\alpha_{t1}$	↑ cGMP-PDE
	$G\alpha_{t2}$	unkown
	$G\alpha_g$	unknown
G_q	$G\alpha_q$	↑ PLCβs
	$G\alpha_{11}$	↑ Bruton's tyrosine kinase ($G\alpha_q$)
	$G\alpha_{14}$	↑ Bruton's tyrosine kinase
	$G\alpha_{15}$ or $G\alpha_{16}$	↑ K channels
$G_{12/13}$	$G\alpha_{12}$	↑ NHE-1 ↑ PLD
	$G\alpha_{13}$	↑ p115RhoGEF ↑ iNOS

1.2.3.1 Signaling Through Gα_{11} Protein

Gα_q family consists of Gα_q, Gα_{11}, Gα_{14}, G$\alpha_{15/16}$ (mouse/human orthologues) proteins and control the homeostatic process in digestive, urinary, cardiovascular and central nervous system. Thus, they activate various pathways that include mitogen activated protein kinase (MAPK) and phosphatidylinositol-3-kinase (PI3K)/AKT pathways (Massotte, D., 2015). This G protein family activates phospholipase C (PLC) β isoform. It catalyzes phosphatidylinositol bisphosphate hydrolysis to generate inositol trisphospate (IP 3) and diacylglycerol (DAG) (Mizuno N. *et al.* 2009). Because of IP3 activation, Ca^{2+} ions flux from highly concentrated internal ER stores to low concentrated intracellular cytoplasmic region through channel gating (Massotte, D., 2015). These secondary messengers regulate intracellular Ca^{2+} transportation to stimulate different cellular event via various signaling (Mizuno N. *et al.* 2009).

Another protein that Gα_q interacts with is regulator of G protein signaling (RGS) proteins. They interact via their RGS domain and increase GTPase activation. One of RGS protein subfamily is B/R4 whose members are small proteins including RGS1, RGS2, RGS3, RGS4, RGS5, RGS8, RGS13, RGS16, and RGS18 (Bansal G. *et al.* 2007). Many of them interact with Gα_q family and inhibit inositol lipid/Ca^{2+} signaling. RGS4 protein acts as a GAP by stimulating GTP-ase activation and blocked MAPK activation by bombesin which is G$\alpha_{q/11}$-coupled receptor agonist (Yan Y., *et al*. 1997). Like G$\alpha_{12/13}$ family members, G$\alpha_{q/11}$ is activators of RhoA. However, G$\alpha_{12/13}$ and G$\alpha_{q/11}$ follows different pathways to convey signals from RhoGEFs to RhoA (Fukuhara S *et al*., 1999). Additionally, G$\alpha_{q/11}$ proteins interact with group 1 metabotropic glutamate, M1, M3, M5 muscarinic acetylcoline, 5HT2 serotonergic, α_1 adrenergic, vasopressin, angiotensin II and histamine receptors among other GPCRs (Massotte, D., 2015).

1.2.3.2 Signaling Through G$\alpha_{12/13}$ Protein

Gα_{12} and Gα_{13} proteins that belong to G12 protein family identified in 1991 and share 67 % amino acid sequence identity (Siehler S. 2007). Although these proteins have high percentage of sequence similarity, they can show different response to different agonists and act on distant pathways due to little (16%) similarity of N terminal sequence homology (Williams J. A. 2011).

Gα_{12} interacts with HSP90 and protein phosphatase 2A but Gα_{13} does not (Vaiskunaite R. *et al*. 2001; Zhu D *et al*. 2004). In contrast, Gα_{13} couple to PYK2 however; Gα_{12} doesn't interact with it (Shi C.S. *et al*. 2000). Also Gα_{12} and Gα_{13} follow different Na^+/H^+ exchange pathways (Yamazaki J. *et al*. 2005).

Recent studies showed that Gα_{12} deficient mice are alive without any significant defect, but Gα_{13} protein deficient mice embryos die because of defect in angiogenesis (Offermanns S. *et al.* 1997). This was supported by another study that Gα_{13} protein has a role in the regulation of endothelial cell shape, movement or the interaction of endothelial cells (Worzfeld T. 2008).

Gα_{12} acts in cell-cell interactions, invasion and differentiation (Kelly P. *et al.* 2006). Active G$\alpha_{12/13}$ has a role in inhibition of cadherin-induced aggregation, activation or inhibition Na^+/H^+ exchange, stimulation of smooth muscle contraction, and effect of secretion. Also they are important for platelet activation, cardiovascular function and immune function (Williams J. A. 2011). According to recent studies, developmental defect of nervous system was observed in the lack of Gα_{12}/Gα_{13} and over migration of cortical neurons in particular region is shown in Gα_{12} and Gα_{13} knockout glial and neuronal cells (Moers, A. *et al*. 2008).

Gα_{12}/Gα_{13}-family proteins are important in immune system development, thymocytes, apoptosis, proliferation and cell-cycle progression. Gα_{12} is involved in activation of Bruton's tyrosine kinase protein which has a role in B-cell maturation (Worzfeld T. *et al*. 2008). It has been observed that Gα_{12} and Gα_{13} proteins also related with cancer. Over expression of these proteins stimulates cellular transformation and high expression levels of these proteins are found in many human cancer cell lines and human cancer tissues (Kelly, P. *et al*. 2006). Though it is still unclear, stimulation of RhoA activates mitogen-activated protein cascade. It is important for c-jun and cellular transformation (Yasenetskaya V. *et al.* 1996). Furthermore, Gα_{12} and Gα_{13} have a role in cell adhesion and migration, which is supported by the study with breast cancer cell lines. This study revealed that active Gα_{12} blocks E- cadherin-mediated cell-cell adhesion breast cancer cell lines. Also inhibition of G$\alpha_{12/13}$ pathway can be used for therapeutic applications in cardiovascular diseases because blocking of this signaling pathway causes reduction of arterial hypertension or reduce platelet-dependent thrombosis (Worzfeld T. *et al*. 2008).

This G protein family conveys signals from GPCRs to induce various biological responses such as stress fiber formation, focal adhesion assembly, neurite retraction induction and transformation of fibroblasts by means of Rho activation (Yamazaki J. *et al*. 2005).

RhoGAPs, RhoGTPase nucleotide exchange factors (RhoGEFs) and Guanine nucleotide dissociation inhibitors (GDIs) regulate activation of RhoA (Siehler S. 2007). GTPase activating proteins (GAPs) regulate G protein signals as accelerating G protein inactivation or enhancing G protein function (Siehler S. *et al*.2009). RhoGDI covers the geranyl residue on the C terminus of RhoA. This molecular group is important for

membrane attachment. Thus, RhoGDI causes to remove RhoA from membrane and it

inhibits GTPase cycling (Siehler S. 2007). Regulator proteins of Gα$_{12/13}$ are RhoGEFs which are known as PSD-95/Disc-large/ZO-1 homology (PDZ)-RhoGEF, leukemia-associated RhoGEF (LARG) and lymphoid blast crisis (Lsc)-RhoGEF or (p115-RhoGEF). Lymphoid blast crisis (Lbc)-RhoGEF is activated by only Gα$_{13}$ protein but others are activated by both Gα$_{12}$ and Gα$_{13}$ (Worzfeld T. *et al*. 2008; Fukuhara S. *et al*. 2001). Regulator proteins bind Gα$_{12/13}$ via their RGS domain to activate them and stimulate guanine nucleotide exchange factor (GEF) activity. RhoGEFs change GDP to GTP and thus small monomeric GTPase trigger RhoA to become an active formation. In addition, oligomer form of RhoGEF are not able to interact with RhoA (Worzfeld T. *et al*. 2008; Siehler S. *et al*. 2009) (**Figure 1.6).**
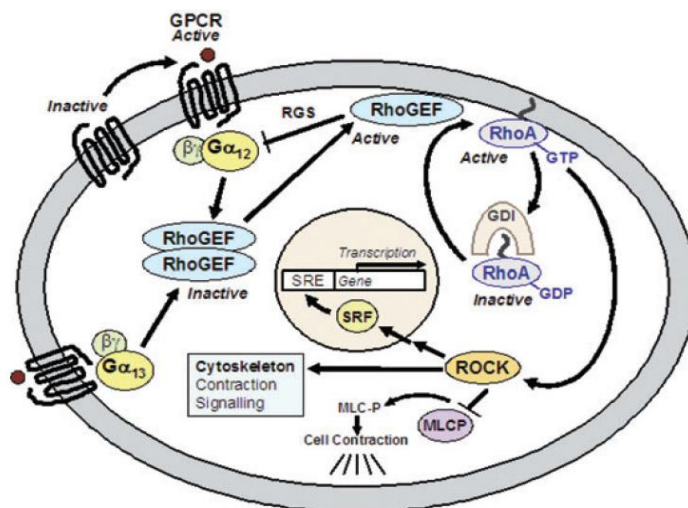
Figure 1.6 Representative image shows Gα$_{12/13}$ proteins intracellular pathway through RhoGEF proteins (Taken from Siehler S. *et al*.2009).

Gα$_{12}$ and Gα$_{13}$ transmit signals through Ras, Rac, Rho, and CDC42 (Cell Division Cycle-42) dependent pathways. These are crucial proteins for cytoskeletal

reorganization, activation of MAPK (Mitogen-Activated Protein Kinase), JNK (Jun N-

terminal kinase), Na^+-H^+(sodium/hydrogen) exchanger, c-Fos, SRE (Serum Response Element) and transcriptional activation of specific primary response genes (Dhanasekaran N. *et al.,* 1996). SRE (Serum Response Element) has a role in transcription of the cytoskeletal and cell cycle entry (Gilchrist A., *et al*., 2002).

Also, $G\alpha_{12/13}$ proteins couple to GPCRs which are purinergic receptors, M1 and M3 muscarinic acetylcholine receptors, receptors for thrombin (PAR-1, PAR-2), thromboxane (TXA2), sphingosine 1-phosphate, lysophosphatidic acid, angiotensin II, serotonin, somatostatin, endothelin, cholecystokinin , V1a vasopressin receptors, D_5 dopamine receptors, A1 adenosine receptors, a1 adrenergic receptors, BB2 bombesin receptors, B2 bradykinin receptors calcium-sensing receptors, KSHV-ORF74 chemokine receptors, receptors and thyroid-stimulating hormone (TSH) receptors (Siehler S. 2009). Many of these receptors interact with only $G\alpha_{12/13}$ protein family. On the other hand, a few receptors also coupling to $G\alpha_{q/11}$ and $G\alpha_i$ proteins (Worzfeld T. 2008).

1.3 GPCRs Oligomerization Detection Methods

In early studies, receptor oligomerization has been detected by using co-immunoprecipitation techniques (Cabello *et al.*, 2009). However, this technique has some disadvantages; such as false positive results due to lack of actual physical contact, necessity of purifying from native environment, non-specific aggregation, harsh and stringent solubilization. These can affect protein oligomerization results (Dziedzicka-Wasylewska *et al.*, 2006). Recently, receptor-receptor interaction experiments have been continued by several approaches; like, protein-protein interaction assays and non-invasive light resonance energy transfer based methods. The most powerful techniques to investigate GPCR dimerization are Bioluminescence resonance energy transfer (BRET), Förster resonance energy transfer (FRET) and bimolecular fluorescence

complementation assay (BiFC) methods (Gandia J. *et al.,* 2008).

1.3.1 Fluorescence (Förster) Resonance Energy Transfer (FRET)

Förster resonance energy transfer (FRET) is a physical process that energy is transferred from excited molecular fluorophore (donor) to acceptor through non-radiative intermolecular long range dipole-dipole coupling. FRET occurs when the molecules are less than 10-100Å apart and donor-acceptor positions are within Förster Radius (the distance when the donor's half of energy is transferred to acceptor, 3-6 nm) (Sekar and Periasamy 2003). It is a kind of quantitative light microscopy technique that provides to detect submicroscopic molecular interaction within cells and organisms (Broussard J.A. *et al.*, 2013).

The GFP (The green Fluorescent protein) from *Victoria aequoria* has been used for discovering the expression and interaction of the proteins which are tagged with this fluorescent molecule. There are many variants of Fluorescent proteins that were generated by site directed mutations. Pairs of these fluorescent proteins could be used as fluorescent resonance energy transfer (FRET) partners (Milligan *et al.*, 2005). To select FRET pairs, there are several properties that has to be carried to obtain efficient energy transfer; for example, the overlap between the emission spectrum of donor and the excitation spectrum of the acceptor must be high (>30%) and reasonable separation in emission spectra between donor and acceptor leads to each fluorophore to be measured independently (Pollok and Heim. 1999). In addition, the FRET experiments may produce background signal that could be refered as a FRET bleedthrough. Spectral

overlap between donor and acceptor emission spectra must be controlled to prevent appropriate FRET signal (Milligan *et al.*, 2005).

26
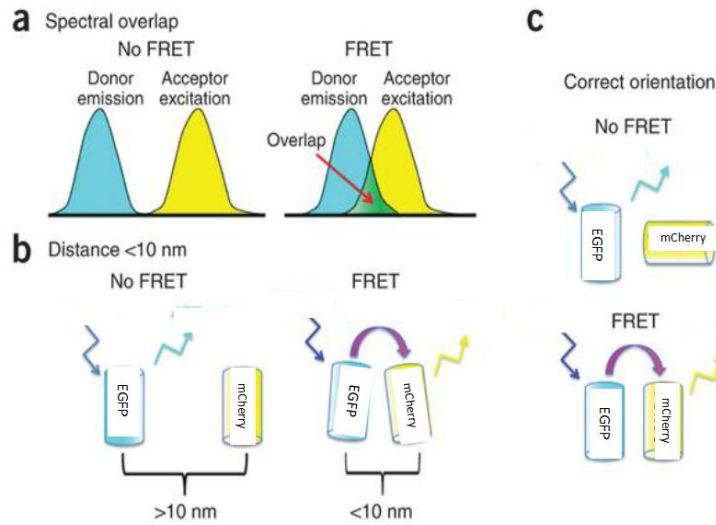
Figure 1.7 Different conditions about FRET occurance. Spectral overlap (a) Distance (b) and correct orientation (c) (adapted from Broussard *et al.*, 2013).

FRET occurs when two fluorophores are in close proximity, usually less then 100 Å. The overlap between emission spectrum of the donor molecule and excitation spectrum of the acceptor molecule must be high enough to optain a good FRET pair. Moreover, donor and acceptor molecules must be oriented properly for the dipole-dipole interaction to occur (Milligan & Bouvier, 2005).

The optimal quantitative determination of FRET between pairs could be measured by determining the FRET efficiency as energy transfer includes electromagnetic dipolar interactions and efficiency inversely related to sixth power of the distance which separates fluorophores. Thus this is shown by Förster equation and calculated with the formula as shown below (Day and Davidson 2012).

$$E = \frac{R_0^6}{R_0^6 + r^6}$$

R0: Förster distance, the separation distance between specific donor and acceptor where energy transfer is 50 % efficient. Due to the sixth power relationship, FRET efficiency can decrease strongly when separation distance increase. It bases on the spectral properties of specific donor and acceptor.

r: is the donor-to acceptor distance (Day and Davidson 2012)

Cyan (CFP) and yellow (YFP) emitting fluorescent proteins were used as a FRET pair in many studies, but this pair has a lot of crosstalk between donor and acceptor. On the other hand in some studies EGFP and mCherry were used as FRET pairs. EGFP, which is a modified version of GFP protein, is used as FRET donor because of its brightness and large stoke shift. Moreover, mCherry protein that was first produced from DsRed (red fluorescent protein) has large absorption cross section and high photo stability properties. Thus it has been used efficiently as a good FRET acceptor (Albertazzi *et al.*, 2009).

Although a spectral overlap is necessary for FRET, it could generate crosstalk signal mixing with the acceptor emission channel. This occurs because of direct excitation of the acceptor by donor excitation wavelength.
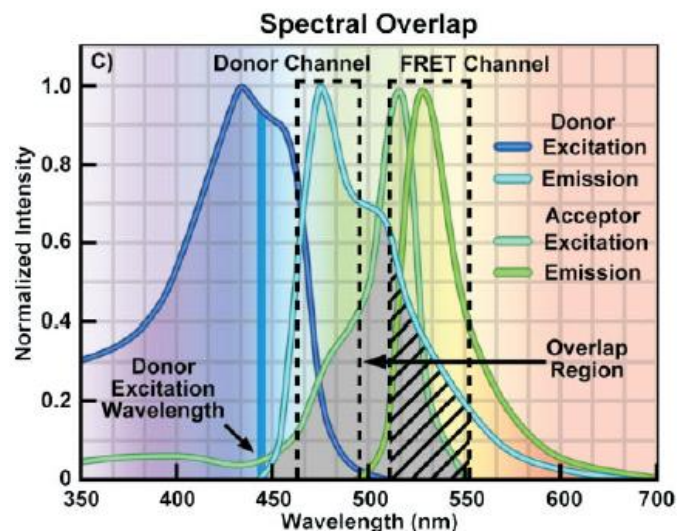
Figure 1.8 The excitation and emission fluorescence spectrum for donor and acceptor is shown. Spectral overlap between the donor emission and acceptor excitation (shaded region). FRET detection Channels are shown by dashed boxes. The arrow indicates overlap region (adapted from Day and Davidson 2012).

FRET technique can be used for studies focusing on protein dimerization/oligomerization, protein-protein interaction in live cells (Milligan and Bouvier 2005) and also used for protein structure, conformation, hybridization, and automated sequencing of nucleic acids.

Although FRET has been used in many different studies, it has some limitations. For instance, fluorophores should interact with accurate sites of molecule; otherwise nonspecific interactions may affect FRET signals. The wavelength which excite donor molecule, may also excite the acceptor; thus noise signal can be produced and influence FRET calculations (Day *et al*., 2001).

29

1.3.2. Bimolecular Fluorescence Complementation Assay (BiFC)

The bimolecular fluorescence complementation assay (BiFC) technique could be used for visualization of protein complexes and interactions in live cells and organisms. In this method, the non-fluorescent fragments of fluorescent protein can associate and create a fluorescent complex (Kerppola, T. K. 2006). When the proteins under question fused with fragments and the proteins interact with eachother the non-fluorescent fragments of fluorescent protein will come in to close proximity thus can regain the fluorescent property. This fluorescent signal shows occurrence of target proteins interaction and location (Kerppola, T. K. 2008). The principles of BiFC assay is shown in **Figure 1.9.**
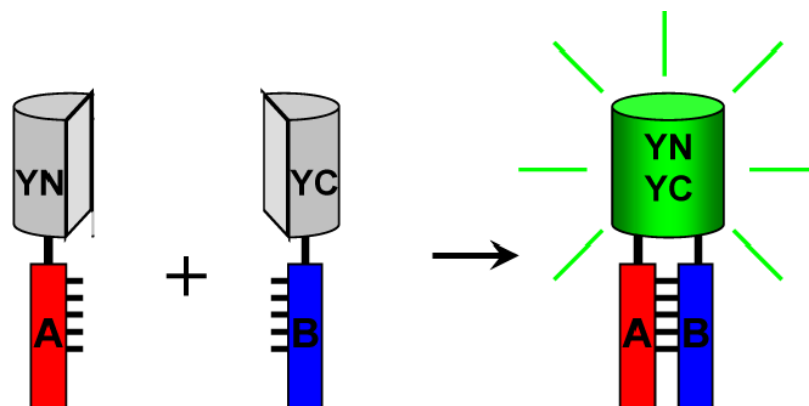
Figure 1.9 Shematic image of bimolecular fluorescence complementation assay (BiFC). It is based on two fragments association. In the image, fragment fused A and B proteins' interaction is shown. When the proteins interact, non-fluorescent fragments are brought together and fluorescent signal occurs (Hu *et al.,* 2002).

Recently this technique has been used for determining the membrane topology and effects of small molecules on protein complexes (Zamyatni *et al.,* 2006). Most methods like co-purification and affinity precipitation assays are not enough for detection of

protein interaction in their native environment as they require removal of proteins from the cell. The most preferred methods for studying protein interaction are FRET, BiFC, fluorescence correlation spectroscopy and image correlation spectroscopy (Kerppola 2006).

However, there are some limitations of BiFC method; Firstly time limitation is a problem. The fluorophore formation occurrence takes time and it can prevent real-time detection of rapid changes in interactions (Demidov *et al.,* 2006). Also, this complex formation can be reversible in protein degradation conditions and this also cause to decreasing of fluorophore signal. Additionally, fragments may prevent or change the function and structure of target protein. Thus, fragment fused proteins which has improper orientation may not complement each other. This could leads to false negatives where fluorescent signal cannot be detected although there is an interaction.

1.4. Aim of Study

Adenosine 2A (A_{2A}) and Dopamine 2 (D_2) receptors are G-protein coupled receptors (GPCRs) which oligomerize in neuron cells. A_{2A} and D_2 receptors signal through G proteins that stimulate or inhibit different pathways. Interaction of G proteins with these receptors is important to explain physiologycal and pharmacological approachs more detail.

Our aim is to optimize the labeling protocol of $G\alpha_{q11}$, $G\alpha_{12,}$ $G\alpha_{13}$ proteins and to detect interaction of $G\alpha_{12/13}$ and $G\alpha_{q11}$ protein families with A_{2A}, D_2R and A_{2A}/A_{2A} homodimer receptors by using Förster Resonance Energy transfer (FRET) method in live cell cultures. It has been shown that these G proteins are coupled with other types of Adenosine and Dopamine receptors, but it is currently not known if $G\alpha_{q/11}$ and $G\alpha_{12/13}$

proteins interact with A_{2A}, D_2 receptors or A_{2A}/A_{2A} homodimer. For this purpose, we tagged $G\alpha_{12}$, $G\alpha_{13}$, $G\alpha_{11}$ proteins with EGFP and mCherry fluorophores. Afterwards, $G\alpha_{11}$-A_{2A}, $G\alpha_{11}$-D_2R, $G\alpha_{11}$-A_{2A}/A_{2A}; $G\alpha_{12/13}$-A_{2A}, $G\alpha_{12/13}$-D_2R and $G\alpha_{12/13}$-A_{2A}/A_{2A} were transfected to N2a cells. Interactions were imaged under confocal microscope and quantified by pixFRET method.

This study investigates new approaches to analyze double and triple protein interactions with the combination of BiFC and FRET methods. Future studies using these techniques could be used to study effects of new drugs on protein protein interactions, such as receptor $G\alpha$ interaction, in cell culture.

CHAPTER 2

MATERIALS AND METHODS

2.1 Materials

2.1.1 Mouse Neuroblastoma Neuro2a (N2a) Cell Line and Cell Media

Mouse Neuroblastoma cell line Neuro 2a (N2a) was chosen to express and visualize fluorescent protein tagged A_{2A}, D_2 receptors and $G\alpha_{11}$, $G\alpha_{12}$, $G\alpha_{13}$ proteins, because they can differentiate into neurons within a few days and extensively used to study signaling pathways, protein protein interactions. These constructs were transfected to N2a cells which was supplied by ŞAP Institute, Ankara, TURKEY.

N2a cell line's growth medium consist of 44,5 % Dulbecco's Modified Eagle Medium (D-MEM) high glucose with L-glutamine (Invitrogen, Cat#41966029), OptiMEM®I, 44,5 % Reduced Serum Medium with L-glutamine (Invitrogen, Cat#31985047), 10 % Fetal Bovine Serum (Invitrogen, Cat#26140-079) and 1% Penicillin/Streptomycin solution (Invitrogen, Cat#15140-122). To sterilize, medium was filtered by using Milipore Stericup® Filter Unit. Cells were grown in Nuve® EC 160 CO2 incubator, at 37 °C with 5 % CO_2. Nuve® LN 120 laminar flow cabinet was used for all cell culture studies. Formulation of D-MEM and PBS are in Appendix A. Cells were passaged every 3 or 4 days when they reach enough (90 %) confluency. Phosphate Buffered Saline

(PBS) solution (Appendix A) was used for washing waste materials and dead cells during cell passage. To dissociate cells from the T25 flask, Trypsin-like solution, TrypLE™ Express with Phenol Red (Invitrogen, Cat#12605-028) was used.

2.1.2 Bacterial Strain and Bacterial Culture Media

To amplify plasmids, *Escherichia coli* XL1blue and *Escherichia coli* DH5α strains were used. They were grown in Luria Bertani (LB) Solution liquid or solid form (Appendix B). The components of LB Solution were dissolve in distilled water and sterilized at 121 °C for 20 minutes by use of Nüve OT 40L autoclave. According to plasmids, ampicillin (100 μg/mL) or kanamycin (50 mg/mL) antibiotics were used for selection. Cells were incubated in solid cultures at 37 °C for 12-16 hours in an incubator ZHWY-200B by Zhicheng Instruments; on the other hand cells were grown in liquid cultures in the rotary shaker incubator at 200 rpm.

2.1.3. Plasmids, Primers, and Sequencing

GNA11 in pCR-BluntII-TOPO vector (Accession Number: HsCD00346196), and GNA13 in pDONR221 vector (Accession Number: HsCD00045589) and GNA12 in pcDNA3.1 (+) vector (Accession Number: GNA1200000) were obtained from PlasmID, Harvard Medical School (MA, USA). cDNA of EGFP in pEGFP-N1 vector (Accession Number: AAB02574) and mCherry in pCS2-mCherry vector (Accession Number: ACO48282) were gifted by Prof. Dr. Henry Lester, California Institute of Technology (CA, USA). pcDNA3.1(-) (Appendix D) was gifted by Assoc. Prof. Dr. Ayşe Elif Erson Bensan, Middle East Technical University, Turkey.

Primers (Appendix E) were obtained from Sentegen (Ankara, Turkey) and Integrated

DNA Technologies (IDT) (IO, USA). Sequencing of mCherry/EGFP tagged G protein genes were done by Molecular Cloning Laboratories (MCLAB) (CA, USA).

2.1.4. Chemicals and Materials

The chemicals which are used in this thesis were purchased from Sigma Chemical Company (NY, USA) and Applichem (Darmstadt, Germany). DNA Polymerases for PCR reaction, T4 Ligases, GeneRuler 100bp plus (#SM0321) and GeneRuler 1kb (#SM0313) DNA ladders were obtained from Thermo Scientific (MA, USA). Gel extraction kit was obtained from QIAGEN (Düsseldorf, Germany). Restriction enzymes were purchased from New England Biolabs (MA, USA). For PCR purification and plasmid isolation GeneJET PCR Purification Kits and Plasmid Miniprep Kit were used and supplied by Thermo Scientific (MA, USA). Transfection of pcDNA 3.1 (-) plasmids to N2a cells, Lipofectamine® LTX and Plus™ Reagent by Invitrogen (CA, ABD) were used. To analyses the function of G proteins, RhoA G-LISA Activation Assay Kit (calorimetric format) by Cytoskeleton (CO, USA) was used. Glass bottom dishes were purchased from In Vitro Scientific (CA, USA). Live cell imaging studies were done by using by Leica Microsystems CMS GmBH's DMI4000B confocal microscope with Andor DSD2 spinning differential disc confocal device. PixFRET a plug-in for ImageJ program was used for analysis of images.

2.2 Methods

2.2.1. Preparation of Competent *E. coli* Cells by Rubidium Chloride Method

XL1blue and DH5α strains of *Escherichia coli* cells were used for preparation of competent cell. A single colony was chosen from streak plate and inoculated into 4 ml of

liquid LB medium then left in a shaker incubator (225 rpm) at 37 °C for 12-16 hours. On the following day, entire inoculum was added to 250 ml of LB medium containing 20 mM $MgSO_4$ in 1L Erlenmeyer flask and grown until optical density of culture reaches 0.4-0.6 at 600 nm (nearly 2-3 hours). When the required density was obtained, culture was centrifuged at 4.500 x g for 5 min at 4 °C by transferring the whole culture to 50 ml falcon tubes. At the end of centrifugation, supernatant was removed and remaining pellet was resuspended in 20 ml TFB1 and kept on ice for 5 min. After chilling on ice, cells were centrifuged at 4.500 x g for 5 min at 4 °C and then supernatant was removed, remaining pellet was dissolved in 2 ml ice cold TFB2. Cells were incubated on ice for 60 min. After the incubation, in 1.5 ml Eppendorf tubes cells were 100 μl aliquoted and quick-frozen in liquid N_2 and store at -70 °C. Preparation of TFB1 and TFB2 were summarized in table 2.1

Table 2.1 250ml TFB1 and 100 ml TFB2 solution preparation.

TFB1 250ml	
30 mM potassium acetate	0.74 g
10 mM $CaCl_2$	1.25 ml of 2M
50 mM $MnCl_2$	2.47 g
100 mM RbCl	3.023 g
15% glycerol	37.5ml

TFB2 100ml	
10 mM MOPS or PIPES	0.335 g
75 mM $CaCl_2$	3.75 ml of 2 M
10 mM RbCl	0.12 g
15% glycerol	15 ml

2.2.2. Transformation of Competent *E. Coli* cells

Competent *E. Coli* cells from -80 °C freezer chilled on ice for 15 minutes. 50-100 ng of plasmid or 5 μl of ligation / PCR product was added to competent cells. Afterwards, cells were chilled on ice for 30 minutes. To apply heat shock, cells were incubated at 42 °C for 30 second. After the heat shock step, they were chilled on ice for 5 min. In the

following step, 900 µl of liquid LB media was added and cells were incubated at 37 °C in a shaker incubator (220 rpm) for 60 minutes. Next, cells were centrifuged at 4000 rpm for 3 minutes. After centrifugation, 800 µl of supernatant was discarded from every tubes and remaining 100 µl suspension was spread to LB agar plate with ampicillin by using glass beads. Then, plates were gently shaken; and glass beads were removed. Then incubated at 37 °C for ~16 hours.

2.2.3. Plasmid Isolation from *E. Coli*

One colony was picked from LB agar plate and inoculated into 4 ml liquid LB medium with ampicillin (100 mg/ml), then left in shaker incubator (200 rpm) at 37 °C for ~16 hours. By using Thermo Scientific® GeneJET Plasmid Miniprep Kit, plasmid DNA was isolated from *E. Coli*. According to manufacturer's instructions; *E. Coli* culture in LB media was centrifuged 4000 rpm for 5 min. After that, pellet was resuspended in 250 µl of resuspention solution and transferred to Ependorf tubes. Then, 250 µl lysis solution and 350 µl neutralization solution were added. After mixing by inverting tubes 4-6 times, they were centrifuged at 13000 rpm for 5 minutes. Immediately, supernatant was transferred to supply GeneJET spin column by pipetting and then, centrifuged at 13000 rpm for 1 minute. After that, the flow was discharged and columns were back into the collection tubes. Washing step was repeated in two times, 500 µl wash solution was added and centrifuged at 13000 rpm for 1 minute. Finally, the spin column transfer into Ependorf tubes and 100 µl nuclease free water was added centrifuged for 1 min. Plasmid DNA in Ependorf tubes was obtained.

2.2.4. Restriction enzyme digestion

All restriction enzymes were supplied from New England Biolabs Inc. (NEB).

According to NEB's instructions, 1 unit of restriction enzyme require to digest 1 µg of DNA in a 50 µl volume. Restriction enzyme double digestion for the 300-600ng of DNA was optimized such as, 0.2 µl of each restriction enzyme was used with 1.5 µl CutSmart® NEB buffer and completed to 20 µl with nuclease free water, then incubated at 37 °C for 2 hours.

2.2.5. Ligation

Gα proteins were transferred from original vectors to pcDNA 3.1 (-) vector in order to be expressed in mammalian cells. For this purpose, digestion and ligation reactions were used. Inserts and vectors were digested and run on the gel. 1 µl of T4 DNA ligase enzyme (NEB, Cat#0202T), 2 µl 1X T4 DNA ligase buffer (Appendix C) and nuclease free water was added to extracted inserts and vectors and volume was completed to 10 µl. Insert and vector's amounts were calculated via NEBioCalculator tool and a molar ratio of 1:5 vectors to insert was considered, then incubated at room temperature for 2 hours.

2.2.6. Polymerase Chain Reaction (PCR)

In the first PCR reaction, EGFP and mCherry fluorescent protein genes were amplified with 24 bp long overhangs, matching to target integration site of G protein gene with 18 bp long linker. In this study, receptor genes were labeled from five different positions avoiding functionally active sites. 5' of the forward primer involves an overhang homologous to 24 bp before the target position and 18bp long linker (TCTGGAGGAGGAGGATCT) and first 24 bp of the fluorescent protein genes. The 5' of the reverse primer involves an overhang homologous to 24 bp of G protein sequence which follows 18 bp same linker and last 24 bp of fluorescent protein genes without the stop codon. At the end of reaction, the PCR product had full length fluorescent protein

gene with overhang homologous to G protein genes and this was used as double stranded DNA primer in second PCR reaction.

Table 2.2 Conditions of optimized PCR to amplify EGFP and mCherry genes by adding 24bp overhangs

Reagents	Amounts			
Template (EGFP_ pcDNA /mCherry_pcDNA)	100-150 ng			
5X Phire Reaction Buffer	10 μl			
Phire Hot Start II DNA Polymerase	1 μl	Pre-denaturation	98°C/90s	
dNTPs (25 mM)	1 μl	Denaturation	98°C/5 s	
Forward Primer (20 pmol)	1 μl	Annealing	60°C /5s	35 cycles
Reverse Primer (20 pmol)	1 μl	Extension	72°C/28s	
MgCl$_2$	1 μl	Final extension	72°C/60s	
Nuclease-free Water	Completed to 50 μl			

2.2.7. Agarose Gel Electrophoresis

PCR and restriction enzyme digestion products sizes were confirmed with this method. 1 % agarose gel weight to volume ratio was used. To prepare the gel, required amount of agarose was weighted, and then dissolved in 1X TAE by using microwave oven. When it got cool, EtBr was added. It was used for DNA visualization under UV light. After that, it was poured into the tray. 6X DNA loading dye (Thermo Scientific, #R0611) was added to mixture. GeneRuler DNA Ladders (Thermo Scientific) and sample-dye mix were loaded into the wells. Lastly, gel was run at 90-100 V for 40-45 minutes in 1X TAE Buffer.

2.2.8. DNA extraction from Agarose Gel

Samples were controlled and QIAGEN® Gel Extraction Kit (Cat# 28704) was used to extract samples from the gel. Then, DNA fragments were excised from the gel by scalpel then gel slices were weighted and they were put into the ependorf tubes. Considering gel slices weight, 3 volumes buffer QC was added to 1 volume gel (100 mg gel ~ 100 µl), and then incubated at 50 °C, 15 minutes. During that time, tubes were vortexed every 2-3 minutes. Then one gel volume isopropanol was added and transferred into the spin colon. After that, centrifuged for 1 minutes and flow was discarded. Then 750 µl buffer PE was added to colums, centrifuged 1 min. The colums were placed into ependorf tubes then 50 µl nuclease free water was added and centrifuge for 1 minutes 13000 rpm.

2.2.9. Determination of DNA Amount

NanoDrop 2000 spectrophotometer from Thermo Scientific® was used to quantify DNA concentration, after plasmid isolation or gel extraction.

2.2.10. PCR Integration Method (Overlap Extension PCR Method),

The G protein genes were tagged with EGFP and mCherry fluorophores from different positions by using Overlap Extension PCR Method. By this method, two consecutive PCR reactions occur. The first PCR reaction condition was shown in Table 2.2. and product was used as double stranded DNA primer in second PCR reaction. The optimal ratio of template (G protein gene plasmid) to insert was 1:5. Overlap extention PCR reaction condition is shown in table 2.3.

41

Table 2.3 Second PCR reaction conditions

Reagent	Amount				
5X Phusion Reaction Buffer	10 μl				
Phusion HF HS Polymerase	1 μl	Pre-denaturation	98°C/30s		
dNTPs (25 mM)	1 μl	Denaturation	98°C/10s		
DMSO	1 μl	Annealing	56°C/30s	35 cycles	
Template (Gα₁₁,Gα₁₂,Gα₁₃ in pcDNA	100 ng	Extension	72°C/6min		
1st PCR product	500 ng	Final extension	72°C/10min		
Nuclease-free Water	Completed to 50 μl				

2.2.11. Transfection of eukaryotic expression vectors to N2a cells

Live N2a cells were transfected with expression vectors containing fluorescent protein gene tagged G protein genes by using Lipofectamine™ LTX with Plus™ reagents (from Invitrogen®) 90.000 cells were seeded on a glass bottom dish and grown for one day in normal growth media. The following day, 200 ng of plasmid was diluted in 100 μl of OptiMEM® and 4 μl of Plus™ reagent was added. The mixture was incubated at room temperature for 15 minutes. During the incubation, 4 μl of Lipofectamine LTX diluted in 100 μl of OptiMEM and added to the first mixture after incubation. Then the last mixture was incubated at room temperature for 20 minutes. At that time, the medium on the cells was removed and cells were washed with 1 ml of sterile 1X PBS solution. After washing step, 1 ml of OptiMEM® was added. At the end of incubation, final mixture was added to cells. Then, cells were incubated for 3 hours in the 5 % CO_2 incubator at 37 °C. After 3 hours, 2 ml of normal growth medium was added on the cells and they were grown for 24 hours, before imaging.

2.2.12. G-Lisa RhoA activation assay

G-lisa RhoA activation assay kit was used to detect whether mCherry tagged $G\alpha_{12/13}$ proteins are still functionally active. The RhoA G-LISA® kit consists of Rho GTP-binding protein binded to the wells of a 96 well plate. The principle of kit is based on separating active GTP-bound Rho and inactive GDP-bound Rho in cell lysate. When active GTP-bound Rho binds to the wells of plate, inactive GDP-bound Rho removed during washing step of the kit protocol and a RhoA specific antibody detects bound

active RhoA. It is important to optimize the assay that Cells were plated and grown to desired confluency, the amount of applied lysis solution and LPA to activate $G\alpha_{12/13}$ proteins were determinded during optimization. Moreover, to prepare lysates rapid processing (<10 min) on ice is important as GTP bound Rho is naive to hydrolysis during and after cell lysis causing Rho inactivation.

2.2.12.1. Conditions of Preparing Cell Lysate

75.000 live N2a cells were seeded on a 35 mm glass bottom dish and grown for one day in growth media at 37 °C incubator. Next day $G\alpha_{13}$ wild type, $G\alpha_{13}$-mcherry, $G\alpha_{12}$ wild type and $G\alpha_{12}$- EGFP, $G\alpha_{11}$ wild type and $G\alpha_{11}$-mCherry plamids were transfected. Before Rho stimulation, cells were kept in serum starvation media that leads low levels of Rho activity before the assay. 30-50 % confluency was determined as optimal condition for preparing cell lysate (Vouret-Craviari *et al.,* 2002). When N2a cells reached 30-50 % confluency, cell media was changed with serum starvation media which include 0.5 % Fetal Bovine serum then cells were grown for 24 hours in 37 °C CO_2 incubator. After incubation, N2a cells were placed on ice and media was aspirated off. Then cells were stimulated with 10ul LPA/1.5 ml stok solution. It was prepared with

0.3mM LPA solution that is dissolved in 1ml phosphate buffered saline (PBS) in the presence of 0.1% bovine serum albumin BSA (w/v) (essentially fatty acid free) (Kranenburg, O. *et al.,* 1999; Yamada, T. *et al.,* 2005). Then LPA solution was discharged and cells were washed with 2 ml ice cold PBS buffer. All buffer was aspirated. inorder not to dilute the lysis buffer. The G-LISA® kit manufacturer indicates that kit uses 25 µl of lysate (0.4-2 mg/ml lysate protein concentration) per assay and recommended lysate concentration is 0.5 mg/ml. To make lysate at this concentration

range, lysis buffer was adjusted depending on cell and plate type. 230 µl ice-cold lysis buffer was applied every 35 mm dishes and cell lysates were immediately harvested with cell scraper. Then cell lysates were transferred to pre-chilled 1.5 ml microfuge tubes on ice and centrifuged at 10,000 xg, 4 °C for 1 min. 20 µl of lysate was saved for protein quantification and 100 µl aliquoted samples were frozen in liquid nitrogen urgently. The rest of lysates were stored at -80 °C.

2.2.12.2 Lysate Protein Concentration Measurement

To optimized protein concentration as 0.5 mg/ml, different amounts of lysis buffer were tried and 230 µl lysis buffer was found as an optimum amount. 1 ml of Precision Red^{TM} Advanced Protein Assay Reagent and 20 µl of lysates or lysis buffer for blank were added into disposable cuvettes. After incubation for 1 min, absorbance of lysates was read with the lysis buffer blank at 600 nm. Lysates' absorbance value was multiplied by 5 to gain protein concentration in mg/ml. It is important that all samples must have equal protein concentration. Cell extracts were equalized with ice cold lysis buffer. Protein concentration was calculated by using the formula below.

$$C=\frac{A}{\varepsilon l}$$

c = protein concentration (mg/ml), A = absorbance reading, l = pathlength (cm) ε = extinction coefficient ([mg/ml]-1 cm-1)

To obtain 0.5 mg/ml protein concentration, 20 µl lysate sample in 1ml Precision Red reagent should give 0.1 absorbance reading (50 is the dilution factor for the lysate).

$$C = \frac{A}{\varepsilon l} = \frac{0.1}{10 \times 1} \times 50 = 0.5 \text{ mg/ml}$$

2.2.12.3. G-Lisa RhoA activation assay Protocol

After optimizing cell lysate concentration, buffers for blank and positive control were prepared. To prepare buffer blank 60 µl Lysis Buffer was mixed with 60 µl ice-cold Binding Buffer and placed on ice. For positive control sample 12 µl Rho Control Protein was mixed with 48 µl Cell Lysis Buffer and 60 µl Binding Buffer then mix was placed on ice. The strips were placed placed on ice. With 100 µl ice-cold water, the powder in the wells was solved. After that frozen cell lysates were thawed in a water bath at room temperature and placed on ice immediately after thawing. Ice-cold lysis buffer was added. 90 µl lysates of $G\alpha_{11}$, $G\alpha_{11}$-mCherry, $G\alpha_{12}$, $G\alpha_{12}$-EGFP, $G\alpha_{13}$ and $G\alpha_{13}$-mcherry plasmids transfected cells were aliquot for triplicate assays into ice-cold microcentrifuge tubes. Then ice-cold Binding Buffer added to each tube and vortexed for 3-5 s on a high setting and returned to ice. Water was removed completely from the microplate wells by 6-7 vigorous pats onto paper towels. This step is very critical for reducing the background readings. Then 50 µl of buffer blank control pipetted into duplicate wells, A1 and B1. 50 µl RhoA positive controls pipetted into duplicate wells C1 and D1. 50 µl of equalized cell lysates were added to wells as $G\alpha_{13}$-wt was pipetted into E1, F1and G1; $G\alpha_{13}$-mCherry was pipetted into H1, A2 and B2; $G\alpha_{12}$-wt was pipette into C2, D2 and E2; $G\alpha_{12}$-EGFP was pipetted into F2, G2 and H2. $G\alpha_{11}$-wt was pipetted into A3, B3 and

C3; Gα$_{11}$.mCherry was pipetted into D3, F3 and G3. After that, plate was placed on a cold orbital microplate shaker at 4 °C for 30 minutes. By the time of incubation, anti-RhoA primary antibody was diluted to 1/250 in Antibody Dilution Buffer. For 16 wells (2 strips), 1 ml final volume was adequate. After 30 minutes, solution was removed from wells and washed two times with 200 µl Wash Buffer, and then Wash Buffer was discharged. 200 µl of room temperature Antigen Presenting Buffer was pipette urgently into the wells and incubated at room temperature for 2 minutes. Antigen Presenting Buffer was flicked out vigorously and wells were washed three times with 200 µl of room temperature Wash Buffer. After that 50 µl of diluted anti-RhoA primary antibody was added to the wells and incubated on 200-400 rpm orbital microplate shaker at room temperature for 45 minutes. During the incubation, secondary HRP labeled antibody was diluted to 1/62.5 in Antibody Dilution Buffer.

For 16 wells (2 strips), 1 ml final volume was adequate. Then the anti-RhoA primary antibody flicked out vigorously and washed three times with 200 µl of room temperature Wash Buffer. Afterward, 50 µl of diluted secondary antibody was added to each well and left the plate on a microplate shaker (200–400 rpm) at room temperature for 45 minutes while secondary antibody was incubated, an aliquot of HRP detection reagents A and B was thawed in a room temperature water bath and removed as soon as they are thawed. 400 µl HRP detection reagents A and B were mixed equal volumes just before the end of the secondary antibody incubation and mixture was protected from light. Then secondary antibody was removed and wells were washed three times with 200 µl of room temperature Wash Buffer. After that, 50 µl mixed HRP detection reagent was pipetted per wells and incubate at 37 °C for 10-15 minutes. Then, 50 µl of HRP Stop Buffer was added to the wells. Finally, the signal was read by using a microplate spectrophotometer at 490nm wavelenght.

2.2.13. Imaging with Spinning Disc Confocal Microscope

After N2a cells were transfected with fluorophore tagged Gα proteins and A2A/D2 receptors, they grown for 1 day and cells were imaged by Leica DMI 4000 equipped with Andor DSD2 spinning disk confocal microscope with 63X oil N1.4 objectie lens. Andor DSD2 spinning disk confocal microscope has maximum 22 frames per second as a frame rate with $370 - 700$ nm excitation range and $410 - 750$ nm emission range. Many rotating holes, inside the confocal disc, help to reject non-focused light quickly and let the focused light reach direct to the sample. Thus images are sharper and more detailed.

EGFP fluorophore was excited with range of 470-500 nm wavelengths and emitted at 500-550 nm wavelengths given green signal. In addition, mCherry fluorophore was excited with the range of 560-600 nm wavelengths and emitted at 600-650 nm wavelengths given red signal. To get FRET signal, fluorophores were excited at 470 nm wavelength from EGFP (donor) channel, and emitted at 650 nm from mCherry (acceptor) channel. DSD Spinning disc was shown in figure 2.1.
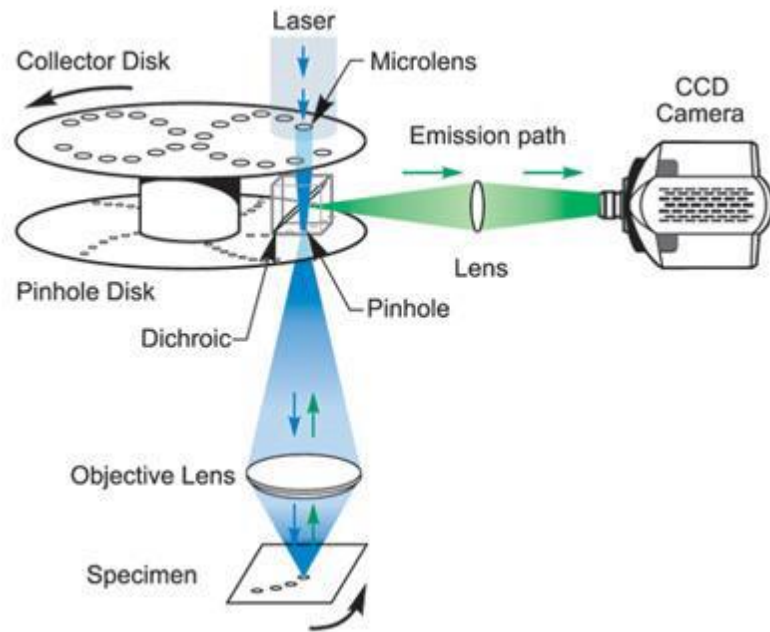
Figure 2.1. A schematic image representing DSD Spinning disc device.

2.2.14. Image Analysis with Pix-FRET Program

FRET method allows discovering interaction between two fluorophores; however spectral bleed-through (SBE) is very important while doing FRET analysis. Spectral overlap occurs when acceptor is excited at donor excitation wavelength range and donor emits light in acceptor wavelength spectra. Thus, PixFRET program can eliminate false FRET signal according to spectral overlap (Feige *et al.*, 2005). For this purpose, while imaging the cells, three different groups were present; only donor, only acceptor and both donor and acceptor. In the first group, only donor tagged proteins were transfected to N2a cells and imaged from two channels; FRET and donor channel. From FRET channel, fluorophores were excited with donor wavelength and picking signals from

acceptor spectra. From donor channel, fluorophores were excited with donor wavelength and picking signals from donor spectra. In the other group, only acceptor tagged proteins were transfected to N2a cells and imaged from two channels; FRET and acceptor channel. From FRET channel, fluorophores were excited with donor wavelength and picking signals from acceptor spectra. From acceptor channel, fluorophores were excited with acceptor wavelength and picking signals from acceptor spectra. In the third group, both donor and acceptor tagged proteins were transfected to N2a cells and imaged from three channels; FRET, donor and acceptor channels. From FRET channel, fluorophores were excited with donor wavelength and picking signals from acceptor spectra. From donor channel, fluorophores were excited with donor wavelength and collecting signals from donor spectra. From acceptor channel, fluorophores were excited with acceptor wavelength and picking signals from acceptor spectra. Using these groups of images, PixFRET algorithm normalized bleed-throughs and FRET efficiency was calculated.

CHAPTER 3

RESULTS AND DISCUSSION

3.1 Analysis of Interaction between Adenosine A_{2A} and/or Dopamine D_2 Receptors with $G\alpha_{11}$, $G\alpha_{12}$, $G\alpha_{13}$ proteins

G protein interaction with Adenosine (A_{2A}) and Dopamine (D_2) receptors were investigated with (Forster Resonance Energy) FRET technique. For this purpose, $G\alpha_{11}$, $G\alpha_{12}$ and $G\alpha_{13}$ proteins were labeled with mCherry and EGFP fluorescent proteins. Also, A_{2A} and D_2 receptors were pre-tagged with EGFP and mCherry fluorescent proteins by Sinem Çelebiöven and Gökhan Ünlü during their thesis studies. Labelled proteins were transfected to N2a cells. To investigate interaction, images were taken from live cells by using confocal microscope, and FRET efficiency was analyzed with pixFRET program.

3.1.1 Labeling G protein genes with EGFP and mCherry Tags Using PCR Integration Method

These genes were tagged from different positions regarding to their functional regions. NCBI conserved domain program was used to detect these regions. Considering to active sites, proteins were labeled at 5 different loop positions. To label $G\alpha_{11}$, $G\alpha_{12}$ and $G\alpha_{13}$ protein genes with EGFP and mCherry fluorophores, PCR integration method was applied. In the first PCR reaction, EGFP and mCherry coding sequences were amplified with 24 bp overhangs and linker (TCTGGAGGAGGAGGATCT) according to insertion

positions. For this purpose, primers were designed and given in Appendix E, pcDNA 3.1(-) vectors containing EGFP and mCherry genes were used as templates to amplify EGFP and mCherry proteins. The 1st PCR products were then run on 1 % agarose gel as seen in Figure 3.1.

Figure 3.1 Image of PCR amplified EGFP and mCherry fragments with Gα_{11}, Gα_{12} and Gα_{13} overhangs and the linker (lane 1-6). Fermentas® GeneRuler™ 1kb plus DNA Ladder was used.

As it is shown in agarose gel image, EGFP and mCherry tags gave bands around 700 bp (EGFP and mCherry tags are 711 bp; overhangs are 24 bp, linker is 18 bp long). These products were extracted from the gel than used as a primer of the 2nd PCR reaction during plasmids containing Gα_{11}, Gα_{12} or Gα_{13} protein genes were used as template of the reaction. 2nd PCR reaction condition was given in methods in **Table 2.3.**

After 2nd PCR reaction, DpnI enzyme digestion was applied to PCR products to eliminate the template plasmids (containing untagged Gα_{11}, Gα_{12} or Gα_{13} protein genes). DpnI enzyme digestion has a crucial role in 2nd PCR reaction. This enzyme recognizes methylated GATC sequences; therefore methylated template plasmids are digested but

PCR products remain intact. After incubation for 3 hours at 37 °C, DpnI enzyme digested 2nd PCR products were transformed to *E. coli* cells and cells were grown on Ampicillin (for $G\alpha_{12}$) or kanamycin (for $G\alpha_{11}$ and $G\alpha_{13}$) containing plates. After 16 hours incubation existed colonies were picked and grown in liquid medium, then plasmids were isolated from the cells. To control insert size of isolated plasmids, digestion was applied.

The wild type $G\alpha_{11}$ protein gene was between *EcoRI;* restriction sites within plasmids. So to control EGFP and mCherry insertion, plasmids containing $G\alpha_{11}$ protein gene was digested with *EcoRI* enzyme. In addition, $G\alpha_{12}$ gene was between *Nhe1 and Xba1* restriction sites so inserts were controlled by double digestion at these restriction sites. On the other hand Wild type $G\alpha_{13}$ protein gene was in Gatewate cloning vector, and it was not between common restriction sites, but *EcoRV* restriction site was located in this plasmid. Thus, to control the insert, digestion through *EcoRV* restriction site was applied. After digestion for 3 hours at 37 °C, digested plasmids were run on 1 % agarose gel as seen in Figure 3.2, 3.3 and 3.4.
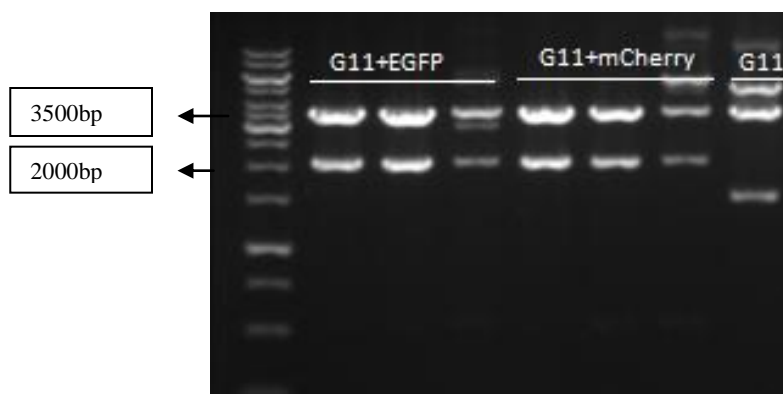
Figure 3.2 Image of *EcoRI*; digestion screening of $G\alpha_{11}$ protein gene tagged with EGFP and mCherry in pENTR223 vector. 1 kb DNA Ladder was used. The wells were loaded with Gα11+EGFP (1, 2, 3), $G\alpha_{11}$+mCherry (4, 5, 6), $G\alpha_{11}$ (7). Upper bands display remaining pcDNA sequence after digestion.

As expected wild type $G\alpha_{11}$ protein is 1261 bp long, $G\alpha_{11}$ + EGFP and $G\alpha_{11}$ + mCherry fusions showed ~750 bp increase in size when it is compared with wild type $G\alpha_{11}$. $G\alpha_{11}$ + EGFP and $G\alpha_{11}$ + mCherry fusion genes were sequenced to confirm that $G\alpha_{11}$ protein was successfully labeled with EGFP and mCherry portion from 244th Amino acid. The coding sequences of $G\alpha_{11}$ + EGFP and $G\alpha_{11}$ + mCherry fusions are given in Appendix F.
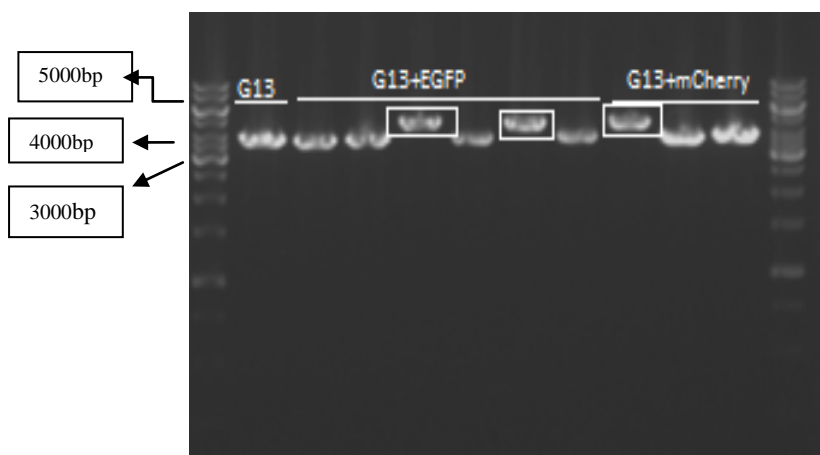
Figure 3.3 Agarose gel electrophoresis image of *EcoRV*; digestion screening of $G\alpha_{13}$ protein gene tagged with EGFP and mCherry in pENTR223 vector. Fermentas[®] GeneRuler™ 1 kb DNA Ladder was used. The wells were loaded with $G\alpha_{13}$ (1), $G\alpha_{13}$ + EGFP (2, 3, 4, 5, 6), $G\alpha_{13}$ + mCherry (7, 8, 9). Positive insert results were shown in rectangular shape.

$G\alpha_{13}$ protein constructs were single digested to control the insert. As expected wild type pENTR223-$G\alpha_{13}$ vector is 4250 bp long, pENTR223-$G\alpha_{13}$ + EGFP and pENTR223-$G\alpha_{13}$ + mCherry fusions showed ~750 bp increase in size when it is compared with wild type pENTR223-$G\alpha_{13}$. As it is shown $G\alpha_{13}$ protein was successfully labeled with EGFP and mCherry portion from 260th Amino acid. The coding sequences of $G\alpha_{13}$ + EGFP and $G\alpha_{13}$ + mCherry fusions are given in Appendix F.
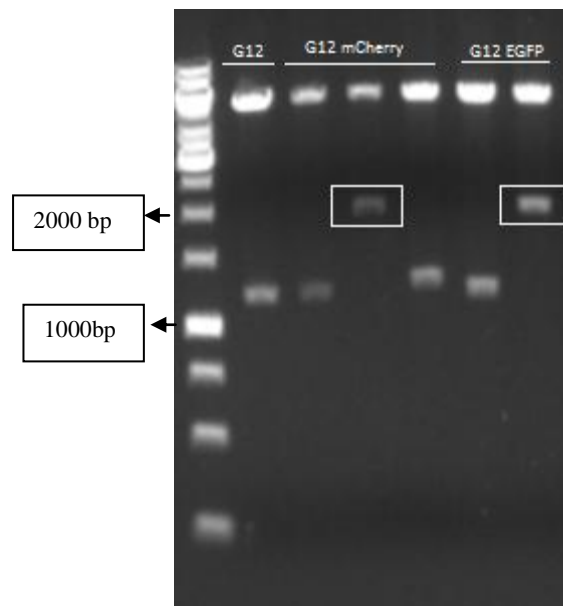
Figure 3.4 Image of *Nhe1 and Xba1*; double digestion screening of $G\alpha_{12}$ protein gene tagged with EGFP and mCherry in pcDNA 3.1(-)vector. 1 kb DNA Ladder was used. The wells were loaded with $G\alpha_{12}$ (lane 1), $G\alpha_{12}$ + mCherry (lane 2, 3, 4); $G\alpha_{12}$ + EGFP (lane 5, 6).

$G\alpha_{12}$ protein constructs were double digested to control the insert. As expected wild type $G\alpha_{12}$ protein gene is 1203 bp long, $G\alpha_{12}$ + EGFP and $G\alpha_{12}$ + mCherry fusions showed ~750 bp increase in size when it is compared with wild type $G\alpha_{12}$. $G\alpha_{12}$ + EGFP and $G\alpha_{12}$ + mCherry fusion genes were sequenced to confirm that $G\alpha_{12}$ protein was successfully labeled with EGFP and mCherry portion from 265th Amino acid. The coding sequences of $G\alpha_{11}$ + EGFP and $G\alpha_{11}$ + mCherry fusions are given in Appendix F.

3.1.2 Transferring Gα protein genes into a mammalian expression vector pcDNA

Labeled Gα protein genes were in different plasmid vectors, that two of them ($G\alpha_{11}$ in pCR-BluntII-TOPO and $G\alpha_{13}$ in pDONR221) were not expressed in mammalian cell lines. Thus, they were cloned to pcDNA 3.1(-) plasmids by using PCR method. In this

PCR reaction, primers were designed to add restriction enzyme sites to EGFP/mCherry tagged Gα protein genes. PCR products and pcDNA 3.1(-) plasmids were digested with these restriction enzymes. After digestion for 2 hours at 37 °C, digested plasmids were run on 1 % agarose gel. Then Gel extraction and ligation protocols were applied as given in methods. Ligation products were transformed in *E. coli* cells and were grown on kanamycin containing plates. After 24 hours, from every plate, three colonies were picked and grown in liquid medium. Then, plasmids were isolated and screened with double digestion to check insert.

After these experiments, $G\alpha_{11}$ + EGFP and $G\alpha_{11}$ + mCherry fusion genes which were between *Xho1* and *Kpn1* restriction sites were obtained within pcDNA 3.1(-). In order to control the size changes, plasmids were digested with these two enzymes and run on 1 % agarose gel as seen in Figure 3.5
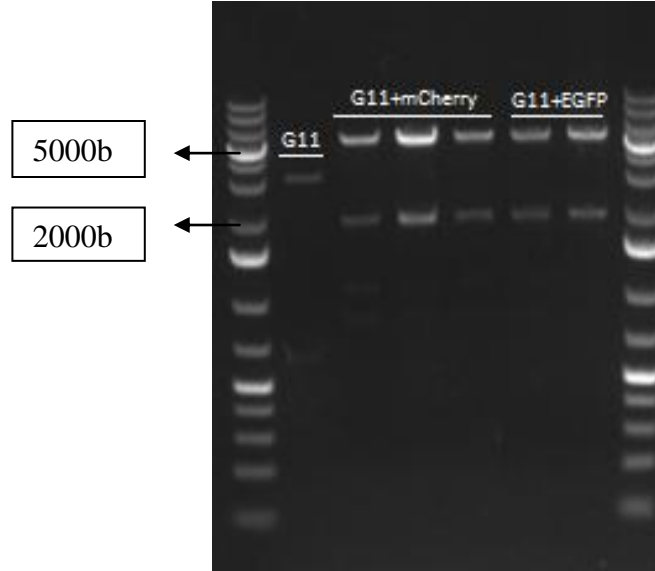
Figure 3.5 Image of *Xho1* and *Kpn1*; double digestion screening of Gα$_{11}$ protein gene tagged with EGFP and mCherry in pcDNA 3.1 (-) vectors. 1 kb plus DNA Ladder was used. The wells were loaded with Gα$_{11}$ in pcDNA 3.1 (lane 1), Gα$_{11}$ + mCherry in pcDNA 3.1 (-) (lane 2, 3, 4), Gα$_{11}$ + EGFP in pcDNA 3.1 (-) (lane 5, 6).

Gα$_{11}$ protein constructs were double digested to control the insert. As expected wild type pcDNA 3.1 (-) vector is 5428 bp long, Gα$_{11}$ + EGFP and Gα$_{11}$ + mCherry inserts are ~ 2000 bp size (Gα$_{11}$ is 1338 bp; mCherry and EGFP are 711bp) . After size control, Gα$_{11}$+EGFP in pcDNA 3.1 (-) and Gα$_{11}$+mCherry in pcDNA 3.1 (-) fusion genes were sequenced to confirm that Gα$_{11}$ protein was successfully labeled and cloned to pcDNA 3.1 (-). The coding sequences are given in Appendix F.

Gα$_{13}$ + EGFP and Gα$_{13}$ + mCherry fusion genes which were between *Xho1* and *Kpn1* restriction sites were obtained within pcDNA 3.1(-). In order to control the size changes, plasmids were digested with these two enzymes and run on 1 % agarose gel as seen in Figure 3.6
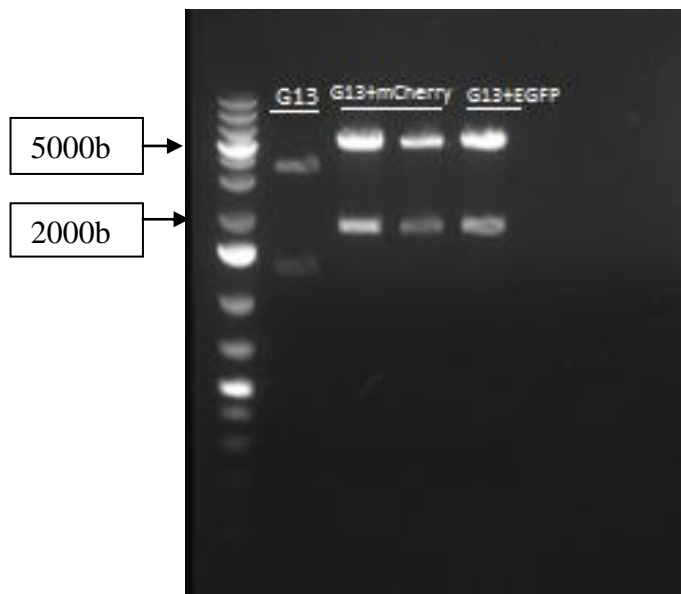
**Figure 3.6** Image of *Xba1 and Kpn1*; double digestion screening of Gα$_{13}$ protein gene tagged with EGFP and mCherry in pcDNA 3.1 (-) vectors. Fermentas$^{®}$ GeneRuler™ 1 kb plus DNA Ladder was used. The wells were loaded with Gα$_{13}$ in pcDNA 3.1 (-) (lane 1), Gα$_{13}$ + mCherry in pcDNA 3.1 (-) (lane 2, 3); Gα$_{13}$ + EGFP in pcDNA 3.1 (-) (lane 4).

Gα$_{13}$ protein constructs were double digested to control the insert. As expected wild type pcDNA 3.1 (-) vectors is 5428 bp long, Gα$_{13}$ + EGFP and Gα$_{13}$ + mCherry inserts are ~ 2000 bp size (Gα$_{13}$ is 1134 bp mCherry and EGFP are 711 bp). After size control, Gα$_{13}$ + EGFP in pcDNA 3.1 (-) and Gα$_{13}$ + mCherry in pcDNA 3.1 (-) fusion genes were sequenced to confirm that Gα$_{13}$ protein was successfully labeled and cloned to pcDNA 3.1 (-). The coding sequences are given in Appendix F . Gα$_{12}$ protein gene was ordered in pcDNA 3.1 (+) so it was not transferred to pcDNA again.

3.2 Imaging with Confocal Microscopy in Live Cell

Gα proteins tagged from different positions' with Fluorescens labels were imaged and

the signals were recorded. The localization of tagged proteins and whether there is an interaction with adenosine (A_{2A}) and dopamine (D_2) receptors were investigated. For this purpose, fluorophore labeled Gα subunits were transfected to N2a cells. These Gα proteins were co-transfected with fluorophore tagged Adenosine (A_{2A}) and Dopamine (D_2) receptors respectively. Also, triple interactions were analyzed between $Gα_{11}$ and adenosine homodimers (A_{2A}/A_{2A}); $Gα_{13}$ and adenosine homodimers (A_{2A}/A_{2A}). Three different plasmids, $Gα_{11}$ or $Gα_{13}$, N-EGFP tagged A_{2A} and C-EGFP tagged A_{2A}, were co-transfected to N2a cells by using Lipofectamine™ LTX with Plus reagent. After transfection, live cells were incubated for one day and imaged via spinning disc confocal microscope. Images gathered from FRET channels were analyzed via PixFRET plugin of Image J as described in method section.

3.2.1 Visualization of mCherry Fluorophore Tagged $Gα_{11}$ Protein in live Cells

Gα proteins were tagged from five different positions to test the effect of tagging position on protein location and function. To see the fluorescent signal, EGFP/mCherry tagged proteins from different positions were transfected into N2a cells. As mentioned in methodology, 200 ng of fluorescent tagged Gα protein containing plasmids were transfected to N2a cells by using Lipofectamine^{TM} LTX with Plus^{TM} reagents. Next day, cells were observed under Leica DMI 4000 equipped with Andor DSD2 spinning disk confocal microscope with 63X oil N1.4 objective.

Images of $Gα_{11}$ gene tagged from 18th, 82nd, 126th, 244th and 294th amino acid positions were shown in figure 3.7.
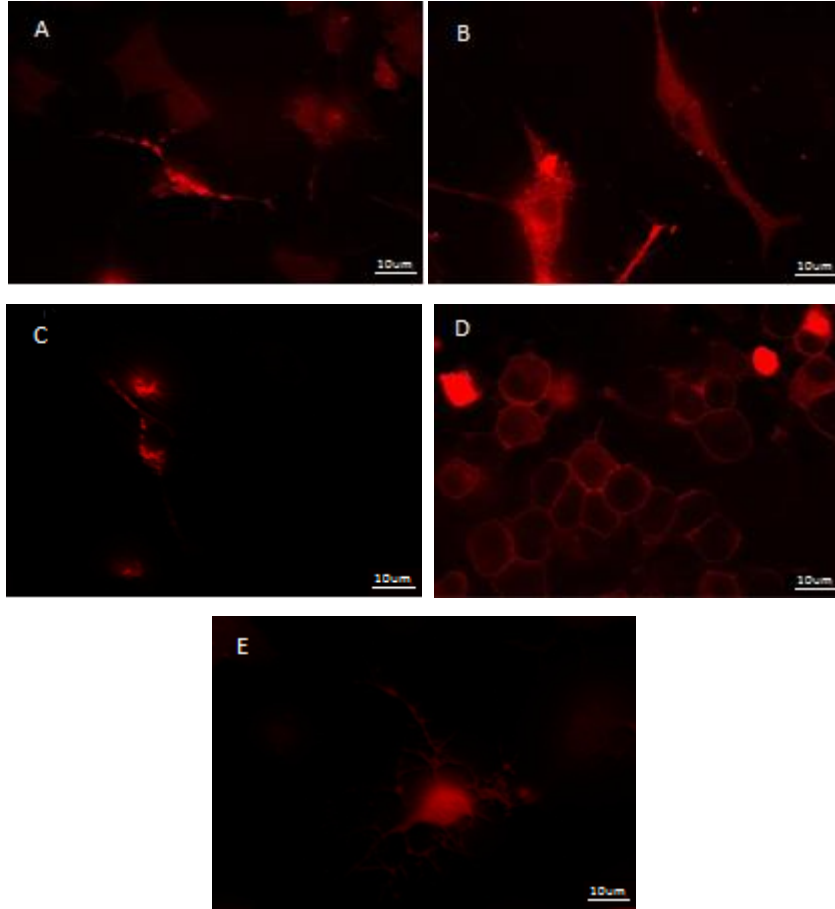
Figure 3.7 N2a cells transfected with $G\alpha_{11}$ labeled with mCherry from its 18th amino acid (A), $G\alpha_{11}$ labeled with mCherry from its 82nd amino acid (B), $G\alpha_{11}$ labeled with mCherry from its 126th amino acid (C), $G\alpha_{11}$ labeled with mCherry from its 244th amino acid (D), $G\alpha_{11}$ labeled with mCherry from its 294th amino acid (E), fusion proteins. Images were taken from mCherry channel with 63X oil N1.4 objective.

All tagged $G\alpha_{11}$ genes (from 18th, 82nd, 126th, 244th and 294th amino acid positions) gave positive mCherry signal, but fusion gene localizations were different. Only tagging at position 244th resulted in proper expression pattern on the plasma membrane resembling normally G protein localization. Proteins tagged at position 126th were located mostly in

cytosol and some on the membrane. However, proteins labeled at 18th, 82nd and 294th positions were expressed in cytosol and probably defective at trafficking to the plasma membrane. Also labeling from improper positions may lead to changing protein's 3D structure or some functions, which could prevent proper localization, lead to aggregation or even cell death. Images of $G\alpha_{11}$ gene labeled with mCherry from its 244th amino acid position were shown in figure 3.8.
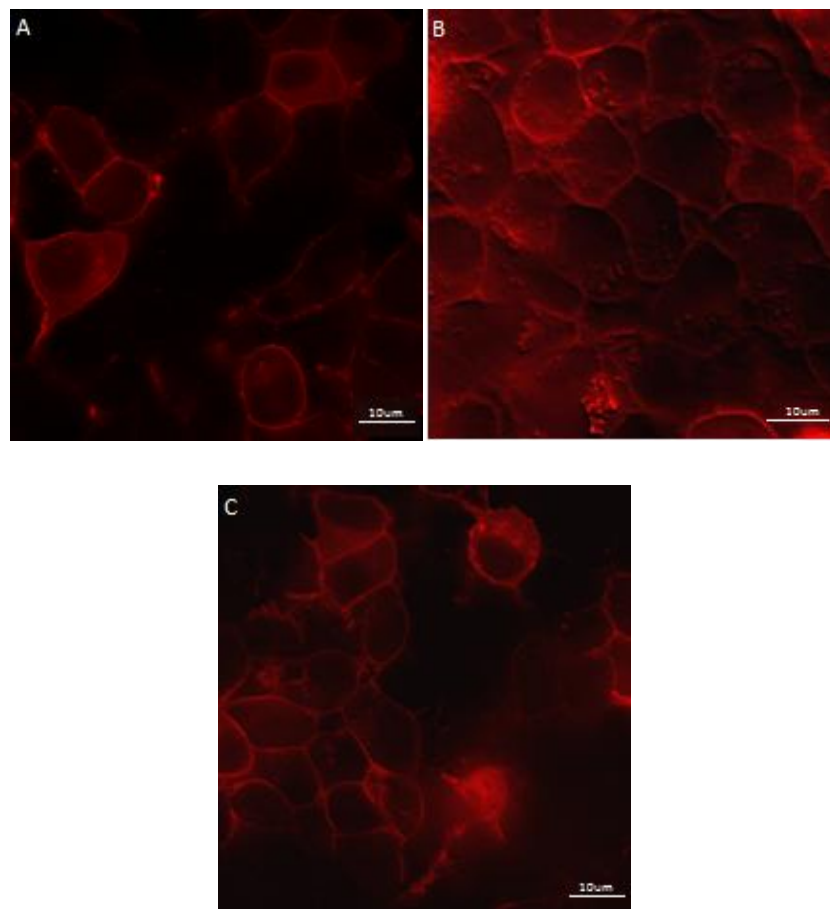
Figure 3.8 $G\alpha_{11}$ labeled with mCherry from its 244th amino acid (A, B and C) Images were taken from mCherry channel.

It has been shown that fluorescent protein labeling from 244th amino acid is optimum position for $G\alpha_{11}$ protein. Because, this position did not affect the protein's targeting to the membrane. $G\alpha_{11}$ + mCherry fusion protein has been located on the cell membrane in specific manner demonstrated in figure 3.8. Therefore interaction experiments were carried out with this construct.

3.2.2 Visualization of EGFP Fluorophore Tagged $G\alpha_{12}$ Protein in live Cells

Like $G\alpha_{11}$; $G\alpha_{12}$ protein was tagged from five different positions to see whether the positions can affect protein location and function. None of the mCherry tagged $G\alpha_{12}$ proteins positive mCherry signal, tagging carried out more than two times from various positions. However EGFP tagged $G\alpha_{12}$ protein gave positive green signal, thus in the rest of the study EGFP tagged $G\alpha_{12}$ proteins were used. To see the fluorescent signal, 200 ng of EGFP tagged $G\alpha_{12}$ protein gene containing plasmid were transfected to N2a cells. Images of $G\alpha_{12}$ protein tagged from 92nd, 142nd, 265th, 320th and 365th amino acid positions were shown in figure 3.9.

,
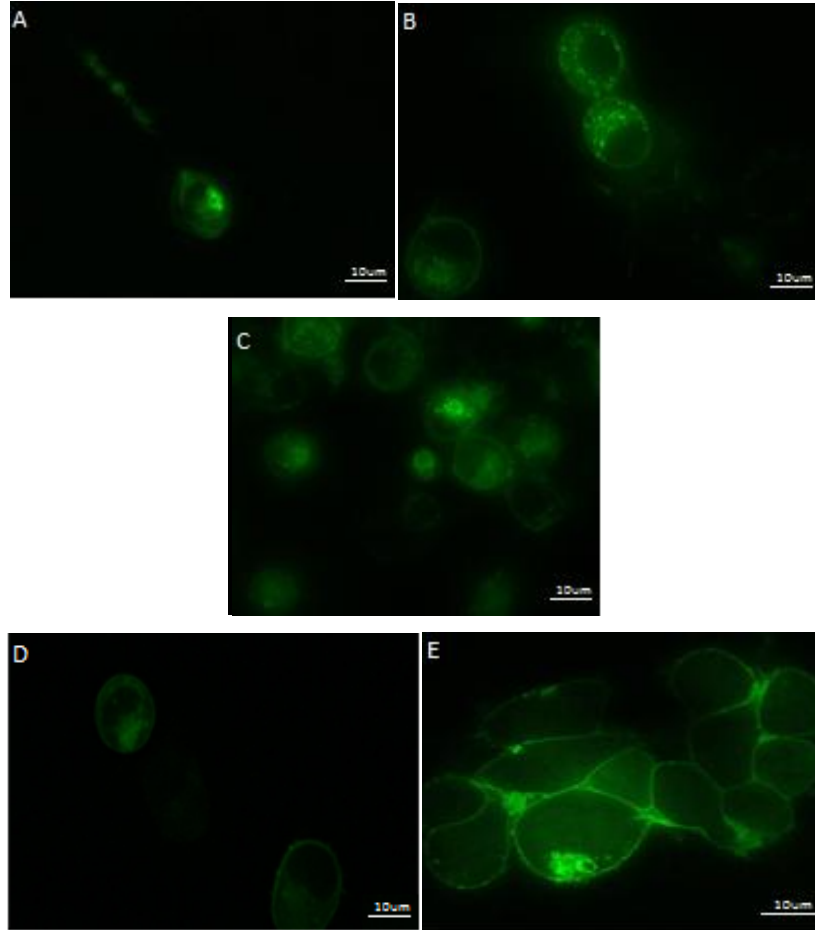
Figure 3.9. N2a cells transfected with $G\alpha_{12}$ labeled with EGFP from its 92nd amino acid (A), $G\alpha_{12}$ labeled with EGFP from its 142nd amino acid (B), $G\alpha_{12}$ labeled with EGFP from its 320th amino acid (C), $G\alpha_{12}$ labeled with EGFP from its 365th amino acid (D), $G\alpha_{12}$ labeled with EGFP from its 265th amino acid (E), fusion proteins. Images were taken from EGFP channel.

It is shown that $G\alpha_{12}$ protein tagged from 92nd, 142nd, 265th, 320th and 365th amino acid positions have signals but except the position of 265, EGFP signal is mostly located in the cytosole. On the other hand, proteins tagged from position 265 were expressed well on the plasma membrane. Images of $G\alpha_{12}$ labeled with EGFP from its 265th amino acid position were shown in figure 3.10.
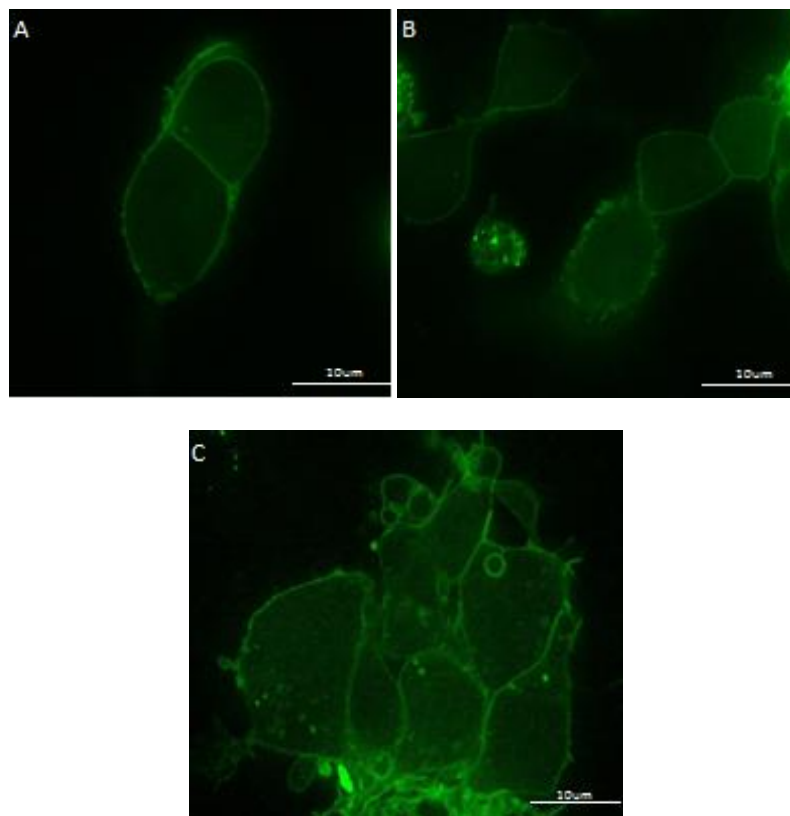
Figure 3.10 Gα$_{12}$ labeled with EGFP from its 265th amino acid (A, B and C) Images were taken from EGFP channel.

Gα$_{12}$ protein labeling from 265th amino acid was targeting to the plasma membrane. Therefore interaction experiments were continued with this construct.

3.2.3 Visualization of mCherry Fluorophore Tagged Gα$_{13}$ Protein in live Cells

Same protocol was applied for Gα$_{13}$ protein labeling from five different positions. To see the fluorescent signal, 200ng of mCherry tagged Gα$_{13}$ protein coding plasmids were transfected to N2a cells. Images of Gα$_{13}$ protein tagged from 75th, 147th, 174th, 260th and 338th amino acid positions were shown in figure 3.11
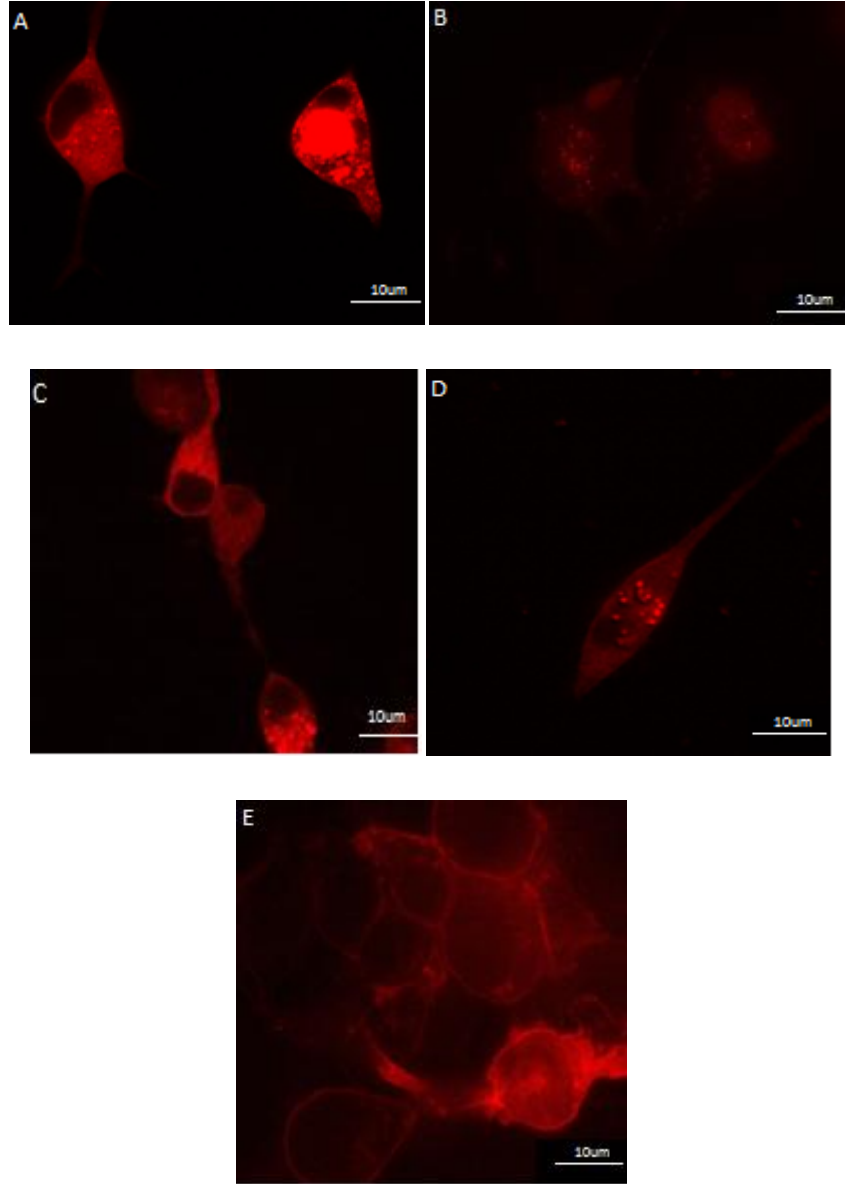
Figure 3.11 N2a cells transfected with Gα13 protein labeled with mCherry from its 75th amino acid (A), Gα$_{13}$ protein labeled with mCherry from its 147th amino acid (B), Gα$_{13}$ protein labeled with mCherry from its 174th amino acid (C), Gα$_{13}$ protein labeled with mCherry from its 260th amino acid (D), Gα$_{13}$ protein labeled with mCherry from its 338th amino acid (E) Images were taken from mCherry channel.

It is shown that $G\alpha_{13}$ protein tagged from 147th, 174th, 260th and 338th amino acid positions gave the mCherry signal. The position of 260th protein signal is located on the plasma membrane. Images of $G\alpha_{13}$ labeled with mCherry from its 260th amino acid position were shown in figure 3.11.
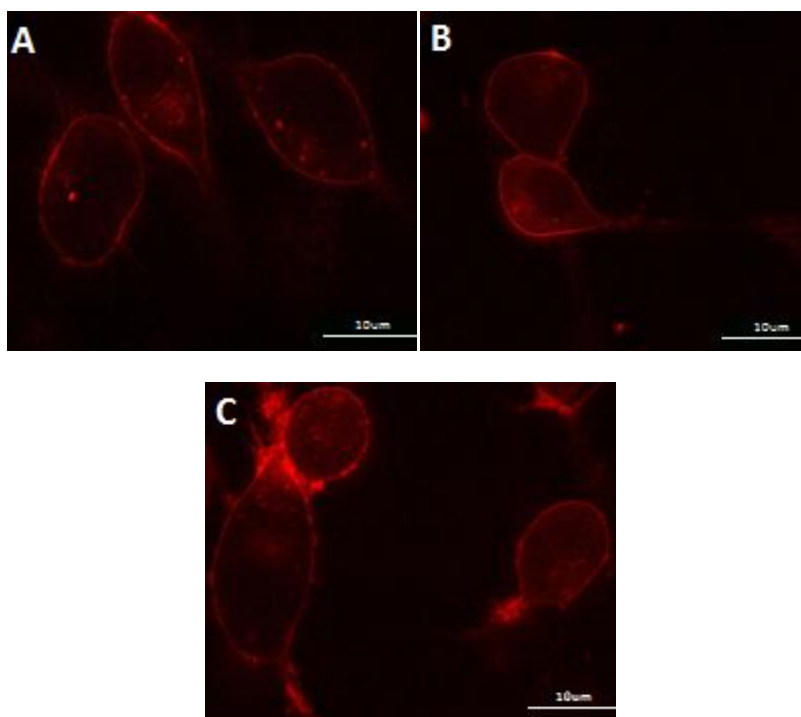
Figure 3.12 $G\alpha_{13}$ labeled with mCherry from its 260th amino acid (A, B and C) Images were taken from mCherry channel.

$G\alpha_{13}$ protein labeled from 260th amino acid was targeting to the plasma membrane. Therefore interaction experiments were continued with this construct.

3.3 Functionality Assay

$G\alpha_{11}$-mCherry244, $G\alpha_{12}$-EGFP265 and $G\alpha_{13}$-mCherry260 labelled proteins were

compared with untagged $G\alpha_{11}$, $G\alpha_{12}$ and $G\alpha_{13}$ proteins according to their function. For this purpose, Lipophosphotidic acid (LPA) was used to activate RhoA and active RhoA was detected with RhoA G-LISA Ativation Assay kit. The amount of RhoA shows activity of G proteins. According to statistical analysis, labeled $G\alpha$ proteins' RhoA functions are not different from wild type ones. Functional analysis of wild type and labeled $G\alpha$ protein were shown in Figure 3.13.
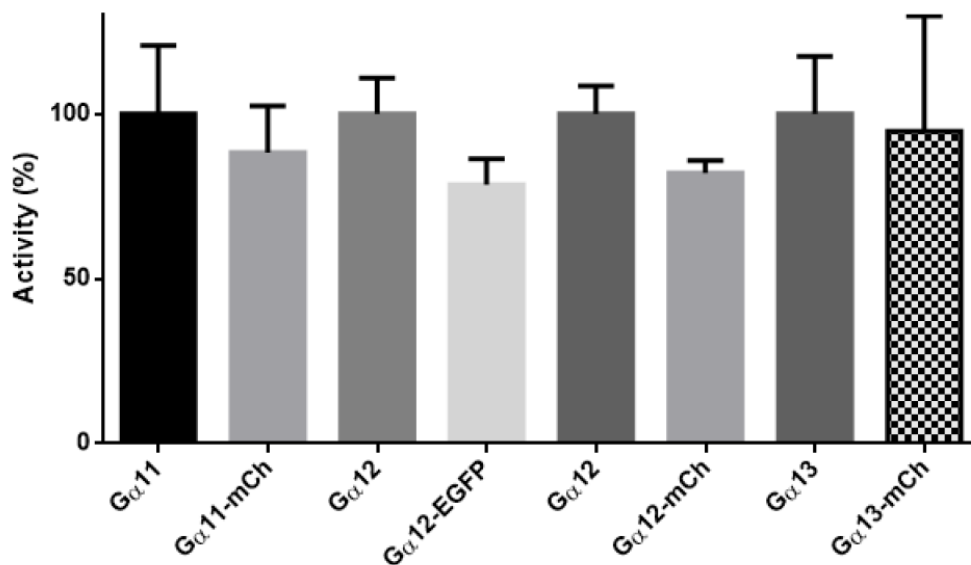
Figure 3.13 RhoA G-LISA Ativation Assay kit was used to obtain RhoA levels of wild type and tagged G proteins.The percentage of RhoA levels were calculated and student T-test result shows the activity of $G\alpha_{11}$-mCherry244, $G\alpha_{12}$-EGFP265, $G\alpha_{13}$-mCherry260, wild type $G\alpha_{13}$, wild type $G\alpha_{12}$ and wild type $G\alpha_{11}$ in pcDNA 3.1(-) vectors were not different from each other respectivley.

Statical analyses of the results show that $G\alpha_{11}$-mCherry244 and wild type $G\alpha_{11}$, $G\alpha_{12}$-EGFP265 and $G\alpha_{12}$, $G\alpha_{13}$-mCherry260 and $G\alpha_{13}$ are not different functionally. Similar active RhoA levels indicate that tagging positions of proteins are not the functional

regions and these regions are not effect proteins activity.

3.4. Gα$_{11}$ protein Interactions

3.4.1 Detection of physical interactions between Adenosine A$_{2A}$ and Gα$_{11}$ protein by using FRET technique

Adenosine A$_{2A}$ receptor and Gα$_{11}$ protein genes were obtained in pDNR-Dual and pCR-BluntII-TOPO vectors, respectively. A$_{2A}$ receptor was tagged with EGFP fluorescent protein from C-termini of the receptor; All of the details about tagging A$_{2A}$ receptor were carried out in our laboratory and described in the thesis titled "Detection of Homo/Hetero-Dimerizations Between Adenosine A$_{2A}$, Dopamine D$_2$ And NMDA Receptors By Use of FRET and BiFC Assays" by Sinem Çelebiöven. Gα$_{11}$ protein was tagged with mCherry fluorescent protein from its 244th amino acid position by using PCR integration method and transferred into pcDNA 3.1 (-) for expression directly into N2a cells; this was done by cutting from *Xhol* and *KpnI* sites and cloning between same restriction sites of pcDNA 3.1 (-).

By using pre-prepared A$_{2A}$R+EGFP constructs, N2a cells were co-transfected with 200 ng of pcDNA 3.1(-)_A$_{2A}$R+EGFP and 200 ng of pcDNA 3.1(-)_Gα$_{11}$+mCherry to investigate possible physical interactions between Gα$_{11}$ proteins and Adenosine A$_{2A}$ receptors. Images were taken from three different petri dishes N2a cells transfected with A$_{2A}$R+EGFP, Gα$_{11}$+mCherry and co transfeced with both A$_{2A}$R+EGFP and Gα$_{11}$+mCherry. After 24 hours, transfected N2a cells were imaged under Leica DMI 4000 equipped with Andor DSD2 spinning disk confocal microscope with 63X oil N1.4 objective. By using PixFRET program, FRET efficiency was calculated and presented using artificial colors indicating the efficiency percentage. These colors represent

different range of FRET efficiency, such as, blue pixels show 1-10 %; green pixels 11-20 %; yellow pixels 21-30 %; red pixels 31-40 % and gray pixels 41-50 % efficiency. For bleed-through elimination, images from only $A_{2A}R$+EGFP and only $G\alpha_{11}$+mCherry transfected N2a cell were used in this program. Images of mCherry tagged $G\alpha_{11}$ protein, EGFP tagged A_{2A} receptor, and FRET efficiency were shown in figure 3.14. Extra images presented in appendix H.
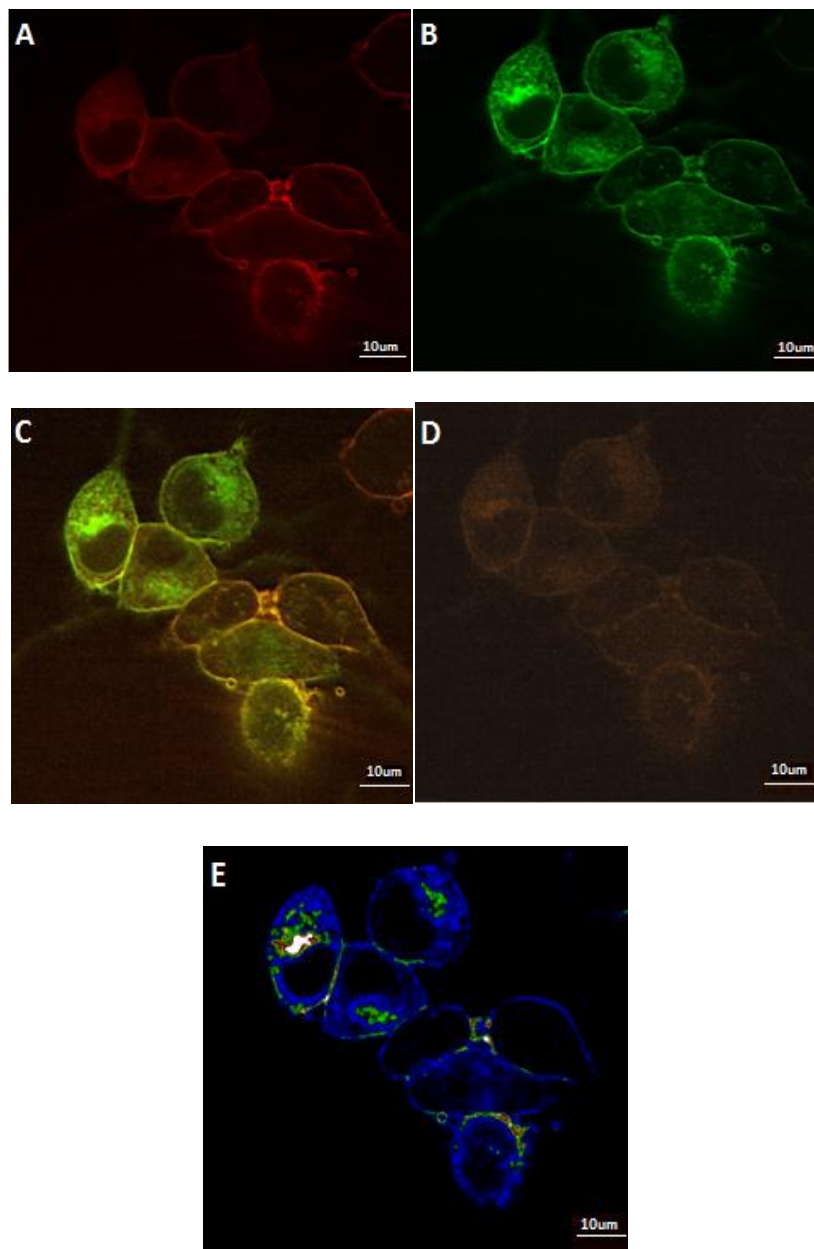
Figure 3.14 N2a cells transfected with A_{2A}+EGFP and $G\alpha_{11}$+mCherry. Images were taken from mCherry channel excitation at 583 nm shows $G\alpha_{11}$+mCherry (A), EGFP channel excitation at 482 nm shows A_{2A}+EGFP (B), multiple channel shows co-localization of A_{2A}+EGFP and $G\alpha_{11}$+mCherry. (C) FRET channel shows FRET signal (D) FRET efficiency shows pixels where FRET occurs (E).

After getting images, FRET efficiency was calculated by using imageJ pixFRET program. Histograms of region of interest were given the pixel counts and values of FRET efficiencies. To determine $G\alpha_{11}$ protein and A_{2A} receptor interaction, images from the cell treated with $A_{2A}R$+EGFP and $G\alpha_{11}$+mCherry proteins were analyzed and mean of total efficiencies were calculated. FRET efficiency was found 6.3 % for $G\alpha_{11}$ protein - A_{2A} receptor.

Specific ranges of FRET efficiencies were calculated and percentage of every range (1-10 %, 10-20 %, 20-30 %, 30-40 % and 40-50 %) was computed from the histograms of PixFRET program obtained for every range.

3.4.2 Detection of physical interactions between Dopamine D_2 and $G\alpha_{11}$ protein by using FRET techniques

Dopamine D_2 receptor and $G\alpha_{11}$ protein genes were obtained in pDONR221 and -BluntII-TOPO vectors, respectively. Dopamine receptor was tagged with EGFP fluorescent protein from C-termini of the receptor. All of the details about tagging D_2 receptor were carried out in our laboratory and described in the thesis written by Sinem Çelebiöven. $G\alpha_{11}$ protein gene was tagged with mCherry fluorescent protein as it is described in methods.

By using pre-prepared D_2R + EGFP constructs, N2a cells were transfected with 200 ng of pcDNA 3.1(-)_D_2R + EGFP and 200 ng of pcDNA 3.1(-)_$G\alpha_{11}$ + mCherry to investigate possible physical interactions between them. After that, images were taken from three different petri dishes N2a cells transfected with D_2R + EGFP, $G\alpha_{11}$ + mCherry and co transfeced with both D_2R + EGFP and $G\alpha_{11}$ + mCherry. After 24 hours, transfected N2a cells were imaged. By using PixFRET program, FRET efficiency was calculated. For bleed-through elimination, images from only D_2R + EGFP and only $G\alpha_{11}$

+ mCherry transfected N2a cell images were used with this program. Images of mCherry tagged Gα_{11} protein, EGFP tagged D2R receptor and FRET efficiency were shown in figure 3.15. Extra images were in appendix H.
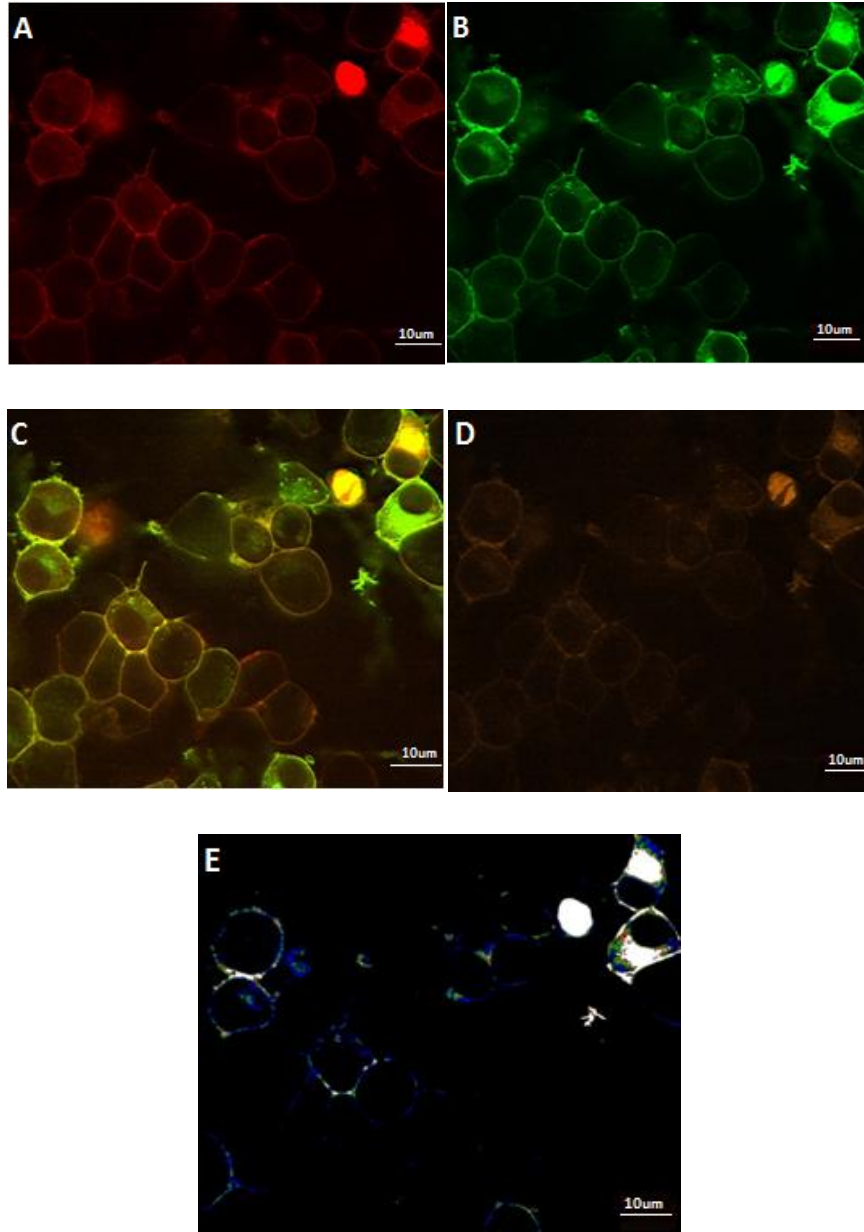
Figure 3.15 N2a cells transfected with D_2R + EGFP and $G\alpha_{11}$ + mCherry. Images were taken from mCherry channel excitation at 583 nm shows $G\alpha_{11}$ + mCherry (A), EGFP channel excitation at 482 nm shows D_2R + EGFP (B), multiple channel shows co-localization of D_2R + EGFP and $G\alpha_{11}$ + mCherry. (C) FRET channel shows FRET signal (D) FRET efficiency shows pixels where FRET occurs (E).

After getting images, FRET efficiency was calculated by using imageJ pixFRET program. Histograms of region of interest were given the pixel counts and values of FRET efficiencies. To determine $G\alpha_{11}$ protein and A_{2A} or D_2 receptor interaction, images from the cell treated with D_2R + EGFP and $G\alpha_{11}$ + mCherry proteins and A_{2A} + EGFP and $G\alpha_{11}$ + mCherry were analyzed and mean of total efficiencies were calculated.

Specific range of FRET efficiencies for $G\alpha_{11}+A_{2A}$ and $G\alpha_{11}+ D_2R$ was calculated and percentage of every range is shown in figure 3.16.
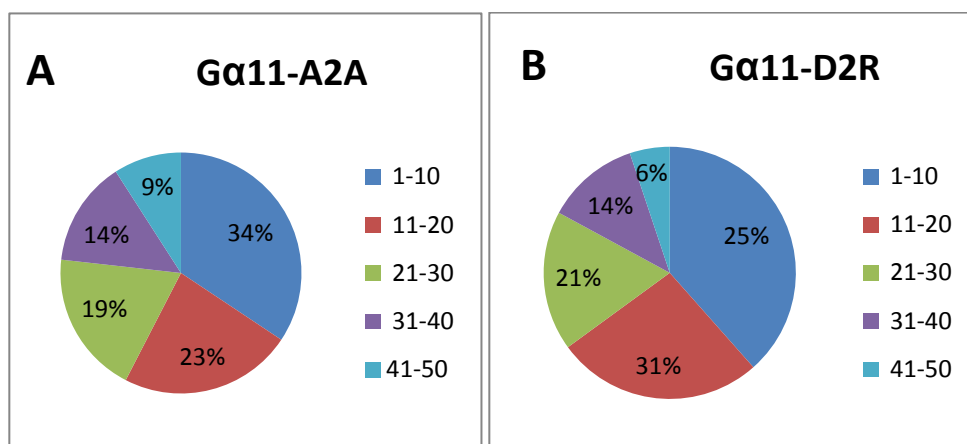
Figure 3.16 20 images were analyzed by pixFRET program, FRET efficiency of $G\alpha_{11}$-A_{2A} and $G\alpha_{11}$-D_2R were calculated, and percentage of every range was demonstrated. These ranges (1-10 %, 10-20 %, 20-30 %, 30-40 % and 40-50 %) were computed from the histograms of PixFRET program obtained for every range. Mean distributions of efficiency ranges in N2a cells co-transfected with A_{2A} + EGFP and $G\alpha_{11}$ + mCherry genes (A). Co-transfected with D_2R + EGFP and $G\alpha_{11}$ +mCherry genes (B)

The percentage of 1-10 % represent mostly background FRET signal so the real signal shows from the percentage of 11-50 %. The pie chart of $G\alpha_{11}$-D_2R has higher value of 11-50 % percentage of FRET efficiency range than $G\alpha_{11}$-A_{2A}.

3.4.3. Triple interaction detection between Adenosine homodimer and $G\alpha_{11}$ protein by using FRET techniques

Adenosine receptor was tagged with split EGFP fluorescent protein genes from C-termini and N- termini of the receptor. The non fluorescent fragments (N-EGFP and C-EGFP) of EGFP fluorescent protein can associate and create a fluorescent complex. Thus, when the A_{2A} receptors homodimerize, N-EGFP and C-EGFP fragments interact, and complex molecule produces detectable fluorescent signal. The details about tagging A_{2A} receptor with split EGFP fluorescent protein are mentioned in the thesis written by Sinem Çelebiöven.

By using pre-prepared $A_{2A}R$ + C-EGFP and $A_{2A}R$ + N-EGFP constructs, N2a cells were transfected with 500 ng of pcDNA 3.1(-)_$A_{2A}R$+C-EGFP, 500 ng of pcDNA 3.1(-)_$A_{2A}R$+N-EGFP and 200 ng of pcDNA 3.1(-)_$G\alpha_{11}$ + mCherry to investigate possible physical interactions between them. Images were taken from three different petri dishes N2a cells transfected with $A_{2A}R$ + C-EGFP and $A_{2A}R$ + N-EGFP; $G\alpha_{11}$ + mCherry; co-transfected with three of them $A_{2A}R$ + C-EGFP, $A_{2A}R$ + N-EGFP and $G\alpha_{11}$ + mCherry. After 24 hours, transfected N2a cells were imaged and FRET efficiency was calculated. For bleed-through elimination, images from only $G\alpha_{11}$ + mCherry; $A_{2A}R$ + C-EGFP and $A_{2A}R$ + N-EGFP transfected petri dishes were used in this program. Images of mCherry tagged $G\alpha_{11}$ protein, N-EGFP; C-EGFP tagged A_{2A} receptor, and FRET efficiency were shown in figure 3.17.
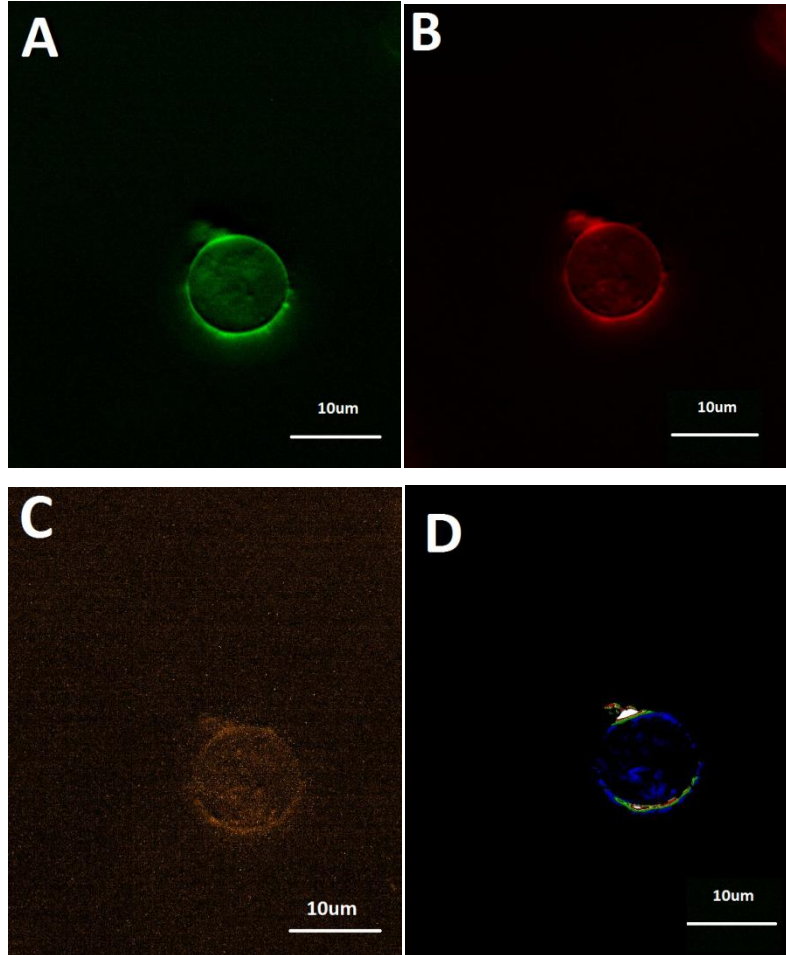
Figure 3.17 N2a cells transfected with A_{2A} + C-EGFP, A_{2A} + N-EGFP and $G\alpha_{11}$ + mCherry. Images were taken from EGFP channel excitation at 482 nm shows A_{2A} + C-EGFP and A_{2A} + N-EGFP (A), mCherry channel excitation at 583 nm shows $G\alpha_{11}$ + mCherry (B) FRET channel shows FRET signal (C) FRET efficiency shows pixels where FRET occurs (D).

After getting images, FRET efficiency was calculated by using imageJ pixFRET program. Histograms of region of interest were given the pixel counts and values of FRET efficiencies. To determine $G\alpha_{11}$ protein and A_{2A} homodimer receptor interaction, images from the cell treated with $A_{2A}R$ + C-EGFP, $A_{2A}R$ + N-EGFP and $G\alpha_{11}$ + mCherry proteins were analyzed and mean of total efficiencies were calculated. Average

FRET efficiency was found as 4.1 % for $G\alpha_{11}$ - A_{2A} homodimer however the circular cell morphology is an indication of death or very sick cells. Specific range of A_{2A}/A_{2A}-$G\alpha_{11}$ and A_{2A}/A_{2A}-$G\alpha_{13}$ FRET efficiencies were calculated from the histograms of PixFRET program and percentage of every range (1-10 %, 10-20 %, 20-30 %, 30-40 % and 40-50 %) was shown in figure 3.18.
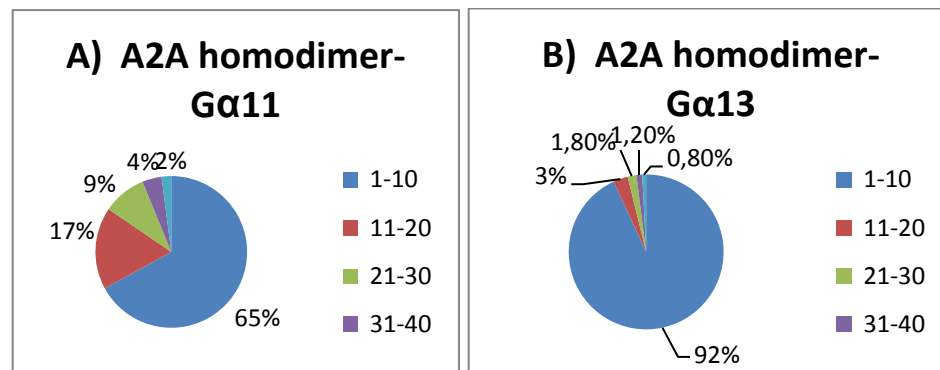
Figure 3.18. 20 images were analyzed by pixFRET program, FRET efficiency of A_{2A} + N-EGFP, A_{2A} + C-EGFP and $G\alpha_{11}$ + mCherry were calculated, and percentage of every range was demonstrated. These ranges (1-10 %, 10-20 %, 20-30 %, 30-40 % and 40-50 %) were computed from the histograms of PixFRET program obtained for every range. Mean distributions of efficiency ranges in N2a cells co-transfected with A_{2A} + N-EGFP, A_{2A} + C-EGFP and $G\alpha_{11}$ + mCherry genes (A). Co-transfected with A_{2A} + N-EGFP, A_{2A} + C-EGFP and $G\alpha_{13}$ + mCherry genes (B)

According to FRET results, images taken from N2a cells transfected with three different plasmid, $G\alpha_{11}$ + mCherry, A_{2A} + N-EGFP and A_{2A} + C- EGFP, shows the percentage of % 11-50 FRET efficiency range was low. It shows the possibility of interaction between $G\alpha_{11}$ and A_{2A}/A_{2A} is little. On the other hand, $G\alpha_{13}$ and homodimer A_{2A} do not interact according to very low FRET efficiency.

3.5. Gα$_{12}$ protein Interactions

3.5.1 Detection of physical interactions between Adenosine A$_{2A}$ and Gα$_{12}$ protein by using FRET technique

Gα$_{12}$ protein genes were obtained in pcDNA 3.1 (+) vectors. A$_{2A}$ receptor was tagged with mCherry fluorescent protein genes from C-termini of the receptor; all of the details about these tagging A$_{2A}$ receptor is mentioned in a thesis written by Sinem Çelebiöven. Gα$_{12}$ protein was tagged with EGFP fluorescent protein from its 265th amino acid position by using PCR integration method.

By using pre-prepared A$_{2A}$R + mCherry constructs, N2a cells were co-transfected with 200 ng of pcDNA 3.1(-)_A$_{2A}$R + mCherry and 200 ng of pcDNA 3.1(+)_Gα$_{12}$ + EGFP to investigate possible physical interactions between Adenosine A$_{2A}$ receptors and Gα$_{12}$ proteins. Images were taken from three different petri dishes N2a cells were transfected with A$_{2A}$R + mCherry, Gα$_{12}$ + EGFP and co-transfected with both A$_{2A}$R + mCherry and Gα$_{12}$ + EGFP.

Images of mCherry tagged A$_{2A}$ receptor, EGFP tagged Gα$_{12}$ protein, and FRET efficiency were shown in figure 3.19. Extra images are in appendix H.
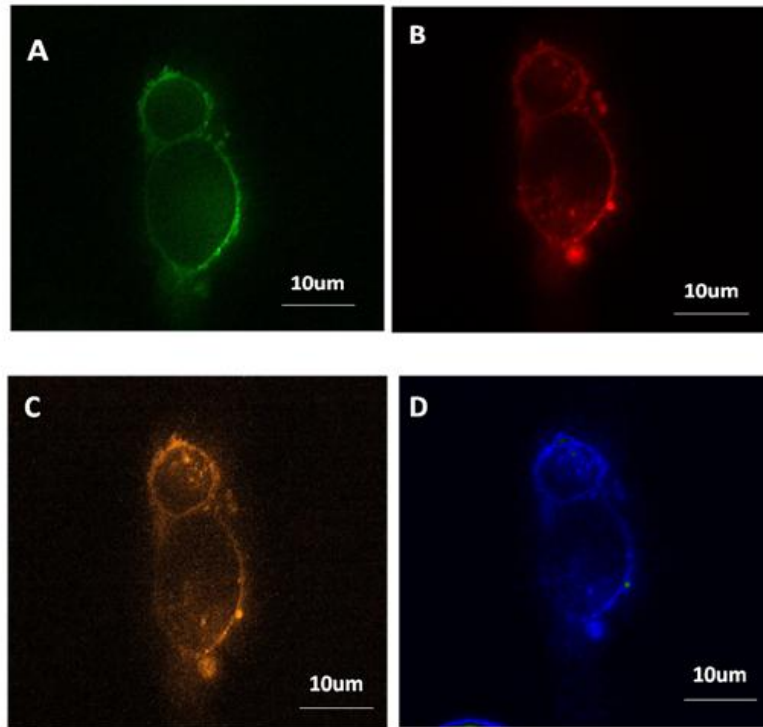
Figure 3.19 N2a cells transfected with A_{2A} - mCherry and $G\alpha_{12}$ + EGFP. Images were taken from EGFP channel excitation at 482 nm shows $G\alpha_{12}$ + EGFP (A), mCherry channel excitation at 583 nm shows A_{2A} - mCherry (B), FRET channel shows FRET signal (C) FRET efficiency shows pixels where FRET occurs (D).

FRET efficiency was calculated by using imageJ pixFRET program. Histograms of region of interest were given the pixel counts and values of FRET efficiencies. To detect $G\alpha_{12}$ protein and A_{2A} receptor interaction, images from the cell transfected with $A_{2A}R$ + mCherry and $G\alpha_{12}$ + EGFP proteins were analyzed. Specific range of FRET efficiencies was calculated and percentage of every range was computed (see figure 3.20).
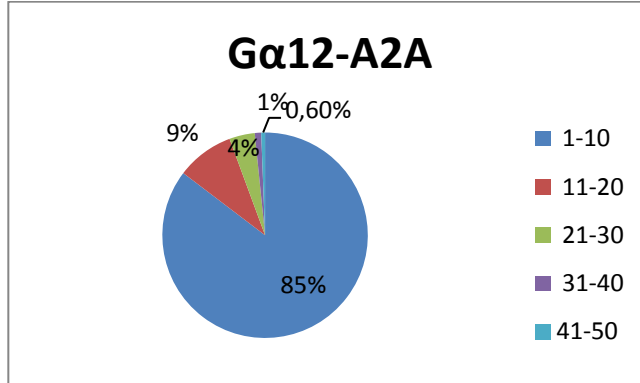
Figure 3.20 20 images were analyzed by pixFRET program, FRET efficiency of $A_{2A}R$ + mCherry, and $G\alpha_{12}$ + EGFP was calculated, and percentage of every range was demonstrated. These ranges (1-10 %, 10-20 %, 20-30 %, 30-40 % and 40-50 %) were computed from the histograms of PixFRET program obtained for every range. Mean distributions of efficiency ranges in N2a cells co-transfected with $A_{2A}R$ + mCherry, and $G\alpha_{12}$ + EGFP genes.

According to FRET results, percentage of 1-10% efficiency range was 85 %; percentage of 11-20 % efficiency range was 9 %; percentage of 21-30 % efficiency range was 4 %; percentage of 31-40 % efficiency range was 1 %; percentage of 41-50 % efficiency range was 0.6 % respectively. The percentage of 11-50 % FRET efficiency was very low so there is no interaction between $A_{2A}R$ and $G\alpha_{12}$ protein.

3.6. $G\alpha_{13}$ protein Interaction

3.6.1 Detection of physical interactions between Adenosine A_{2A} and $G\alpha_{13}$ protein by using FRET technique

Adenosine A_{2A} receptor and $G\alpha_{13}$ protein genes were obtained in pDNR-Dual and pDONR221 vectors, respectively. A_{2A} receptor was tagged with EGFP fluorescent protein from C-termini of the receptor as it is mentioned before. Moreover, $G\alpha_{13}$ protein

was tagged with mCherry fluorescent protein from its 260th amino acid position by using PCR integration method and transferred into pcDNA 3.1 (-) for expression directly into N2a cells; this was done by cutting from *Xbal* and *KpnI* sites and cloned between same restriction sites of pcDNA 3.1 (-).

By using $A_{2A}R$+EGFP constructs prepared previously in our laboratory, N2a cells were co-transfected with 200 ng of pcDNA 3.1(-)_$A_{2A}R$+EGFP and 200 ng of pcDNA 3.1(-)_$G\alpha_{13}$ + mCherry to investigate interactions between Adenosine A_{2A} receptors and $G\alpha_{13}$ proteins. Images were taken from three different petri dishes N2a cells transfected with $A_{2A}R$ + EGFP, $G\alpha_{13}$ + mCherry and co-transfected with both $A_{2A}R$ + EGFP and $G\alpha_{13}$ + mCherry. After 24 hours, transfected N2a cells were imaged and FRET efficiency was calculated. For bleed-through elimination, images from only $A_{2A}R$ + EGFP and only $G\alpha13$ + mCherry transfected N2a cell images were used in this program. Images of mCherry tagged $G\alpha_{13}$ protein, EGFP tagged A_{2A} receptor, and their FRET efficiencies were shown in figure 3.21. Extra images are in appendix H.
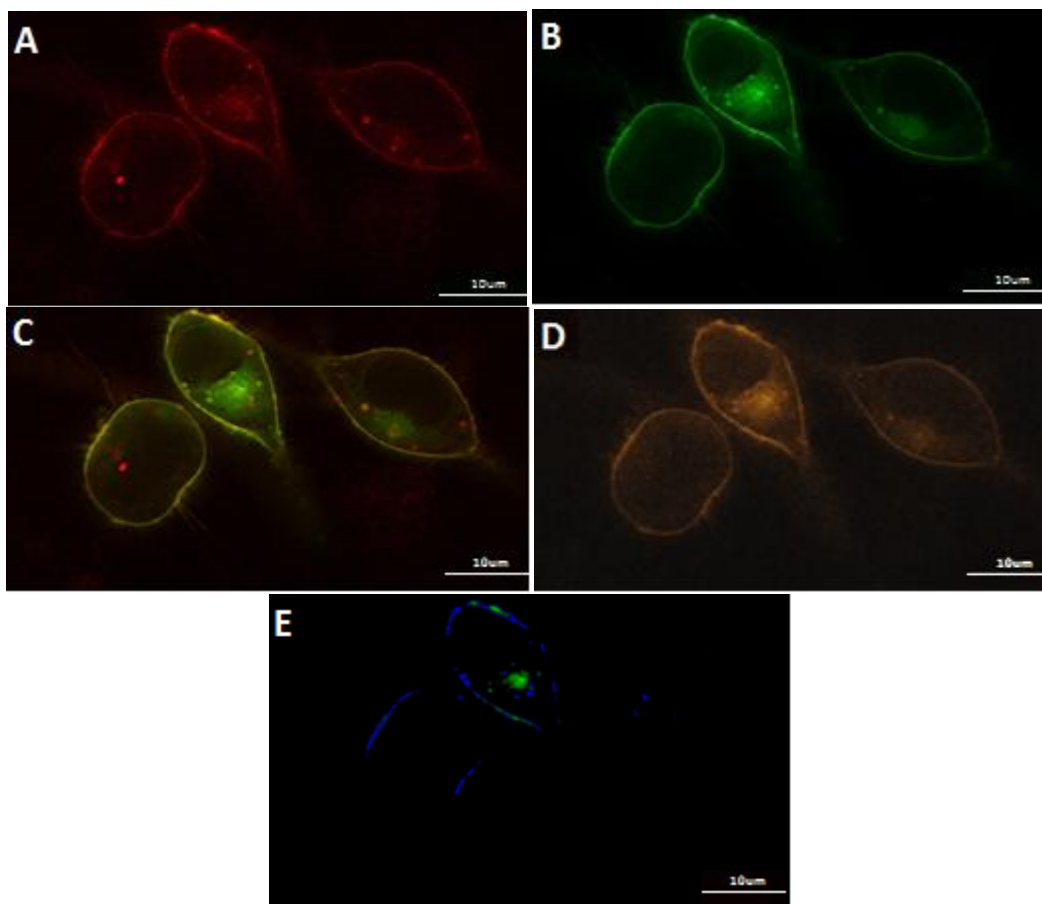
Figure 3.21 N2a cells transfected with $A_{2A}R$ + EGFP and $G\alpha_{13}$ + mCherry. Images were taken from mCherry channel excitation at 583 nm shows $G\alpha_{13}$ + mCherry (A), EGFP channel excitation at 482 nm shows $A_{2A}R$ + EGFP (B), Multiple channel shows co-localization of $A_{2A}R$+ EGFP and $G\alpha_{13}$ + mCherry (C) and FRET channel shows FRET signal (D) FRET efficiency shows pixels where FRET occurs (E).

After getting images, FRET efficiency was calculated by using imageJ pixFRET program. Histograms of region of interest were given the pixel counts and values of FRET efficiencies. To determine $G\alpha_{13}$ protein and A_{2A} receptor interaction, images from the cell treated with $A_{2A}R$ + EGFP and $G\alpha_{13}$ + mCherry proteins were analyzed and

82

mean of total efficiencies were calculated. It is found that average FRET efficiency was 7.1 % for $G\alpha_{13}$-A_{2A}.

For $G\alpha_{13}$-A_{2A}, total means of FRET efficiency was compared with other proteins. Also, specific range of FRET efficiencies was calculated and percentage of every range was computed from the histograms of PixFRET program.

3.6.2 Detection of physical interactions between Dopamine D_2 receptor and $G\alpha_{13}$ protein by using FRET technique

By using pre-prepared D_2R+EGFP constructs, N2a cells were transfected with 200 ng of pcDNA 3.1(-)_D_2R + EGFP and 200 ng of pcDNA 3.1(-)_$G\alpha_{13}$ + mCherry to investigate possible physical interactions between them. After that, images were taken from three different petri dishes N2a cells transfected with D_2R + EGFP, $G\alpha_{13}$ + mCherry and co-transfected with both D_2R + EGFP and $G\alpha_{13}$ + mCherry. After 24 hours, transfected N2a cells were imaged under Leica DMI 4000 equipped with Andor DSD2 spinning disk confocal microscope with 63X oil N1.4 objective By using PixFRET program, Fret efficiency was calculated. For bleed-through elimination, images from only D_2R + EGFP and only $G\alpha_{13}$ + mCherry transfected N2a cell images were used in this program. Images of mCherry tagged $G\alpha_{13}$ protein, EGFP tagged D_2R receptor, and FRET efficiency was shown in figure 3.22. Extra images are in Appendix H.
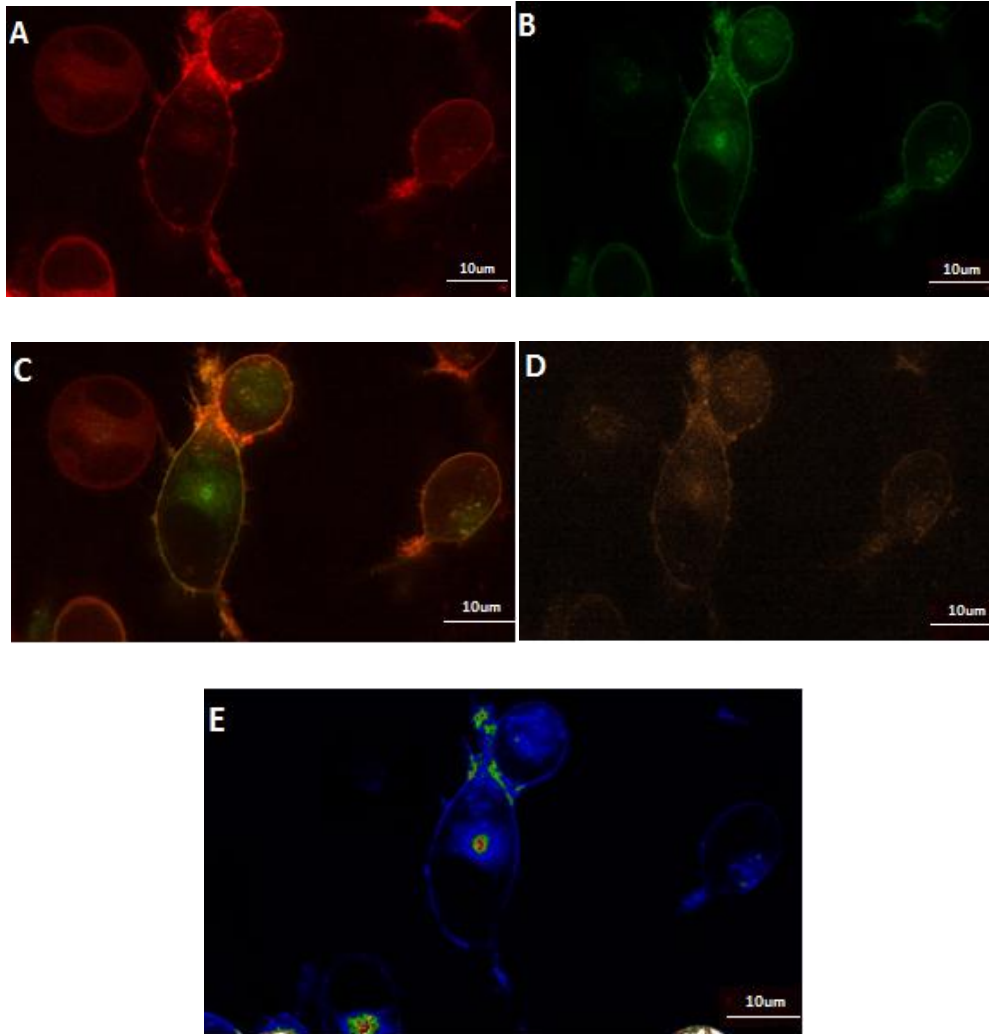
Figure 3.22 N2a cells transfected with D_2R + EGFP and $G\alpha_{13}$ + mCherry. Images were taken from mCherry channel excitation at 583 nm shows $G\alpha_{13}$ + mCherry (A), EGFP channel excitation at 482 nm shows D_2R + EGFP (B), Multiple channel shows co-localization of D_2R + EGFP and $G\alpha_{13}$ + mCherry (C) and FRET channel shows FRET signal (D) FRET efficiency shows pixels where FRET occurs (E).

After getting images, FRET efficiency was calculated by using imageJ pixFRET program. Histograms of region of interest were given the pixel counts and values of

FRET efficiencies. To determine $G\alpha_{13}$ protein and D_2 receptor interaction, images from the cell treated with D_2R + EGFP and $G\alpha_{13}$ + mCherry proteins were analyzed. Specific range of $G\alpha_{13}$ -D_2R and $G\alpha_{13}$-A_{2A} FRET efficiencies were shown in figure 3.23.
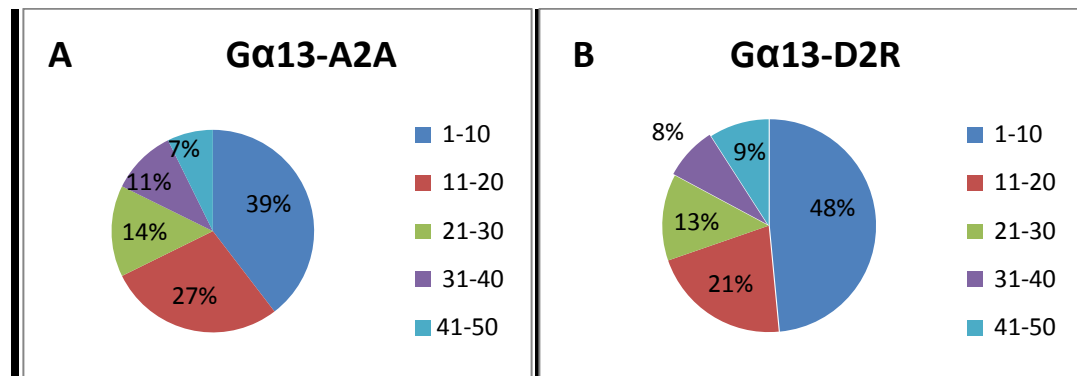
Figure 3.23 20 images were analyzed by pixFRET program, FRET efficiency of $G\alpha_{13}$-A_{2A} and $G\alpha_{13}$-D_2R were calculated, and percentage of every range was demonstrated. These ranges (1-10 %, 10-20 %, 20-30 %, 30-40 % and 40-50 %) were computed from the histograms of PixFRET program obtained for every range. Mean distributions of efficiency ranges in N2a cells co-transfected with A_{2A} + EGFP and $G\alpha_{13}$ + mCherry genes (A). Co-transfected with D_2R + EGFP and $G\alpha_{13}$ +mCherry genes (B)

The pie chart of $G\alpha_{13}$-A_2A has higher value of 11-50 % percentage of FRET efficiency range than $G\alpha_{13}$-D_2R.

3.6.3. Triple interaction detection between Adenosine homodimer and $G\alpha_{13}$ protein by using FRET technique

N2a cells were transfected with 500 ng of pcDNA 3.1(-)_$A_{2A}R$ + C-EGFP, 500 ng of pcDNA 3.1(-)_$A_{2A}R$+N-EGFP and 200 ng of pcDNA 3.1(-)_$G\alpha_{13}$ + mCherry to investigate possible physical interactions between A_{2A} homodimer and $G\alpha_{13}$. Images

were taken from three different petri dishes N2a cells transfected with $A_{2A}R$ + C-EGFP and $A_{2A}R$ + N-EGFP; $G\alpha_{13}$ + mCherry; co-transfected with three of them $A_{2A}R$ + C-EGFP, $A_{2A}R$ + N-EGFP and $G\alpha_{13}$ + mCherry. As described before, after 24 hours, transfected N2a cells were imaged and FRET efficiency was calculated. Images of mCherry tagged $G\alpha_{13}$ protein, N-EGFP, C-EGFP tagged A_{2A} receptor, and FRET efficiency were shown in figure 3.24.
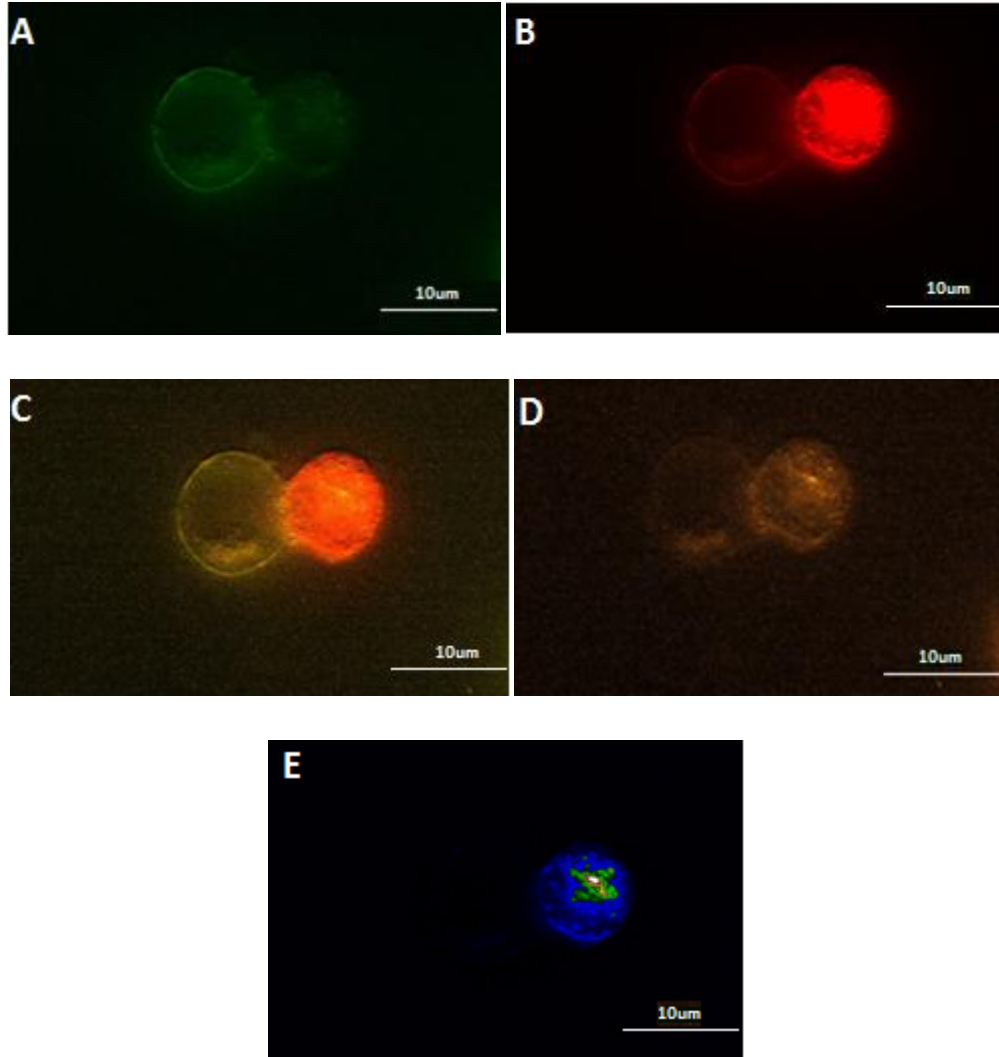
Figure 3.24 N2a cells transfected with A_{2A} + C-EGFP, A_{2A} + N-EGFP and $G\alpha_{13}$ + mCherry. Images were taken from EGFP channel excitation at 482 nm shows A_{2A} + C-EGFP and A_{2A} + N-EGFP (A) mCherry channel excitation at 583 nm shows $G\alpha_{13}$ + mCherry (B) Multiple channel shows co-localization of A_{2A} + C-EGFP, A_{2A} + N-EGFP and $G\alpha_{13}$ + mCherry. (C) FRET channel shows FRET signal (D) FRET efficiency shows pixels where FRET occurs (E).

After getting images, FRET efficiency was calculated by using imageJ pixFRET program. Histograms of region of interest were given the pixel counts and values of

FRET efficiencies. To determine $G\alpha_{13}$ protein and A_{2A} homodimer receptor interaction, images from the cell treated with $A_{2A}R+C$-EGFP, $A_{2A}R+N$-EGFP and $G\alpha_{13}$+mCherry proteins were analyzed and mean of total efficiencies were calculated. FRET efficiency was found 1.6 % for $G\alpha_{13}$ - homodimer A_{2A}. This means there is no interaction between A_{2A}/A_{2A} receptor and $G\alpha_{13}$, or the cells expressing these proteins are not healthy as seen from the morphology of the cells thus the FRET reported for these conditions are not reliable. Specific range of FRET efficiencies were calculated and percentage of every range was shown (see figure 3.18).

Total means of FRET efficiencies were calculated and compared with other proteins shown in figure 3.2
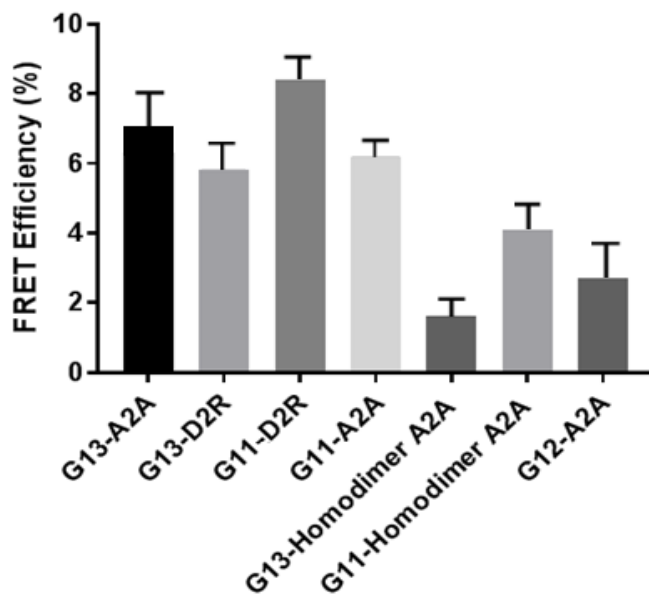
Figure 3.25 Graph of mean FRET efficiency for N2a cells transfected with $G\alpha_{13}$+mCherry-A_{2A}+EGFP, $G\alpha_{13}$+mCherry-D_2R+EGFP, $G\alpha_{11}$+mCherry-A_{2A}+EGFP, $G\alpha_{11}$+mCherry-D_2R+EGFP, $G\alpha_{13}$+mCherry-A_{2A}+NEGFP-A_{2A}+CEGFP, $G\alpha_{11}$+mCherry-A_{2A}+NEGFP-A_{2A}+CEGFP and $G\alpha_{12}$+EGFP-A_{2A}+mCherry genes. Mean of FRET efficiency for $G\alpha_{13}$-A_{2A} 7.1 %; $G\alpha_{13}$-D_2R 6.2 %; $G\alpha_{11}$-D_2R 8.4 %; $G\alpha_{11}$-A_{2A} 6.3 %; $G\alpha_{11}$-A_{2A} homodimer 4.1 %; $G\alpha_{13}$-A_{2A} homodimer 1.6 %; $G\alpha_{12}$-A_{2A} 2.7 %.

Mean of FRET efficiency was calculated and compared for each protein shown in colon graphic. With this analysis, it has been demonstrated that, images obtained from $G\alpha_{11}$+mCherry and D_2R+EGFP transfected N2a cells has the highest FRET signal, mostly coming from cell membrane. This indicates $G\alpha_{11}$ protein interacts with D_2R receptor more than other ones. Additionally, $G\alpha_{13}$-A_{2A} protein receptor interaction has been shown with 7.1 % FRET efficiency on average which is less than $G\alpha_{11}$-D_2R dimer but higher than the others. These proteins probably interact with each other. On the other hand mean of FRET efficiency of $G\alpha_{13}$ and $G\alpha_{11}$-homodimer A_{2A}, $G\alpha_{12}$-A_{2A} gave very low signal and the calculated FRET efficiency was not trustable. Low FRET signal shows slight interaction or no interact with each other. Another possibility is that these proteins are interacting but the configuration and the distance between the fluorophores are not suitable to observe FRET. In our study as we tested several positions for each tagging this possibility is less likely to occur but still probable. Triple interaction of A_{2A} homodimer and $G\alpha_{11}$ or $G\alpha_{13}$ is hard to detect. Additionally, this would be due to plasmid transfection efficiency. It is possible that N2a cells can take two different plasmids inside of the cell more easily than three different plasmids ($G\alpha_{13}$, A_{2A}-N EGFP and A_{2A}-C EGFP) at the same time. Although A_{2A}-N EGFP and A_{2A}-C EGFP split proteins were in close distance to give FRET signal, they may not orient properly to complement each other.

CHAPTER 4

CONCLUSION

The aim of our study was to analyze the expression of fluorescently labeled $G\alpha_{11}$, $G\alpha_{12}$, $G\alpha_{13}$ proteins in live N2a (mouse neuroblastoma) cells and investigate interaction of these G proteins with Adenosine A_{2A}, dopamine D_2 receptors and adenosine homodimer A_{2A}/A_{2A} by using Bimolecular Fluorescence Complementation (BiFC) and Fluorescent Resonance Energy Transfer (FRET) assays.

$G\alpha_{11}$, $G\alpha_{12}$, $G\alpha_{13}$ proteins were successfully labeled with both EGFP and mCherry proteins from five different positions and were transfected into N2a cells to see the fluorescent signal location and intensity. mCherry tagged $G\alpha_{11}$ and $G\alpha_{13}$ proteins had very good signal intensity, but $G\alpha_{12+}$mCherry proteins did not gave detectable fluorescent signals. Therefore in this study, for FRET experiments, EGFP tagged $G\alpha_{12}$ fused proteins were used. After the construction of the tagged protein genes, $G\alpha_{11,}$ $G\alpha_{12,}$ $G\alpha_{13}$ protein coding gene carriying plasmids were transfected to N2a cells, $G\alpha_{11+}$mCherry 244th, $G\alpha_{12+}$EGFP 265th and $G\alpha_{13+}$mCherry 260th position signals were detected mostly on the plasma membrane with high intensity. For these tagged G proteins, RhoA functional assay was done, results suggest that tagging was successful and protein function was not altered. Fluorophore tagged $G\alpha_{11,}$ $G\alpha_{12,}$ $G\alpha_{13}$ proteins and their wild types are not significantly different from each other. These results indicate, tagging positions of proteins are not interfaring with the functional regions and these regions do not affect proteins activity.

Possible dimerization of $G\alpha_{11}$, $G\alpha_{12}$, $G\alpha_{13}$ and A_{2A}, D_2R, A_{2A}/A_{2A} were studied with FRET method. At the end of FRET study, dimerization of $G\alpha_{11}$-A_{2A}, $G\alpha_{11}$-D_2R, $G\alpha_{11}$-A_{2A}/A_{2A}; $G\alpha_{12}$-A_{2A}, $G\alpha_{12}$-D_2R, $G\alpha_{12}$-A_{2A}/A_{2A}; $G\alpha_{13}$-A_{2A}, $G\alpha_{13}$-D_2R, $G\alpha_{13}$-A_{2A}/A_{2A} have been observed and quantified in live N2a cells. Imaging had been carried out using spinning disc confocal microscopy and FRET signal of these dimers was calculated by pixFRET computer application. Interaction of these proteins with A_{2A} and D_2R receptors has been shown using FRET method for the first time. Also both BiFC and FRET techniques were used to study triple interaction comprising A_{2A} homodimer and $G\alpha$ proteins in a single complex. Combination of these two methods' optimization was used to understand homo-or heterooligomeric protein complexes consist of $G\alpha$ proteins and receptors interaction.

According to recent studies, it is not certain that $G\alpha_{q/11}$ protein interacts with A_{2A} or D_2 receptors. D_2 receptor is coupled to $G\alpha_{i/o}$ but D_1/D_2 heteromer formation binds to $G\alpha_{q/11}$ to activate PLC signaling. On the other hand, D_3 receptor which is the other member of D_2 like receptors signal via $G\alpha_o$, $G\alpha_z$ and $G\alpha_{q/11}$ with regard to different cell types (Neve A.K *et al.,* 2004) (Ferré S. *et al*., 2008). In our study, experiment result shows 11-20 % percentage of FRET efficiency range of $G\alpha_{11}$-D_2R was 31 %. This indicates that, there is an interaction between $G\alpha_{11}$ and D_2 receptor on plasma membrane. However, we cannot rule out the possibility of D_2 receptor which was shown to couple with $G\alpha_{11}$ protein in our study may also couple with D_1 receptor as a D_1/D_2 heteromer formation and what we observe was due to D_1-$G\alpha_{11}$ interaction. Further studies are needed to identify that if D_2 receptor couples with $G\alpha_{11}$ protein was heteromer or monomer formation.

Moreover, it has been suggested that $A_{2A}R$ may signal through $G\alpha_{12/13}$ proteins in human endothelial cells. Also, in human microvascular cells, $A_{2B}R$ has a role in angiogenic factor expression via $G\alpha_q$, and possibly via $G\alpha_{12/13}$ (Feoktistov I. et al., 2002). $G\alpha_{12/13}$

protein regulates actin cytoskeleton and cell migration through activation of Rho kinases. In addition, cell migration is effected with A_{2A} receptor positively (Connor K. and Chen M. 2013; Fernandez P. *et al.,* 2012). In this study, interaction of $G\alpha_{13}$ protein with A_{2A} receptor has been shown by using FRET method for the first time. However, there is no significant FRET results obtained from $G\alpha_{12}$ protein and A_{2A} receptor interaction.

Mean of FRET efficiency and different FRET efficiency ranges were calculated and compared with each protein. With this analysis, it has been demonstrated that, images taking from $G\alpha_{11}$+mCherry and D_2R+EGFP transfected N2a cells; $G\alpha_{13}$+mCherry and A_{2A}+EGFP have high FRET signal mostly coming from cell membrane. $G\alpha_{13}$-D_2R, $G\alpha_{11}$-A_{2A} and $G\alpha11$-A_{2A}/A_{2A} pairs gave less signal than $G\alpha_{11}$-D_2R and $G\alpha_{13}$-A_{2A} ones. To be sure if they are also interacting with each other, further experiments should be done to support this idea, because their FRET signal was not very low like $G\alpha_{12}$-A_{2A} and $G\alpha_{13}$-A_{2A}/A_{2A} pairs. According to our results, $G\alpha_{12}$-A_{2A} and $G\alpha_{13}$-A_{2A}/A_{2A} probably are not coupling with each other.

In further studies, positive and negative control should be added to confirm our FRET analysis. For this purpose, another subtype of Adenosine and Dopamine receptors which are certainly interact with $G\alpha_{11,}$ $G\alpha_{12,}$ $G\alpha_{13}$ proteins should be taged with fluorescent protein as a positive control. For negative control, receptors that are not coupled with these G proteins should be choosen and FRET signals should be compared. In addition, triple interaction of these receptors and G proteins should be studied such as, D_2R and A_{2A} heterodimer or D_2R and D_2R homodimer interaction with $G\alpha_{11}$, $G\alpha_{12}$ and $G\alpha_{13}$ proteins. Since, different dimers may cause receptors to follow different pathways. Also, $G\alpha_{11}$ and D_1/D_2 triple interaction should be conducted to further analyze our $G\alpha_{11}$-D_2 receptor interaction result.

REFERENCES

Abbracchio M.P., Burnstock G., Verkhratsky A., Zimmermann H. (2009) Purinergic signaling in the nervous system: an overview, *Trends Neurosci*. 32, 19–29.

Agnati L.F., Ferre S., Lluis C., Franco R., Fuxe K. (2003) Molecular mechanisms and therapeutical implications of intramembrane receptor/receptor interactions among heptahelical receptors with examples from the striatopallidal GABA neurons, *Pharmacol. Rev*. 55, 509–550.

Albertazzi L., Marchetti A. L., Ricci F. and Beltram F. (2009) Quantitative FRET Analysis With the E0GFP-mCherry Fluorescent Protein Pair, *Photochemistry and Photobiology* 85, 287–297.

Ares-Santos S., Granado N. & Moratalla R. (2013) The role of dopamine receptors in the neurotoxicity of methamphetamine, *Journal of Internal Medicine*. 273, 437–453.

Bansal G., Druey K.M., and Xie Z. (2007) R4 RGS Proteins: Regulation of G Protein Signaling and Beyond, *Pharmacol* 116(3), 473–495.

Beaulieu J.M., Gainetdinov R. R., Sibley D.R. (2011) The Physiology, Signaling, and Pharmacology of Dopamine Receptors, *Pharmacological Reviews* 63 (1), 182-217.

Bhattacharyya R., Wedegaertner B.P. (2000) Ga13 Requires Palmitoylation for Plasma Membrane Localization, Rho-dependent Signaling, and Promotion of p115-RhoGEF Membrane Binding, *J Biol Chem* Vol. 275, 14992–14999.

Bourne, H. R., Sanders, D. A. and McCormick, F. (1991) The GTPase superfamily conserved tructure and molecular mechanism, *Nature* 349, 117-27.

Broussard J.A., Rappaz B., Webb J.D., and Brown M.C. (2013) Fluorescence resonance energy transfer microscopy as demonstrated by measuring the activation of the serine/threonine kinase Akt, *Nat Protoc.* 8(2), 265–281.

Cabrera-Vera, T. M., Vanhauwe, J., Thomas, T. O., Medkova, M., Preininger, A., Mazzoni, M.R. and Hamm, H. E. (2003) Insights into G protein structure, function, and regulation, *Endocr Rev* 24, 765-81.

Canals M., Marcellino D., Fanelli F., Ciruela F., de Benedetti P., Goldberg S.R., Neve K., Fuxe K., Agnati L.F., Woods A.S., Ferré S., Lluis C., Bouvier M., Franco R. (2003) Adenosine A2A-dopamine D2 receptorreceptor heteromerization: qualitative and quantitative assessment by fluorescence and bioluminescence energy transfer, *J Biol Chem*; 278,46741–9.

Ciruela F., Gómez-Soler M., Guidolin D., Borroto-Escuela D. O., Agnati L. F., Fuxe K., Víctor Fernández-Dueñas (2011) Adenosine receptor containing oligomers: Their role in the control of dopamine and glutamate neurotransmission in the brain, *Biochimica et Biophysica Acta* 1808, 1245–1255.

Ciruela F., Vilardaga J.P., Fernandez-Duenas V. (2010) Lighting up multiprotein complexes: lessons from GPCR oligomerization, *Trends Biotechnol* 28, 407–415.

Clapham D.E. and Neer E.J. (1997) G protein beta gamma subunits, *Pharmacol Toxicol.* 37, 167-203.

Day R. D. and Davidson M.W. (2012) Fluorescent proteins for FRET microscopy: Monitoring protein Interactions in living cells, *Bioessays* 34, 341–350.

Day R. D., Periasamy A., Schaufele F. (2001) Fluorescence Resonance Energy Transfer Microscopy of Localized Protein Interactions in the Living Cell Nucleus. *Methods* 25**,** 4–18.

Demidov V.V., Dokholyan V.N., Witte-Hoffmann C., Chalasani P., Wei Yiu H., Din F., Yu Y., Cantor R.C., Broude N.E. (2006) Fast complementation of split fluorescent protein triggered by DNA hybridization, *National Academy of Sciences* 103, 2052 2056.

Gandia J., Galino J., Amaral O.B. Soriano A., Lluís C., Franco, R., Ciruela F. (2008) Detection of higher-order G protein-coupled receptor oligomers by a combined BRET–BiFC technique. *FEBS Lett*, 582(20), 2979-84

Dhanasekaran N., Dermott J.M. (1996) Signaling by the G12 class of G proteins. *Cellular Signalling***,** Volume 8, Issue 4. Pages 235–245.

Dickenson J.M. and Hill S.J. (1998) Involvement of G-protein βγ subunits in coupling the adenosine A1 receptor to phospholipase C in transfected CHO cells, *Eur J Pharmacol* 355, 85-93.

Donoso M.V., Lopez R., Miranda R., Briones R., Huidobro-Toro J.P. (2005) A2B adenosine receptor mediates human chorionic vasoconstriction and signals through the arachidonic acid cascade, *Am J Physiol Heart Circ Physiol* 288, H2439–H2449.

Dupre D.J., Robitaille M., Ethier L.R., Villeneuve L.R., Mamarbachi A.M., Hebert T.E. (2006) Seven transmembrane receptor core signaling complexes are assembled prior

To plasma membrane trafficking, *J. Biol. Chem*. 281, 34561–34573.

Feoktistov I. and Biaggioni I. (1995) Adenosine A2B receptors evoke interleukin secretion in human mast cells. An enprofylline-sensitive mechanism with implicationsfor asthma. *J. Clin. Invest* 96, 1979–1986.

Feoktistov I., Goldstein A.E., Ryzhov S., Zeng D., Belardinelli L., Voyno-Yasenetskaya T.,Biaggioni I. (2002) Differential Expression of Adenosine Receptors in Human Endothelial Cells Role of A2B Receptors in Angiogenic Factor Regulation. *Circulation Research* 90, 531-538.

Ferré S., Quiroz C., Woods A.S., Cunha R., Popoli P., Ciruela ., Lluis C., Franco R., Azdad K., and Schiffmann S.N. (2008) An Update on Adenosine A2A-Dopamine D2 receptor interactions.Implications for the Function of G Protein-Coupled Receptors, *Curr Pharm Des* 14(15), 1468–1474.

Flower D.R. (1999) Modelling G-protein-coupled receptors for drug design. *Biochim Biophys Acta*. 16;1422(3), 207-34.

Fredholm B.B., Chen J.F., Cunha R.A., Svenningsson P., Vaugeois J.M. (2005) Adenosine and brain function, *Int. Rev. Neurobiol* 63, 191–270.

Fredholm B.B., Irenius E., Kull B., Schulte G. (2001) Comparison of the potency of adenosine as an agonist at human adenosine receptors expressed in Chinese hamster ovary cells, *Biochem. Pharmacol* 61, 443–448

Fredholm B.B. (1995) Purinoceptors in the nervous system, *Pharmacol. Toxicol* 76, 228–239.

Fukuhara S., Chikumi H., Gutkind J.S. (2001) RGS-containing RhoGEFs: the missing link between transforming G proteins and Rho? *Oncogene* 20, 1661–1668.

Fukuhara S., Murga C., Zohar M., Igishi T., Gutkind J.S. (1999) A novel PDZ domain containing guanine nucleotide exchange factor links heterotrimeric G proteins to Rho. *J Biol Chem* 274, 5868–5879.

Garritsen A., Van Galen P. J., and Simonds W. F. (1993) The N-terminal coiled-coil domain of beta is essential for gamma association: a model for G-protein beta gamma subunit interaction. *Proc Natl Acad Sci U S A* 90, 7706-10.

Gilchrist A., Li A., Hamm H.E. (2002) G alpha COOH-terminal minigene vectors dissect heterotrimeric G protein signaling, *Sci STKE* (118):pl1.

Gines S., Hillion J., Torvinen M., Le Crom S., Casado V., Canela E.I., Rondin S., Lew J.Y., Watson S., Zoli M., Agnati L.F., Verniera P., Lluis C., Ferre S., Fuxe K., Franco R. (2000) Dopamine D1 and adenosine A1 receptors form functionally interacting heteromeric complexes, *Proc. Natl Acad. Sci.* 97, 8606–8611.

Hallak H., Muszbek L., Laposata M., Belmonte E., Brass L. F. and Manning D. R. (1994). Covalent binding of arachidonate to G protein alpha subunits of human platelets. *J Biol Chem* 269, 4713-6.

Hanoune J. and Defer N. (2001) Regulation and Role of Adenylyl cyclase isoforms. *Annu Rev Pharmacol Toxicol* 41,145-174.

Hermans M.J.W. (2008) Visualizing G protein signaling in living cells. *Swammerdam Institute for Life Sciences (SILS)*. Chapter 1 GPCR signaling. uvapub:53292.

Hu C.D. and Kerppola T.K. (2003) Simultaneous visualization of multiple protein interactions in living cells using multicolor fluorescence complementation analysis. *Nat Biotechnol* 21,539–45.

Jaber M., Robinson S.W., Missale C., Caron G.M. (1996) Dopamine Receptors and Brain Function. *Neuropharmacology* 35, 1503-1519

Jacobson A.K. and Gao Z.G. (2006) Adenosine receptors as therapeutic targets. *Nat Rev Drug Discov* 5(3), 247–264.

Jiang Y., Ma W., Wan Y., Kozasa T., Hattori S., Huang X. (1998). The G protein Gα12 stimulates Bruton's tyrosine kinase and a rasGAP through a conserved PH/BM domain. *Nature* 395, 808.

Kamiya T, Saitoh O, Yoshioka K, Nakata H. Oligomerization of adenosine A2A and dopamine D2 receptors in living cells. *Biochem Biophys Res Commun* 27(306), 544–9.

Kelly P., Moeller B.J., Juneja J., Booden M.A., Der C.J., Daaka Y., Dewhirst MW., Fields T.A., Casey P.J. (2006) The G12 family of heterotrimeric G proteins promotes breast cancer invasion and metastasis. *Proc Natl Acad Sci* 103, 8173-8178.

Kerppola, T. K. (2006). Design and implementation of bimolecular fluorescence complementation (BiFC) assays for the visualization of protein interactions in living cells, *Nature Protocols 1*, 1278–1286.

Kerppola, T. K. (2008). Bimolecular Fluorescence Complementation: Visualization of Molecular Interactions in Living Cells, *Methods in Cell Biology* 85, 431-70.

Kleuss C., and Krause E. (2003) Galpha(s) is palmitoylated at the N-terminal glycine, *Embo J* 22, 826-32.

Kull B., Svenningsson P., Fredholm BB. (2000) Adenosine A2A receptors are colocalized with and activate Golf in rat striatum, *Mol. Pharmacol*. 58,771–777.

Latek D., Modzelewska A, Trzaskowski B., Palczewski K., Filipek S., (2012) G protein coupled receptors — recent advances, *Acta Biochim Pol*. 59(4), 515–529.

Lee S.P., So C.H., Rashid A.J., Varghese G., Cheng R., Lanca A.J., O'Dowd B.F. George S.R. (2004) Dopamine D1 and D2 Receptor Co-activation Generates a Novel Phospholipase C-mediated Calcium Signal, *J Biol Chem* 279,35671–35678.

Liu L.X., Burgess L.H., Gonzalez A.M., Sibley D.R., Chiodo L.A. (1999) D2S, D2L, D3, and D4 dopamine receptors couple to a voltage-dependent potassium current in N18TG2x mesencephalon hybrid cell (MES-23.5) via distinct G proteins, *Synapse* 31,108–118.

Liu, W. and Northup J. K. (1998). The helical domain of a G protein alpha subunit is a regulator of its effector, *Proc Natl Acad Sci U S A* 95, 12878-83.

Marala R.B. and Mustafa S.J. (1993) Direct evidence for the coupling of A2-adenosine receptor to stimulatory guanine nucleotide-binding-protein in bovine brain striatum, *J. Pharmacol.* 266, 294–300.

Marrari Y., Crouthamel M., Irannejad R., Wedegaertner P.B. (2007). Assembly and Trafficking of Heterotrimeric G Proteins. *Biochemistry*. 46(26), 7665−7677.

Massotte D. (2015) Monitoring endogenous GPCRs: lessons for drug design, *Front Pharmacol.* 6, 146.

Michaelson D., Ahearn I., Bergo M., Young S., Philips M. (2002) Membrane Trafficking of Heterotrimeric G Proteins via the Endoplasmic Reticulum and Golgi, *Molecular Biology of the Cell Vol*. 13, 3294–3302.

Milligan G. and Bouvier M. (2005) Methods to monitor the quaternary structure of G protein-coupled receptors, *FEBS Journal* 272, 2914–2925.

Milligan G. and Kostenis E. (2006) Heterotrimeric G-proteins: a short history. *British Journal of Pharmacology* 147, S46–S55.

Missale C., Nash S.R., Robinson S.W., Jaber M., Caron M.G. (1998) Dopamine receptors: from structure to function, *Physiol Rev* 78,189–225.

Mizuno N. and Itoh H. (2009).Functions and Regulatory Mechanisms of Gq-Signaling Pathways, *Neurosignals* 17,42–54.

Moers A., Nürnberg A., Goebbels S., Wettschureck N., Offermanns S. (2008) Gα12/Gα13 deficiency causes localized over migration of neurons in the developing cerebral and cerebellar cortices, *Mol. Cell. Biol.* 28, 1480–1488.

Neve A.K., Seamans J.K., Trantham-Davidson H. (2004) Dopamine Receptor Signaling. *Journal of Receptors And Signal Transduction* 24, 165–205.

Neves R.S., Ram T. P., Iyengar R. (2002) G Protein Pathways, *Science* 296(5573),1636-9.

Obadiah J., Avidor-Reiss T., Fishburn C.S., Carmon S., Bayewitch M., Vogel Z., Fuchs S., Levavi-Sivan B. (1999) Adenylyl cyclase interaction with the D2 dopamine receptor family: differential coupling to Gi, Gz, and Gs, *Cell Mol Neurobiol* 19,653–664.

Offermanns S., Mancino V., Revel J-P., and Simon M.I. (1997) Vascular system defects and impaired cell chemokinesis as a result of Gα13 deficiency, *Science* 275,533-536.

Offermanns S., Simon M.I. (1995) Gα15 and Gα16 couple a wide variety of receptors to phospholipase C, *J. Biol. Chem* 270:15175–15180.

Oldham W. M. and Hamm E. H. (2008) Heterotrimeric G protein activation by G-protein-coupled receptors, *Nature Reviews Molecular Cell Biology* 9, 60-71

Palmer T.M., Stiles G.L. (1995) Adenosine receptors, *Neuropharmacology* 34,683–694.

Pollok B.A., and Heim R. (1999). Using GFP in FRET-based applications, *Trends Cell Biol.*9, 57–60.

Purves D., Augustine G.J., FitzpatrickD., Katz L.C., LaMantia A.S., McNamara J.O., and Williams S.M.. (2001) *Neuroscience* 10, 87893-742-0.

Ram P.T. and Iyengar R. (2001) G protein coupled receptor signaling through the Src and Stat3 pathway: role in proliferation and transformation, *Oncogene* 20, 1601 1606.

Rashid A.J., So C.H., Kong M.C., Furtak T., El-Ghundi M., Cheng R., O'Dowd B.F.,

and George R.S.(2007) D1–D2 dopamine receptor heterooligomers with unique pharmacology are coupled to rapid activation of Gq/11 in the striatum, *Proc Natl AcadSci U S A*.104(2):654-9.

Reid E.A., Kristo G., Yoshimura Y., Ballard-Croft C., Keith B.J., Mentzer R.M., Lasley R.D (2005). In vivo adenosine receptor preconditioning reduces myocardial infarct size via subcellular ERK signaling, *Am. J. Physiol. Heart Circ. Physiol* 288, 2253–H2259.

Rens-Domiano S. and Hamm H. E. (1995). Structural and functional relationships of heterotrimeric G-proteins, *Faseb J* 9, 1059-66.

Ryzhov S., Goldstein A.E., Biaggioni I., Feoktistov I. (2006) Cross-talk between Gs- and Gq-coupled pathways in regulation of interleukin-4 by A2B adenosine receptors in human mast cells, *Mol. Pharmacol.* 70, 727–735.

Scheffzek K., Ahmadian M. R., Kabsch W., Wiesmuller L., Lautwein A., Schmitz F. and Wittinghofer A. (1997). The Ras-RasGAP complex: structural basis for GTPase activation and its loss in oncogenic Ras mutants. *Science* 277, 333-8.

Schoneberg T., Schulz A., Biebermann H., Hermsdorf T., Rompler H., Sangkuhl K. (2004). Mutant G-protein-coupled receptors as a cause of human diseases *Pharmacol Ther 104*,173–206.

Schulte G. (2002).Adenosine Receptor Signaling and the Activation of Mitogen-Activated Protein Kinases.Department of Physiology and Pharmacology Karolinska Institutet.

Sebastiao A.M., Ribeiro J.A. (2000) Fine-tuning neuromodulation by adenosine, Trends *Pharmacol.* Sci. 21, 341–346.

Sedaghat K., Nantel M.F.,Ginsberg S., Lalonde V., and Tiberi M. (2006) Molecular Characterization of Dopamine D2 Receptor Isoforms Tagged With Green Fluorescent Protein, *Molecular Biotechnology* 34, 1073–6085.

Sekar R.B. and Periasamy A (2003) Fluorescence resonance energy transfer (FRET) microscopy imaging of live cell protein localizations. *The Journal of Cell Biology*, 160;5, 629–633.

Shi C. S., Kehrl J. H, (2001) PYK2 Links $G_q\alpha$ and $G_{13}\alpha$ Signaling to NF-κB Activation. *J. Biol. Chem.* 276, 31845.

Shi CS., Sinnarajah S., Cho H., Kozasa T., Kehrl J.H (2000) G13alpha-mediated PYK2 activation. PYK2 is a mediator of G13alpha -induced serum response element-dependent transcription, *J Biol Chem*. 275(32), 24470-6

Siehler S. (2007) G 12/13 -dependent signaling of G-protein-coupled receptors:disease context and impact on drug discovery*, Drug Discov*. 2(12),1591-1604.

Siehler S. (2009) Regulation of RhoGEF proteins by G12/13-coupled Receptors. *British Journal of Pharmacology* 158, 41–49.

Surmeier D.J, Bargas J., Hemmings Jr H.C., Nairn A.C., Greengard P. (1995) Modulation of calcium currents by a D1 dopaminergic protein kinase/phosphatase cascade in rat neostriatal neurons. *Neuron* 14, 385–397.

Surmeier D.J, Ding J., Day M., Wang Z., Shen W. (2007) D1 and D2 dopamine-receptor modulation of striatal glutamatergic signaling in striatal medium spiny neurons. *Trends Neurosci*. 30, 228–35.

Suzuki N., Hajicek N., Kozasa T., (2009) Regulation and Physiological Functions of G12/13-Mediated Signaling Pathways. *Neurosignals* 17, 55–70.

Taraskevich P.S, Douglas W.W. (1990) Dopamine (D2) or gamma-aminobutyric acid (GABAB) receptor activation hyperpolarizes rat melanotrophs and pertussis toxin blocks these responses and the accompanying fall in $[Ca^{2+}]i$. *Neurosci Lett* 112, 205–9.

Thevananther S., Rivera A. and Rivkeesca A.S. (2001) A1 adenosine receptor activation inhibit neurite process formation by rho kinase mediated pathways. *Molecular Neuroscience*. Vol: 12 No:14

Thomsen W., Frazer J. and Unett D. (2005) Functional assays for screening GPCR targets.
Current Opinion in Biotechnology 16,655–665

Vaiskunaite R., Kozasa T., Voyno-Yasenetskaya T.A. (2001) Interaction between the Ga subunit of heterotrimeric G12 protein and Hsp90 is required for Ga12 signaling, *J. Biol. Chem*. 276, 46088–46093.

Vallone D., Picetti R., Borrelli E., (2000) Structure and function of dopamine receptors. *Neuroscience and Biobehavioral Reviews* 24, 125–132.

Warner D. R. and Weinstein L. S. (1999) A mutation in the heterotrimeric stimulatory guanine nucleotide binding protein alpha-subunit with impaired receptor-mediated activation because of elevated GTPase activity. *Proc Natl Acad Sci U S A* 96, 4268-72.

Wettschureck N. and Offermanns S. (2005) Mammalian G Proteins and Their Cell Type Specific Functions. *Physiol Rev* 85: 1159–1204

Williams J. A. (2011) Galpha12/13. The pancreapedia.Version 1.0, March 1, 2011 [DOI: 10.3998/panc.2011.7].

Wise A., Parenti M., Milligan G (1997) Interaction of the G-protein $G_{11}\alpha$ with receptors and phosphoinositidase C: The contribution of G-protein palmitoylation and membrane association *FEBS Letters* 407(3), 257-260

Woods A.S., Ferre S. (2005) Amazing stability of the arginine-phosphate electrostatic interaction, *J. Proteome Res.* 4,1397–1402.

Worzfeld T., Wettschureck N. and Offermanns S. (2008) G12/G13-mediated signalling in mammalian physiology and disease, *Trends in Pharmacological Sciences*. 29,11.

Wu J., Xie N., Zhao X., Nice E. C., and Huang, C. (2012). Dissection of aberrant GPCR signaling in tumorigenesis a systems biology approach. *Cancer* 116 *Genomics & Proteomics*, *9*, 37–50.

Yamazaki J., Katoh H, Yamaguchi Y., Negishi M. (2005) Two G12 family G proteins, Ga12 and Ga13, show different subcellular localization. *Biochemical and Biophysical Research Communications* 332, 782–786.

Yan Y., Chi P. P. and Bourne R. H. (1997) RGS4 Inhibits G_q-mediated Activation of Mitogen-activated Protein Kinase and Phosphoinositide Synthesis. *The Journal of Biological Chemistry* 272,11924-11927.

Yasenetskaya V., Tatyana A., Michel F. P., Natalie A. G. (1996). Gα12 and Gα13 regulate extracellular signal-regulated kinase and c-Jun kinase pathways by different mechanisms in COS-7 cells. *J. Biol. Chem*. 271, 21081–21087.

Zamyatnin A.A., Solovyev A.G., Bozhkov P.V., Valkonen J.P, Morozov S.Y., Savenkov E.I. (2006) Assessment of the integral membrane protein topology in living cells. *Plant Journal*. 46,145–154.

Zhu D., Kosik K.S., Meigs T. E., Yanamadala V., Denker B. M. (2004) Ga12 directly interacts with PP2A: evidence for Ga12-stimulated PP2A phosphatase activity and dephosphorylation of microtubule- associated protein, tau, *J. Biol. Chem*. 279, 54983–54986.

APPENDİX A

COMPOSITIONS OF CELL CULTURE SOLUTIONS

Table A. 1 Composition of D-MEM with high glucose

COMPONENT	CONCENTRATION (mg/L)
Amino Acids	
Glycine	30
L-Arginine hydrochloride	84
L-Cysteine 2HCl	63
L-Glutamine	580
L-Histidine hydrochloride-H_2O	42
L-Isoleucine	105
L-Leucine	105
L-Lysine hydrochloride	146
L-Methionine	30
L-Phenylalanine	66
L-Serine	42
L-Threonine	95
L-Tryptophan	16
L-Tyrosine	72
L-Valine	94
Vitamins	
Choline chloride	4
D-Calcium pantothenate	4

Table A.4 Continued

Folic acid	4
Niacinamide	4
Pyridoxine hydrochloride	4
Riboflavin	0.4
Thiamine hydrochloride	4
i-Inositol	7.2
Inorganic Salts	
Calcium chloride	264
Ferric nitrate	0.1
Magnesium sulfate	200
Potassium chloride	400
Sodium bicarbonate	3700
Sodium chloride	6400
Sodium phosphate monobasic	141
Other components	
D-Glucose (Dextrose)	4500
Phenol Red	15
Sodium pyruvate	110

Table A. 2 Composition of 1X Phosphate Buffered Saline (PBS) solution

NaCl	8 g/L
KCl	0.2 g/L
Na_2HPO_4	1.44 g/L
KH_2PO_4	0.24 g/L

The components are dissolved within dH2O. After adjustment of pH to 7.4, solution is autoclaved.

APPENDIX B

COMPOSITION AND PREPARATION OF BACTERIAL CULTURE MEDIUM

Luria Bertani (LB) Medium

10 g/L Tryptone

5 g/L Yeast Extract

5 g/L NaCl

15 g/L agar is added for solid medium preparation.

The pH of the medium is adjusted to 7.0.

APPENDIX C

COMPOSITIONS OF BUFFERS AND SOLUTIONS

1X NEB-CutSmartTM Buffer:

50 mM Potassium Acetate

20 mM Tris-acetate

10 mM Magnesium Acetate

100 μg/ml BSA

pH 7.9 at 25°C

1X T4 DNA Ligase Reaction Buffer:

50 mM Tris-HCl

10 mM MgCl2

1 mM ATP

10 mM Dithiothreitol

pH: 7.5 at 25°C

6X Loading Dye :

10 mM Tris-HCl (pH: 7.6)

0.03% Bromophenol Blue

0.03% Xylene Cyanol FF

60% Glycerol

60 mM EDTA

PLASMID MAPS
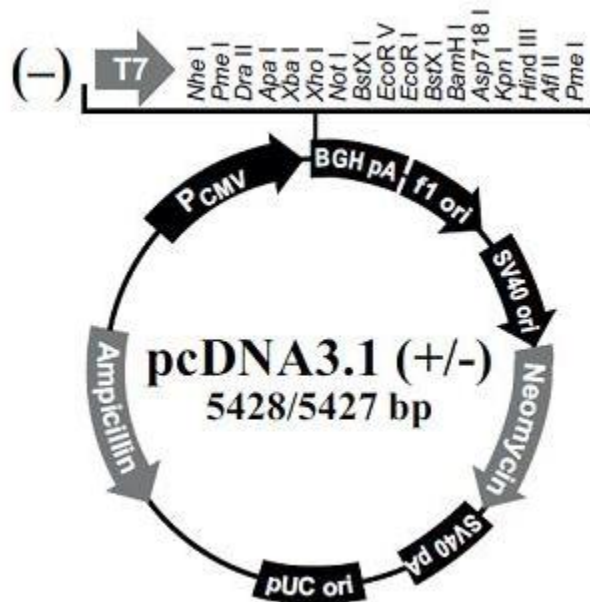
Figure D. 1 Map of pcDNA 3.1 (-) (taken from Invitrogen® Life Technologies)

APPENDIX E

PRIMERS

Table E.1 Primers to amplify EGFP/mCherry tag with Gα overhangs and linker according to insertion position.

Gα11	244aa	EGFP/mCh forward	5'-CAA GTC CTG GTG GAG TCG GAC AAC TCT GGA GGA GGA GGA TCT ATG GTG AGC AAG GGC GAG-3'
		EGFP/mCh reverse	5'-TTT GCT CTC CTC CAT CCG GTT CTC AGA TCC TCC TCC TCC AGA CTT GTA CAG CTC GTC CAT-3'
Gα12	265aa	EGFP/mCh forward	5'-GAC CAG GTC CTC ATG GAG GAC AGG TCT GGA GGA GGA GGA TCT ATG GTG AGC AAG GGC GAG-3'
		EGFP/mCh reverse	5'-GGA CTC CAC CAG CCG GTT GGT GCG AGA TCC TCC TCC TCC AGA CTT GTA CAG CTC GTC CAT-3'
Gα13	260aa	EGFP/mCh forward	5'-GAC CAG GTG CTT ATG GAA GAT CGA TCT GGA GGA GGA GGA TCT ATG GTG AGC AAG GGC GAG-3'
		EGFP/mCh reverse	5'-AGA CTC TGT AAG GCG ATT GGT CAG AGA TCC TCC TCC TCC AGA CTT GTA CAG CTC GTC CAT-3'

Forward primers:

Green region: Last 24 bp before 244th amino acid of Gα_{11}; 265th amino acid of G$\alpha_{12;}$ 260th amino acid of Gα_{13}

Yellow region: linker

Red region: Beginning of EGFP/mCherry sequence

Reverse primers:

Green region: End of EGFP/mCherry sequence

Yellow region: linker

Red region: 18 bp after 244th amino acid of Gα_{11}; 265th amino acid of G$\alpha_{12;}$ 260th amino acid of Gα_{13}

Table E.2 Primers to transfer tagged Gα proteins to pcDNA

Gα11-Xho1 forward	5' GTT GTT GTT CTC GAG ATG ACT CTG GAG TCC ATG ATG 3'
Gα11-Kpn1 reverse	5'-TGC TTA GGT ACC TCA GAC CAG GTT GTA CTC CTT-3'
Gα13-Xba1 forward	5'- GTT GTT TCT AGA ATG GCG GAC TTC CTG CCG- 3'
Gα13-Kpn1 reverse	5'- GTT GTT GGT ACC CTA CTG TAG CAT AAG CTG- 3'

CODING SEQUENCES OF FUSION PROTEINS

Coding sequence of mCherry tagged Gα11 Protein from 244th amino acid region: Black sequence corresponds to Gα11 receptor; blue sequence shows linker while red sequence represents mCherry sequence.

GGCCGGGGGGCGGCGGCGGGCAGGCGGCCGCGTCGGCCGGGGCCGGGACGATGACTCTGAGTCCATGATGG
CGTGTTGCCTGAGCGATGAGGTGAAGGAGTCCAAGCGGATCAACGCCGAGATCGAGAAGCAGCTGCGGCGG
GACAAGCGCGACGCCCGGCGCGAGCTCAAGCTGCTGCTGCTCGGCACGGGCGAGAGCGGGAAGAGCACGTT
CATCAAGCAGATGCGCATCATCCACGGCGCCGGCTACTCGGAGGAGGACAAGCGCGGCTTCACCAAGCTCG
TCTACCAGAACATCTTCACCGCCATGCAGGCCATGATCCGGGCCATGGAGACGCTCAAGATCCTCTACAAG
TACGAGCAGAACAAGGCCAATGCGCTCCTGATCCGGGAGGTGGACGTGGAGAAGGTGACCACCTTCGAGCA
TCAGTACGTCAGTGCCATCAAGACCCTGTGGGAGGACCCGGGCATCCAGGAATGCTACGACCGCAGGCGCG
AGTACCAGCTCTCCGACTCTGCCAAGTACTACCTGACCGACGTTGACCGCATCGCCACCTTGGGCTACCTG
CCCACCCAGCAGGACGTGCTGCGGGTCCGCGTGCCCACCACCGGCATCATCGAGTACCCTTTCGACCTGGA
GAACATCATCTTCCGGATGGTGGATGTGGGGGGCCAGCGGTCGGAGCGGAGGAAGTGGATCCACTGCTTTG
AGAACGTGACATCCATCATGTTCTGGAGGAGGAGGATCTATGGTGAGCAAGGGCGAGGAGGATAACATGGC
CATCATCAAGGAGTTCATGCGCTTCAAGGTGCACATGGAGGGCTCCGTGAACGGCCACGAGTTCGAGATCG
AGGGCGAGGGCGAGGGCCGCCCCTACGAGGGCACCCAGACCGCCAAGCTGAAGGTGACCAAGGGTGGCCCC
CTGCCCTTCGCCTGGGACATCCTGTCCCCTCAGTTCATGTACGGCTCCAAGGCCTACGTGAAGCACCCCGC
CGACATCCCCGACTACTTGAAGCTGTCCTTCCCCGAGGGCTTCAAGTGGGAGCGCGTGATGAACTTCGAGG
ACGGCGGCGTGGTGACCGTGACCCAGGACTCCTCCCTGCAGGACGGCGAGTTCATCTACAAGGTGAAGCTG
CGCGGCACCAACTTCCCCTCCGACGGCCCCGTAATGCAGAAGAAGACCATGGGCTGGGAGGCCTCCTCCGA
GCGGATGTACCCCGAGGACGGCGCCCTGAAGGGCGAGATCAAGCAGAGGCTGAAGCTGAAGGACGGCGGCC
ACTACGACGCTGAGGTCAAGACCACCTACAAGGCCAAGAAGCCCGTGCAGCTGCCCGGCGCCTACAACGTC
AACATCAAGTTGGACATCACCTCCCACAACGAGGACTACACCATCGTGGAACAGTACGAACGCGCCGAGGG

CCGCCACTCCACCGGCGGCATGGACGAGCTGTACAAGTCTGGAGGAGGAGGATCTTTCTCGTCGCCCTCAG
CGAATACGACCAAGTCCTGGTGGAGTCGGACAACGAGAACCGGATGGAGGAGAGCAAAGCCCTGTTCCGGA
CCATCATCACCTACCCCTGGTTCCAGAACTCCTCCGTCATCCTCTTCCTCAACAAGAAGGACCTGCTGGAG
GACAAGATCCTGTACTCGCACCTGGTGGACTACTTCCCCGAGTTCGATGGTCCCCAGCGGGACGCCCAGGC
GGCGCGGGAGTTCATCCTGAAGATGTTCGTGGACCTGAACCCCGACAGCGACAAGATCATCTACTCACACT
TCACGTGTGCCACCGACACGGAGAACATCCGCTTCGTGTTCGCGGCCGTGAAGGACACCATCCTGCAGCTC
AACCTCAAGGAGTACAACCTGGTCTGAGCGCCCAGGCCCAGGGAGACGGGATGGAGACACGGGGCAGGACC
TTCCTTCCACGGAGCCTGCGGCTGCCGGGCGGGTGGCGCTGCCGAGTCCGGGCCGGGGCCTCTGCCGCGGG
AGGAGATTTTTTTTTT

Coding sequence of EGFP tagged Gα12 Protein from 265th amino acid region:

Black sequence corresponds to Gα12 receptor, blue sequence shows linker; while green sequence represents EGFP sequence.

GCTAGCGTTTAAACTTAAGCTTGGTACCACCATGTCCGGGGTGGTGCGGACCCTCAGCCGCTGCCTGCTGC
CGGCCGAGGCCGGCGGGGCCCGCGAGCGCAGGGCGGGCAGCGGCGCGCGCGACGCGGAGCGCGAGGCCCGG
AGGCGTAGCCGCGACATCGACGCGCTGCTGGCCCGCGAGCGGCGCGCGGTCCGGCGCCTGGTGAAGATCCT
GCTGCTGGGCGCGGGCGAGAGCGGCAAGTCCACGTTCCTCAAGCAGATGCGCATCATCCACGGCCGCGAGT
TCGACCAGAAGGCGCTGCTGGAGTTCCGCGACACCATCTTCGACAACATCCTCAAGGGCTCAAGGGTTCTT
GTTGATGCACGAGATAAGCTTGGCATTCCTTGGCAGTATTCTGAAAATGAGAAGCATGGGATGTTCCTGAT
GGCCTTCGAGAACAAGGCGGGGCTGCCTGTGGAGCCGGCCACCTTCCAGCTGTACGTCCCGGCCCTGAGCG
CACTCTGGAGGGATTCTGGCATCAGGGAGGCTTTCAGCCGGAGAAGCGAGTTTCAGCTGGGGGAGTCGGTG
AAGTACTTCCTGGACAACTTGGACCGGATCGGCCAGCTGAATTACTTTCCTAGTAAGCAAGATATCCTGCT
GGCTAGGAAAGCACCAAGGGAATTGTGGAGCATGACTTCGTTATTAAGAAGATCCCCTTTAAGATGGTGGA
TGTGGGCGGCCAGCGGTCCCAGCGCCAGAAGTGGTTCCAGTGCTTCGACGGGATCACGTCCATCCTGTTCT
CTGGAGGAGGAGGATCTATGGTGAGCAAGGGCGAGGAGCTGTTCACCGGGGTGGTGCCCATCCTGGTCGAG
CTGGACGGCGACGTAAACGGCCACAAGTTCAGCGTGTCCGGCGAGGGCGAGGGCGATGCCACCTACGGCAA
GCTGACCCTGAAGTTCATCTGCACCACCGGCAAGCTGCCCGTGCCCTGGCCCACCCTCGTGACCACCCTGA
CCTACGGCGTGCAGTGCTTCAGCCGCTACCCCGACCACATGAAGCAGCACGACTTCTTCAAGTCCGCCATG
CCCGAAGGCTACGTCCAGGAGCGCACCATCTTCTTCAAGGACGACGGCAACTACAAGACCCGCGCCGAGGT
GAAGTTCGAGGGCGACACCCTGGTGAACCGCATCGAGCTGAAGGGCATCGACTTCAAGGAGGACGGCAACA

TCCTGGGGCACAAGCTGGAGTACAACTACAACAGCCACAACGTCTATATCATGGCCGACAAGCAGAAGAAC
GGCATCAAGGTGAACTTCAAGATCCGCCACAACATCGAGGACGGCAGCGTGCAGCTCGCCGACCACTACCA
GCAGAACACCCCCATCGGCGACGGCCCCGTGCTGCTGCCCGACAACCACTACCTGAGCACCCAGTCCAAGC
TTAGCAAAGACCCCAACGAGAAGCGCGATCACATGGTCCTGCTGGAGTTCGTGACCGCCGCCGGGATCACT
CTCGGCATGGACGAGCTGTACAAGTCTGGAGGAGGAGGATCTATGGTCTCCTCCAGCGAGTACGACCAGGT
CCTCATGGAGGACAGGCGCACCAACCGGCTGGTGGAGTCCATGAACATCTTCGAGACCATCGTCAACAACA
AGCTCTTCTTCAACGTCTCCATCATTCTCTTCCTCAACAAGATGGACCTCCTGGTGGAGAAGGTGAAGACC
GTGAGCATCAAGAAGCACTTCCCGGACTTCAGGGGCGACCCGCACAGGCTGGAGGACGTCCAGCGCTACCT
GGTCCAGTGCTTCGACAGGAAGAGACGGAACCGCAGCAAGCCACTCTTCCACCACTTCACCACCGCCATCG
ACACCGAGAACGTCCGCTTCGTGTTCCATGCTGTGAAAGACACCATCCTGCAGGAGAACCTGAAGGACATC
ATGCTGCAGTGA CTCGAGTCTAGAGGGCCCGTTTAAAC

Coding sequence of mCherry tagged Gα13 Protein from 260th amino acid region:
Black sequence corresponds to Gα13 receptor, blue sequence shows linker; while red
sequence represents mCherry sequence.

ATGGCGGACTTCCTGCCGTCGCGGTCCGTGCTGTCCGTGTGCTTCCCCGGCTGCCTGCTGACGAGTGGCGA
GGCCGAGCAGCAACGCAAGTCCAAGGAGATCGACAAATGCCTGTCTCGGGAAAAGACCTATGTGAAGCGGC
TGGTGAAGATCCTGCTGCTGGGCGCGGGCGAGAGCGGCAAGTCCACCTTCCTGAAGCAGATGCGGATCATC
CACGGGCAGGACTTCGACCAGCGCGCGCGCGAGGAGTTCCGCCCCACCATCTACAGCAACGTGATCAAAGG
TATGAGGGTGCTGGTTGATGCTCGAGAGAAGCTTCATATTCCCTGGGGAGACAACTCAAACCAACAACATG
GAGATAAGATGATGTCGTTTGATACCCGGGCCCCCATGGCAGCCCAAGGAATGGTGGAAACAAGGGTTTTC
TTACAATATCTTCCTGCTATAAGAGCATTATGGGCAGACAGCGGCATACAGAATGCCTATGACCGGCGTCG
AGAATTTCAACTGGGTGAATCTGTAAAATATTTCCTGGATAACTTGGATAAACTTGGAGAACCAGATTATA
TTCCATCACAACAAGATATTCTGCTTGCCAGAAGACCCACCAAAGGCATCCATGAATACGACTTTGAAATA
AAAAATGTTCCTTTCAAAATGGTTGATGTAGGTGGTCAGAGATCAGAAAGGAAACGTTGGTTTGAATGTTT
CGACAGTGTGACATCAATACTTTTCCTTGTTTCCTCAAGTGAATTTGACCAGGTGCTTATGGAAGATCGAT
CTGGAGGAGGAGGATCTATGGTGAGCAAGGGCGAGGAGGATAACATGGCCATCATCAAGGAGTTCATGCGC
TTCAAGGTGCACATGGAGGGCTCCGTGAACGGCCACGAGTTCGAGATCGAGGGCGAGGGCGAGGGCCGCCC
CTACGAGGGCACCCAGACCGCCAAGCTGAAGGTGACCAAGGGTGGCCCCCTGCCCTTCGCCTGGGACATCC
TGTCCCCTCAGTTCATGTACGGCTCCAAGGCCTACGTGAAGCACCCCGCCGACATCCCCGACTACTTGAAG

121

CTGTCCTTCCCCGAGGGCTTCAAGTGGGAGCGCGTGATGAACTTCGAGGACGGCGGCGTGGTGACCGTGAC
CCAGGACTCCTCCCTGCAGGACGGCGAGTTCATCTACAAGGTGAAGCTGCGCGGCACCAACTTCCCCTCCG
ACGGCCCCGTAATGCAGAAGAAGACCATGGGCTGGGAGGCCTCCTCCGAGCGGATGTACCCCGAGGACGGC
GCCCTGAAGGGCGAGATCAAGCAGAGGCTGAAGCTGAAGGACGGCGGCCACTACGACGCTGAGGTCAAGAC
CACCTACAAGGCCAAGAAGCCCGTGCAGCTGCCCGGCGCCTACAACGTCAACATCAAGTTGGACATCACCT
CCCACAACGAGGACTACACCATCGTGGAACAGTACGAACGCGCCGAGGGCCGCCACTCCACCGGCGGCATG
GACGAGCTGTACAAGTCTGGAGGAGGAGGATCTCTGACCAATCGCCTTACAGAGTCTCTGAACATTTTTGA
AACAATCGTCAATAACCGGGTTTTCAGCAATGTCTCCATAATTCTGTTCTTAAACAAGACAGACTTGCTTG
AGGAGAAGGTGCAAATTGTGAGCATCAAAGACTATTTCCTAGAATTTGAAGGGGATCCCCACTGCTTAAGA
GACGTCCAAAAATTCCTGGTGGAATGTTTCCGGAACAAACGCCGGGACCAGCAACAGAAGCCCTTATACCA
CCACTTCACCACTGCTATCAACACGGAGAACATCCGCCTTGTTTTCCGTGACGTGAAGGATACTATTCTGC
ATGACAACCTCAAGCAGCTTATGCTACAGTAG

Coding sequence of EGFP tagged A2A receptor: Black sequence corresponds to A2A receptor; while green sequence represents EGFP sequence.

ATGCCCATCATGGGCTCCTCGGTGTACATCACGGTGGAGCTGGCCATTGCTGTGCTGGCCATCCTGGGCAA
TGTGCTGGTGTGCTGGGCCGTGTGGCTCAACAGCAACCTGCAGAACGTCACCAACTACTTTGTGGTGTCAC
TGGCGGCGGCCGACATCGCAGTGGGTGTGCTCGCCATCCCCTTTGCCATCACCATCAGCACCGGGTTCTGC
GCTGCCTGCCACGGCTGCCTCTTCATTGCCTGCTTCGTCCTGGTCCTCACGCAGAGCTCCATCTTCAGTCT
CCTGGCCATCGCCATTGACCGCTACATTGCCATCCGCATCCCGCTCCGGTACAATGGCTTGGTGACCGGCA
CGAGGGCTAAGGGCATCATTGCCATCTGCTGGGTGCTGTCGTTTGCCATCGGCCTGACTCCCATGCTAGGT
TGGAACAACTGCGGTCAGCCAAAGGAGGGCAAGAACCACTCCCAGGGCTGCGGGGAGGGCCAAGTGGCCTG
TCTCTTTGAGGATGTGGTCCCCATGAACTACATGGTGTACTTCAACTTCTTTGCCTGTGTGCTGGTGCCCC
TGCTGCTCATGCTGGGTGTCTATTTGCGGATCTTCCTGGCGGCGCGCGACGACAGCTGAAGCAGATGGAGAGC
CAGCCTCTGCCGGGGGGAGCGGGCACGGTCCACACTGCAGAAGGAGGTCCATGCTGCCAAGTCACTGGCCAT
CATTGTGGGGCTCTTTGCCCTCTGCTGGCTGCCCCTACACATCATCAACTGCTTCACTTTCTTCTGCCCCG
ACTGCAGCCACGCCCCTCTCTGGCTCATGTACCTGGCCATCGTCCTCTCCCACACCAATTCGGTTGTGAAT
CCCTTCATCTACGCCTACCGTATCCGCGAGTTCCGCCAGACCT
TCCGCAAGATCATTCGCAGCCACGTCCTGAGGCAGCAAGAACCTTTCAAGGCAGCTGGCACCAGTGCCCGG
GTCTTGGCAGCTCATGGCAGTGACGGAGAGCAGGTCAGCCTCCGTCTCAACGGCCACCCGCCAGGAGTGTG
GGCCAACGGCAGTGCTCCCCACCCTGAGCGGAGGCCCAATGGCTACGCCCTGGGGCTGGTGAGTGGAGGGA

GTGCCCAAGAGTCCCAGGGGAACACGGGCCTCCCAGACGTGGAGCTCCTTAGCCATGAGCTCAAGGGAGTG
TGCCCAGAGCCCCCTGGCCTAGATGACCCCCTGGCCCAGGATGGAGCAGGAGTGTCCATGGTGAGCAAGGG
CGAGGAGCTGTTCACCGGGGTGGTGCCCATCCTGGTCGAGCTGGACGGCGACGTAAACGGCCACAAGTTCA
GCGTGTCCGGCGAGGGCGAGGGCGATGCCACCTACGGCAAGCTGACCCTGAAGTTCATCTGCACCACCGGC
AAGCTGCCCGTGCCCTGGCCCACCCTCGTGACCACCCTGACCTACGGCGTGCAGTGCTTCAGCCGCTACCC
CGACCACATGAAGCAGCACGACTTCTTCAAGTCCGCCATGCCCGAAGGCTACGTCCAGGAGCGCACCATCT
TCTTCAAGGACGACGGCAACTACAAGACCCGCGCCGAGGTGAAGTTCGAGGGCGACACCCTGGTGAACCGC
ATCGAGCTGAAGGGCATCGACTTCAAGGAGGACGGCAACATCCTGGGGCACAAGCTGGAGTACAACTACAA
CAGCCACAACGTCTATATCATGGCCGACAAGCAGAAGAACGGCATCAAGGTGAACTTCAAGATCCGCCACA
ACATCGAGGACGGCAGCGTGCAGCTCGCCGACCACTACCAGCAGAACACCCCCATCGGCGACGGCCCCGTG
CTGCTGCCCGACAACCACTACCTGAGCACCCAGTCCAAGCTTAGCAAAGACCCCAACGAGAAGCGCGATCA
CATGGTCCTGCTGGAGTTCGTGACCGCCGCCGGGATCACTCTCGGCATGGACGAGCTGTACAAGTAA

Coding sequence of EGFP tagged D2R receptor: Black sequence corresponds to D2R receptor; while green sequence represents EGFP sequence

ATGGATCCACTGAATCTGTCCTGGTATGATGATGATCTGGAGAGGCAGAACTGGAGCCGGCCCTTCAACGG
GTCAGACGGGAAGGCGGACAGACCCCACTACAACTACTATGCCACACTGCTCACCCTGCTCATCGCTGTCA
TCGTCTTCGGCAACGTGCTGGTGTGCATGGCTGTGTCCCGCGAGAAGGCGCTGCAGACCACCACCAACTAC
CTGATCGTCAGCCTCGCAGTGGCCGACCTCCTCGTCGCCACACTGGTCATGCCCTGGGTTGTCTACCTGGA
GGTGGTAGGTGAGTGGAAATTCAGCAGGATTCACTGTGACATCTTCGTCACTCTGGACGTCATGATGTGCA
CGGCGAGCATCCTGAACTTGTGTGCCATCAGCATCGACAGGTACACAGCTGTGGCCATGCCCATGCTGTAC
AATACGCGCTACAGCTCCAAGCGCCGGGTCACCGTCATGATCTCCATCGTCTGGGTCCTGTCCTTCACCAT
CTCCTGCCCACTCCTCTTCGGACTCAATAACGCAGACCAGAACGAGTGCATCATTGCCAACCCGGCCTTCG
TGGTCTACTCCTCCATCGTCTCCTTCTACGTGCCCTTCATTGTCACCCTGCTGGTCTACATCAAGATCTAC
ATTGTCCTCCGCAGACGCCGCAAGCGAGTCAACACCAAACGCAGCAGCCGAGCTTTCAGGGCCCACCTGAG
GGCTCCACTAAAGGGCAACTGTACTCACCCCGAGGACATGAAACTCTGCACCGTTATCATGAAGTCTAATG
GGAGTTTCCCAGTGAACAGGCGGAGAGTGGAGGCTGCCCGGCGAGCCCAGGAGCTGGAGATGGAGATGCTC
TCCAGCACCAGCCCACCCGAGAGGACCCGGTACAGCCCCATCCCACCCAGCCACCACCAGCTGACTCTCCC
CGACCCGTCCCACCATGGTCTCCACAGCACTCCCGACAGCCCCGCCAAACCAGAGAAGAATGGGCATGCCA
AAGACCACCCCAAGATTGCCAAGATCTTTGAGATCCAGACCATGCCCAATGGCAAAACCCGGACCTCCCTC
AAGACCATGAGCCGTAGGAAGCTCTCCCAGCAGAAGGAGAAGAAAGCCACTCAGATGCTCGCCATTGTTCT

CGGCGTGTTCATCATCTGCTGGCTGCCCTTCTTCATCACACACATCCTGAACATACACTGTGACTGCAACA
TCCCGCCTGTCCTGTACAGCGCCTTCACGTGGCTGGGCTATGTCAACAGCGCCGTGAACCCCATCATCTAC
ACCACCTTCAACATTGAGTTCCGCAAGGCCTTCCTGAAGATCCTCCACTGCATGGTGAGCAAGGGCGAGGA
GCTGTTCACCGGGGTGGTGCCCATCCTGGTCGAGCTGGACGGCGACGTAAACGGCCACAAGTTCAGCGTGT
CCGGCGAGGGCGAGGGCGATGCCACCTACGGCAAGCTGACCCTGAAGTTCATCTGCACCACCGGCAAGCTG
CCCGTGCCCTGGCCCACCCTCGTGACCACCCTGACCTACGGCGTGCAGTGCTTCAGCCGCTACCCCGACCA
CATGAAGCAGCACGACTTCTTCAAGTCCGCCATGCCCGAAGGCTACGTCCAGGAGCGCACCATCTTCTTCA
AGGACGACGGCAACTACAAGACCCGCGCCGAGGTGAAGTTCGAGGGCGACACCCTGGTGAACCGCATCGAG
CTGAAGGGCATCGACTTCAAGGAGGACGGCAACATCCTGGGGCACAAGCTGGAGTACAACTACAACAGCCA
CAACGTCTATATCATGGCCGACAAGCAGAAGAACGGCATCAAGGTGAACTTCAAGATCCGCCACAACATCG
AGGACGGCAGCGTGCAGCTCGCCGACCACTACCAGCAGAACACCCCCATCGGCGACGGCCCCGTGCTGCTG
CCCGACAACCACTACCTGAGCACCCAGTCCAAGCTTAGCAAAGACCCCAACGAGAAGCGCGATCACATGGT
CCTGCTGGAGTTCGTGACCGCCGCCGGGATCACTCTCGGCATGGACGAGCTGTACAAGTAA

FILTERS OF CONFOCAL MICROSCOPY
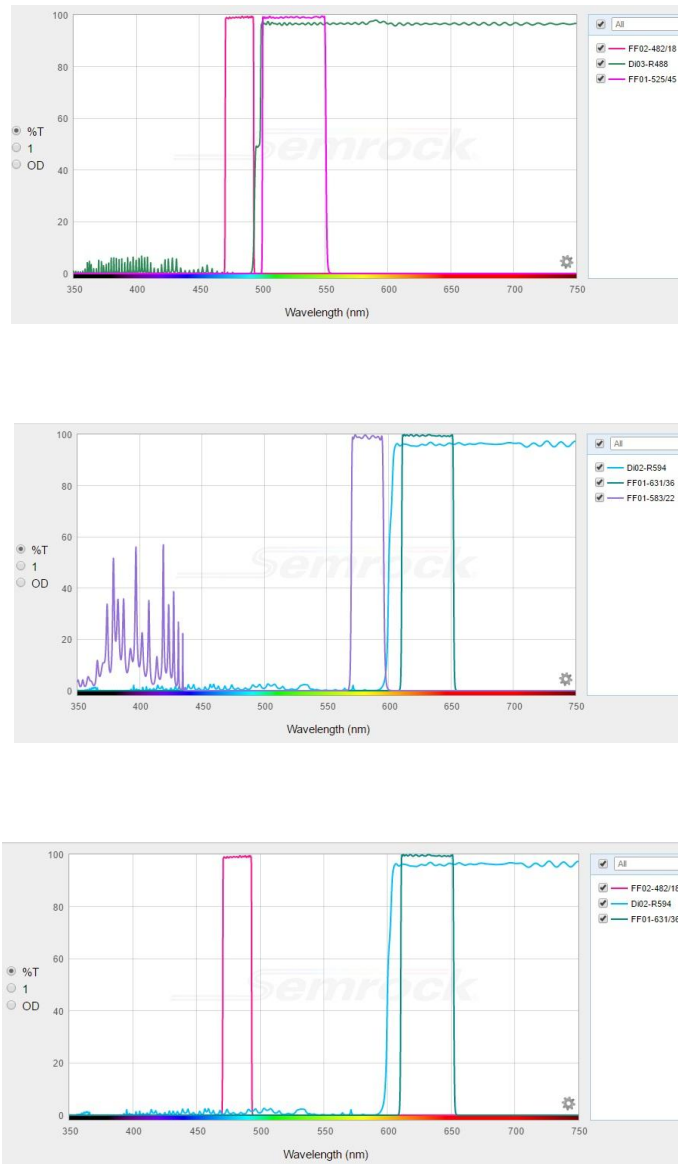
Figure G.1 Wavelenght of EGFP (a),mCherry (b) and FRET(c).

EXTRA IMAGES OF FRET RESUTLTS

Detection of physical interactions between Adenosine A2A and Gα11 protein by using FRET techniques
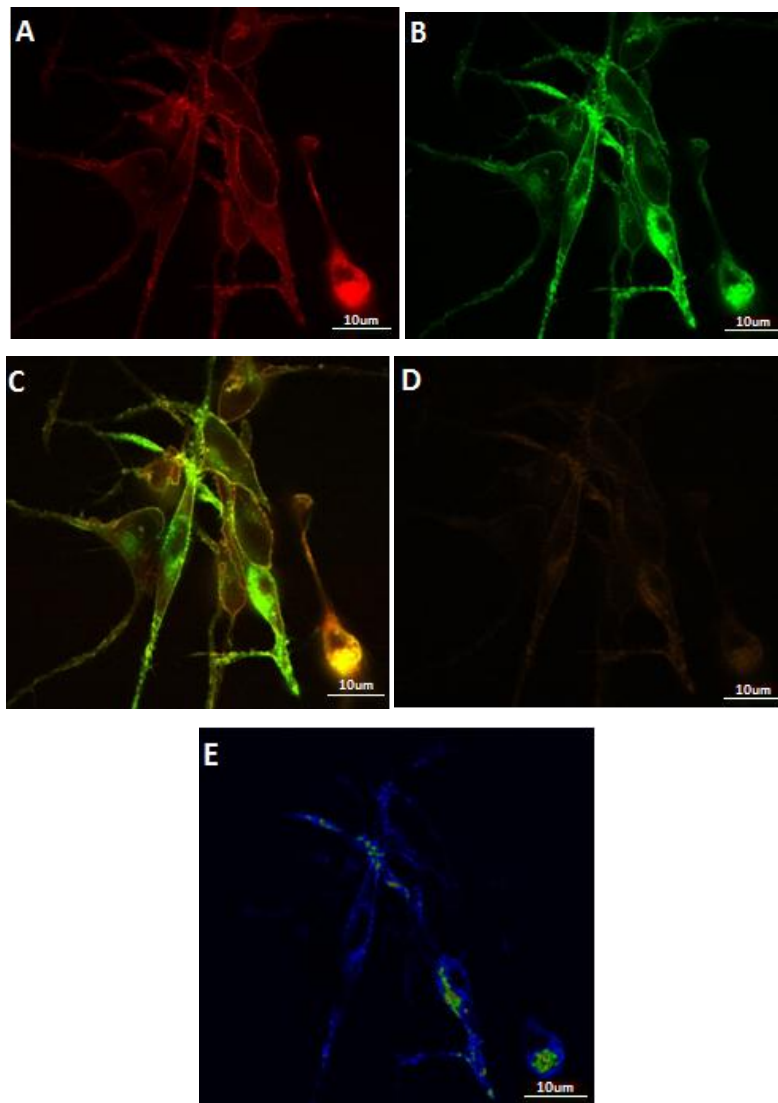
Figure H.1 N2a cells transfected with A2A+EGFP and Gα11+mCherry. Images were taken from mCherry channel excitation at 583 nm shows Gα11+mCherry (A), EGFP channel excitation at 482 nm shows A2A+EGFP (B), Multiple channel shows co-localization of A2A+EGFP and Gα11+mCherry. (C) FRET channel shows FRET signal (D) FRET efficiency shows pixels where FRET occurs (E).

**Detection of physical interactions between Dopamine and Gα11 protein by using FRET techniques**
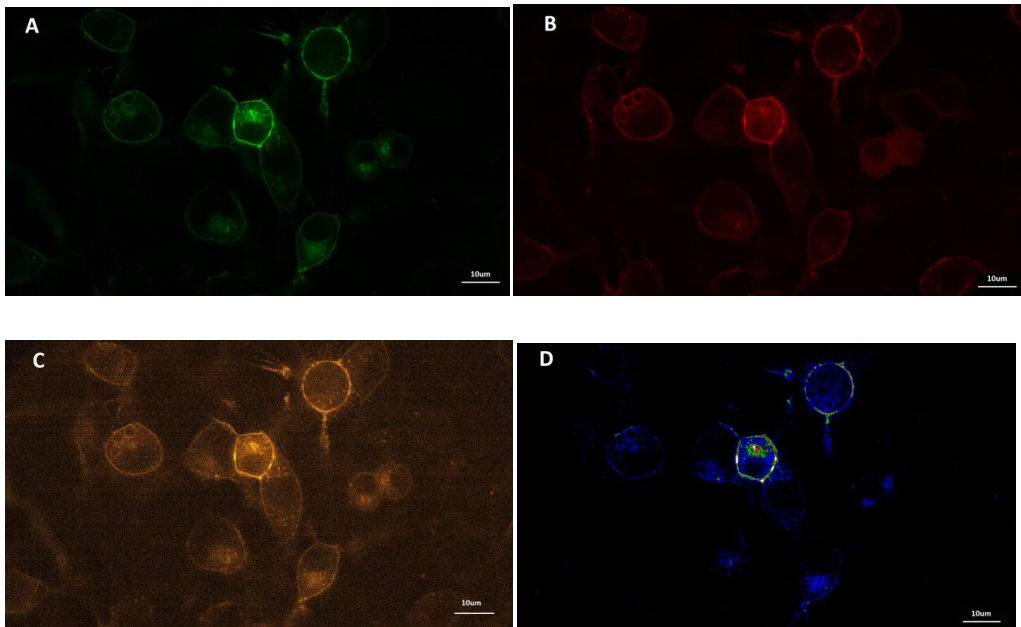
Figure H.3 N2a cells transfected with D2R+EGFP and Gα11+mCherry. Images were taken from EGFP channel excitation at 482 nm shows D2R+EGFP (A), mCherry channel excitation at 583 nm shows Gα11+mCherry (B), FRET channel shows FRET signal (C) FRET efficiency shows pixels where FRET occurs (D).

**Detection of physical interactions between Adenosine A2A and Gα13 protein by using FRET techniques**
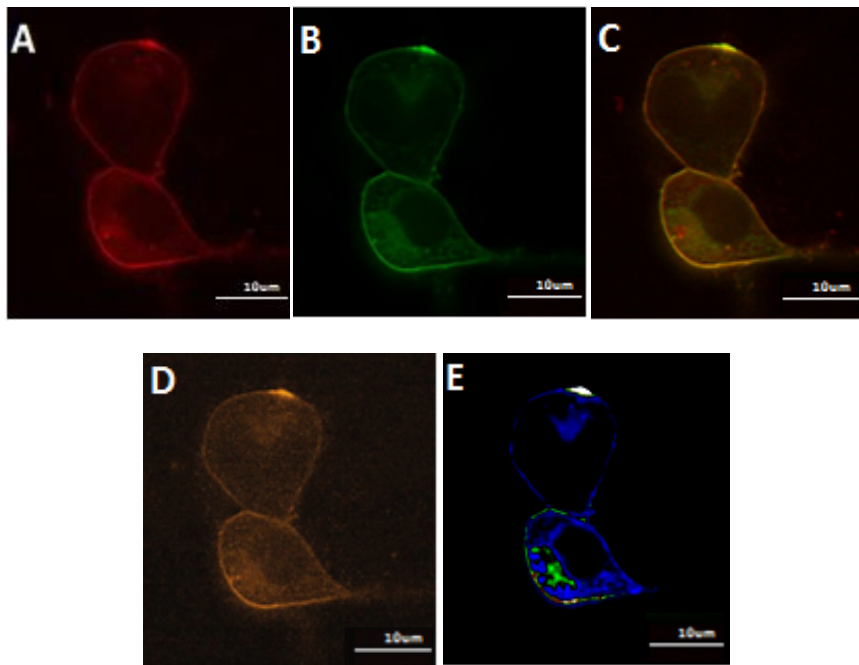
Figure H.4 N2a cells transfected with A2AR+EGFP and Gα13+mCherry. Images were taken from mCherry channel excitation at 583 nm shows Gα13+mCherry (A), EGFP channel excitation at 482 nm shows A2AR+EGFP (B), Multiple channel shows co-localization of A2AR+EGFP and Gα13+mCherry (C) and FRET channel shows FRET signal (D) FRET efficiency shows pixels where FRET occurs (E).

Detection of physical interactions between Dopamine and Gα13 protein by using FRET techniques
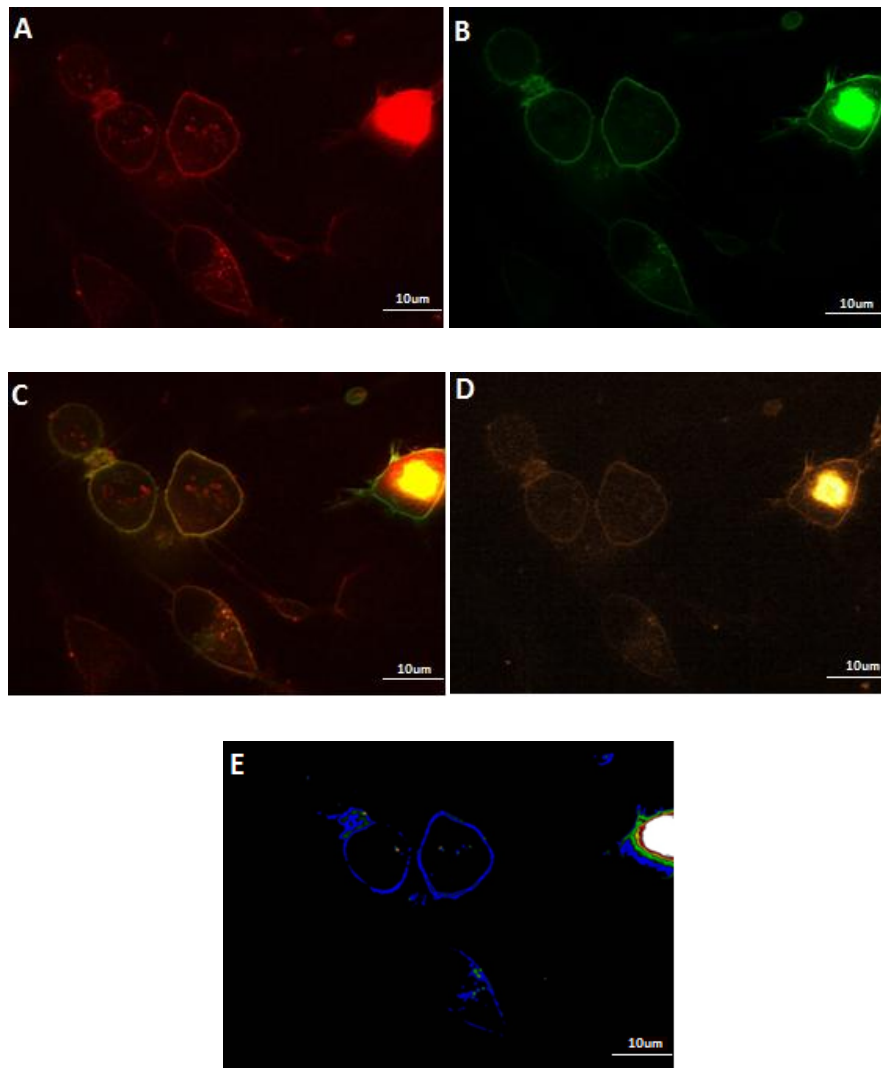

Figure H.6 N2a cells transfected with D2R+EGFP and Gα13+mCherry. Images were taken from mCherry channel excitation at 583 nm shows Gα13+mCherry (A), EGFP channel excitation at 482 nm shows D2R +EGFP (B), Multiple channel shows co-localization of D2R+EGFP and Gα13+mCherry (C) and FRET channel shows FRET signal (D) FRET efficiency shows pixels where FRET occurs (E).